Stony Brook University

Mek1 regulates partner choice during meiotic recombination in yeast

A Dissertation Presented by

HENGYAO NIU

to

The Graduate School

In Partial Fulfillment of the

Requirements

For the Degree of

Doctor of Philosophy

in

Molecular and Cellular Biology

Stony Brook University

August 2007

Stony Brook University
The Graduate School

HENGYAO NIU

We, the dissertation committee for the above candidate for the
Doctor of Philosophy degree, hereby recommended
acceptance of this dissertation

Nancy M. Hollingswoth, Ph.D.
Dissertation Advisor
Professor, Department of Biochemistry and Cell Biology

Aaron Neiman, Ph.D.
Chairperson of Defense
Associate Professor, Department of Biochemistry and Cell Biology

Robert S. Haltiwanger, Ph.D.
Professor, Department of Biochemistry and Cell Biology

Daniel F. Bogenhagen, M.D.
Professor, Department of Pharmological Science

Lorraine S. Symington, Ph.D.
Professor, Department of Microbiology, Columbia University

This dissertation is accepted by the Graduate School

Lawrance Martin
Dean of the Graduate School

Abstract of the Dissertation

Mek1 regulates partner choice during meiotic recombination in yeast

by

Hengyao Niu

Doctor of Philosophy

In

Molecular and Cellular Biology

Stony Brook University

2007

Meiotic recombination between homologs generates crossovers, which are critical for properly segregating homologs at Meiosis I (MI). In contrast, sister chromatids are the preferred templates for mitotic recombination. The bias in meiotic recombination for homologs is created in two ways: (1) a meiosis-specific RecA ortholog, Dmc1, actively promotes recombination between homologous chromosomes; and (2) a barrier to sister chromatid repair (BSCR) suppresses recombination between sister chromatids. Hop1, Red1 and Mek1 are meiosis-specific proteins that form a complex required for BSCR formation. Mek1 is a serine/threonine protein kinase whose activation requires both Hop1 and Red1. Studies on the BSCR can be broken down into two basic questions: (1) how is Mek1 kinase activity regulated to create a BSCR? and (2) what is the mechanism by which Mek1-phosphorylated substrates create a BSCR? My thesis involved experiments designed to address both questions.

The Hop1 protein contains two distinct functional domains: the C–domain, made up of the last 20 amino acids, and the N-domain (the remainder of the protein). My research revealed that the C-domain of Hop1 functions in BSCR formation by promoting Mek1 dimerization, which then enables activation of Mek1 through auto-phosphorylation of conserved threonines in the activation loop of the kinase. This work, in combination with other results from the Hollingsworth lab, has led to a model where DSB formation triggers Hop1 C-domain phosphorylation and Mek1 recruitment to Red1. Subsequent Mek1 auto-activation as a result of Hop1 C-domain promoted dimerization then allows creation of a BSCR in a region around where DSBs are formed.

A selected candidate approach to identify Mek1 targets revealed that Rad54 is a substrate for Mek1 *in vitro*. The *in vitro* Mek1 phosphorylation sites were mapped by mass spectrometry. Overexpression of one phosphorylation site mutant, *rad54-T132A*, allows *dmc1* to sporulate. The resulting spores are viable, indicating that *rad54-T132A* promotes interhomolog recombination and that the BSCR is intact. Therefore, in addition to creating the BSCR, Mek1 regulates meiotic recombination by down-regulating the activity of Rad54.

Table of Content

List of Abbreviations

MI: Meiosis I

MII: Meiosis II

ssDNA: Single stranded DNA

DSB: Double strand break

dHJ: Double Holliday junction

AE: Axial element

SC: Synaptonemal omplex

BSCR: Barrier to sister chromatid repair

1-NA-PP1: 4-amino-1-*tert*-butyl-3-(1'naphthyl)pyrazolo[3,4-*d*]pyrimidine

EDTA: Ethylenediamine tetraacetic acid

EGTA: Ethylene glycol tetraacetic acid

SDS: Sodium dodecyl sufate

PMSF: Phenylmethylsulphonyl fluoride

NPDs: Non-parental ditypes

PCR: Polymerase Chain Reaction

ATP: Adenosine 5'-triphosphate

TCEP-HCl: Tris(2-Carboxyethyl) phosphine Hydrochloride

IPTG: Isopropyl-β -D-1-thiogalactopyranoside

FPLC: Fast Protein Liquid Chromatography

List of Figures

List of Tables

Acknowledgements

I would like to give my special thanks to my advisor, Nancy Hollingsworth for her great mentoring in various aspects of scientific researches from setting up experiments to finishing a manuscript. While I look over the past five years, I am still enjoying the happiness of sharing my every progress with her. I would also like to thank my committees, Aaron Neiman, Daniel Bogenhagen, Robert Haltiwanger and Lorraine Symington for their directions. I would like to acknowledge my current and previous lab members, Lihong Wan, Tracy Callender, Hsiao-Chi Lo, Emily Job, Caroline Park, Dana Schaefer, Theresa de los Santos for their thoughtful ideas and helps with the experiments. It has been a wonderful time to work in the lab. Lihong Wan, Dana Scheafer, Emily Job and Caroline Park have made great contributions to two publications of mine. In addition, I would like to recognize two previous lab members, who I have not overlapped with, Dana Woltering and Bridget Baumgartner for their initial work on Hop1 C domain studies. Furthermore, I would like to acknowledge our collaborators: Lumir Krejci and Valeriya Busygina from Patrick Sung's Lab, Xue Li from Steven Gygi's Lab, Danesh Moazed and Josef Loidl. Lastly I dedicate this dissertation to my wife, Zhixin Chen and my daughter, Vivian Niu.

CHAPTER ONE

INTRODUCTION

I. Meiosis

Mitosis is a process where a single nuclear division segregates sister chromatids and produces genetically identical daughter cells. In constrast, meiosis consists of two nuclear divisions and is specialized to produce haploid gametes from a diploid mother cell. The reduction in chromosome number during meiosis is due to a single round of DNA replication followed by two rounds of chromosome segregation (Figure 1-1). In the first nuclear division (Meiosis I or MI), homologous chromosomes segregate to opposite poles, while in the second nuclear division (Meiosis II or MII), sister chromaids segregate to opposite poles. One cause of infertility in humans arises from failures at Meiosis I, where homologous chromosome mis-segregation results in aneuploid gametes. Most of the time, this aneuploidy produces inviable progeny. In cases where aneuploidy is tolerated, chromosome imbalances may cause genetic disorders such as Down syndrome (CHAMPION and HAWLEY 2002).

Segregation of sister chromatids in mitosis requires that pairs of sister chromatids first be connected by sister chromatid cohesion during DNA replication (UHLMANN and NASMYTH 1998). Centromeres of two sister chromatids are captured by microtubules from opposite poles of the spindle, thereby bi-orienting the chromatids. Sister chromatid cohesion, combined with the pulling forces of microtubules from opposite poles, generates tension which is monitored by the spindle checkpoint to ensure that all pairs of sister

chromatids are bi-oriented at Metaphase (RIEDER *et al.* 1995). At Anaphase, cohesion is removed, thereby allowing sister chromatids to segregate. There are three critical modifications of the mitotic segregation apparatus that allow pairs of homologous sister chromatids to segregate to opposite poles at MI. (1) Recombination between non-sister chromatids of homologous chromosomes generates crossovers. Crossovers, together with sister chromatid cohesion, connect homologs, thereby enabling the chromosomes to segregate to opposite poles when arm cohesion is removed at Anaphase I. (2) The kinetochores of pairs of sister chromatids act as a single unit and are captured by microtubules from the same pole of the spindle, producing mono-orientation of the sisters. (3) Sister chromatid cohesion is removed in two steps. At Anaphase I, arm cohesion is abolished while centromeric cohesion continues to hold sister chromatids together. At meiosis II, centromeric cohesion is lost, thereby allowing sister-chromatid separation (Figure 1-1).

II. Mitotic *Vs.* Meiotic Recombination:

A. Mitotic Recombination:

Mitotic recombination functions to repair DNA damage while preventing loss of heterozygosity and preferentially uses sister chromatids as templates for repair (KADYK and HARTWELL 1992). During mitotic recombination, double-strand breaks (DSBs) are resected to produce 3′ single stranded DNA

(ssDNA) ends (Figure 1-2A). The ends are covered by RPA, a single strand binding protein complex, to remove DNA secondary structure (Figure 1-2B). RPA is replaced by the recombinase Rad51, a step that requires the mediator proteins, Rad52 and Rad55/57 (NEW *et al.* 1998; SHINOHARA and OGAWA 1998; SUNG 1997a; SUNG 1997b) (Figure 1-2C). Rad51 then catalyzes single strand invasion, a process stimulated by the Swi2/Snf2 chromatin remodeling family member, Rad54 (Figure 1-2D) (PETUKHOVA *et al.* 1998). Besides facilitating Rad51 catalyzed strand invasion, Rad54 has also been found to promote DNA repair synthesis and to displace Rad51 from duplex DNA (SOLINGER *et al.* 2002; SUGAWARA *et al.* 2003). Following strand invasion, recombination intermediates may be processed through different pathways to repair breaks (KROGH and SYMINGTON 2004). To facilitate repair between sister chromatids, cohesin, a multi-subunit protein complex that holds sister chromatids together, is loaded post-replicatively to regions as long as 100 kb of DNA on either side of a DSB (STROM *et al.* 2004; UNAL *et al.* 2004).

B. Meiotic Recombination:

The purpose of meiotic recombination is to create physical connections between homologous chromosomes, therefore recombination occurs preferentially between non-sister chromatids. In keeping with this goal, there are a number of unique features to meiotic recombination. First, in meiosis, recombination occurs at high frequency and is initiated by programmed DSBs at

discrete regions known as "hotspots". This process is catalyzed by a conserved meiosis-specific endonuclease, Spo11 (Figure 1-3B) (KEENEY *et al.* 1997) . There are at least nine additional proteins (Rec107/Mer2, Rec102, Rec104, Rec114, Mei4, Ski8, Rad50, Mre11 and Xrs2) that are required for DSB formation (KEENEY 2001; KEENEY and NEALE 2006). After DSBs are created, covalent Spo11-DNA linkages are removed by an endonucleolytic process to free the DSB ends (Figure 1-3C) (NEALE *et al.* 2005). The free 5′ ends are further resected to create 3′ ssDNA (Figure 1-3D). Two RecA orthologs, Rad51 and the meiosis-specific protein Dmc1 (BISHOP *et al.* 1992), are then loaded onto 3′ ends to catalyze strand invasion (Figure 1-3E). Another unique feature of meiotic recombination is the bias for strand invasion into homologous non-sister chromatids, as compared to vegetative cells where sister chromatids are preferred (KADYK and HARTWELL 1992). The resulting recombination intermediates are then designated to become either crossovers with physical exchange of homologous chromosome arms or non-crossovers where genetic information is copied from the repair template without exchange (BISHOP and ZICKLER 2004). Most crossovers come from resolution of double Holliday junctions (dHJs) (ALLERS and LICHTEN 2001). An alternative crossover pathway utilizes Mus81/Mms4, a structure specific endonuclease, to process recombination intermediates into crossovers without forming dHJs (Figure 1-3F) (DE LOS SANTOS *et al.* 2003).

III. Meiotic recombination partner choice.

During meiosis, recombination partner choice is determined at the time of strand invasion, which is regulated in several ways:

A. Factors that promote interhomolog recombination.

Meiotic recombination uses recombination factors that promote Rad51 nucleoprotein filament formation, such as RPA, Rad52 and Rad55/Rad57 (GASIOR *et al.* 1998). In addition, many proteins are involved, including Dmc1, Rdh54 (Tid1), Hop2/Mnd1 and Mei5/Sae3 to promote recombination between non-sister chromatids during meiosis.

a. Dmc1: A meiosis-specific RecA ortholog, Dmc1 is present in many organisms and has been demonstrated to promote inter-homolog recombination in budding yeast (BISHOP *et al.* 1992). In the SK1 strain background of *Saccharomyces cerevisiae*, *dmc1* cells arrest at prophase with hyper-resected DSBs due to a failure in interhomolog strand invasion (BISHOP *et al.* 1992; HUNTER and KLECKNER 2001). However, the presence of *DMC1* does not bypass the requirement for the *RAD51*. In fact, *RAD51* is required for Dmc1 loading, although the reverse is not true (BISHOP 1994; SHINOHARA and SHINOHARA 2004). To assist Dmc1 promoted inter-homolog strand invasion, there are at least five proteins in addition to Rad51 that are involved.

b. Rdh54 (Tid1): Rdh54 shares homology with Rad54. It was initially identified in a yeast two-hybrid screen as a Dmc1-interacting protein (DRESSER *et al.* 1997; KLEIN 1997; SHINOHARA *et al.* 1997). In the absence of *RDH54*, Rad51 and

Dmc1 co-localization on chromosomes is reduced and recombination intermediates are not properly processed, thereby decreasing sporulation (SHINOHARA *et al.* 2000). The meiotic phenotypes of *rdh54Δ* are more severe than those of *rad54Δ*, which, while reducing spore viability to ~50 %, has very little effect on inter-homolog recombination during meiosis (LUI *et al.* 2006; SCHMUCKLI-MAURER and HEYER 2000). This situation is in contrast to DSB repair in vegetative cells, where *rad54* but not *rdh54* has severe effects and sister chromatids are the preferred repair templates (ARBEL *et al.* 1999; KLEIN 1997). *rad54Δ rdh54Δ* eliminates almost all meiotic inter-homolog recombination, indicating that *RAD54* and *RDH54* are partially functionally redundant (SHINOHARA *et al.* 1997). One of Rdh54's *in vivo* functions is to remove non-specific binding of Dmc1 to double strand DNA, presumably to facilitate Dmc1 loading on the ssDNA ends (HOLZEN *et al.* 2006). Although there are no published results yet to demonstrate stimulation of Dmc1 recombinase activity by Rdh54, Rdh54 has been shown to interact with Rad51 *in vitro* and stimulate Rad51 catalyzed D-loop formation (PETUKHOVA *et al.* 2000).

c. Mei5/Sae3: Mei5 and Sae3 form an evolutionary conserved complex that physically interacts with Dmc1. Both proteins co-localize with Dmc1 and are required for Dmc1 function *in vivo* (HAYASE *et al.* 2004; TSUBOUCHI and ROEDER 2004). Either single mutant mimics *dmc1Δ*, where hyper-resected DSBs accumulate and cells arrest at meiotic prophase (HAYASE *et al.* 2004; TSUBOUCHI

and ROEDER 2004). The biochemical activity of Mei5/Sae3 has not yet been determined. In fission yeast, there is one Sae3 homologue, Swi5, and two Mei5 homologues, Swi2 and Sfr1. The Swi5/Sfr1 complex is required for both meiotic and mitotic recombination (AKAMATSU *et al.* 2003; ELLERMEIER *et al.* 2004). The Swi5/Sfr1 complex has been shown to promote strand exchange activity of both the Rad51 ortholog, Rhp51, as well as Dmc1 *in vitro*, where the complex functions as a mediator to promote Rhp51 and Dmc1 nucleoprotein filament formation (HARUTA *et al.* 2006).

d. Hop2/Mnd1: Hop2 and Mnd1 form a heterodimer that prevents strand invasion of non-homologous chromosomes during meiosis. In *hop2* mutants, meiotic DSBs accumulate and non-homologous chromosomes synapse (LEU *et al.* 1998). These phenotypes can be partially explained by the fact that the Hop2/Mnd1 complex stimulates Dmc1 and Rad51 catalyzed D-loop formation (PETUKHOVA *et al.* 2005; PLOQUIN *et al.* 2007). However, the Hop2/Mnd1 complex localizes to chromatin independent of DSB formation and does not co-localize with DSB sites (ZIERHUT *et al.* 2004). The Hop2/Mnd1 complex therefore might have some global functions other than stimulating Dmc1 and Rad51 activity, such as facilitating chromatin accessibility (ZIERHUT *et al.* 2004).

B. Rad51 activity is down-regulated.

Besides the above proteins that assist Dmc1 activity, Rad51 is down-regulated by a meiosis-specific inhibitory protein, Hed1. Although *hed1*

mutants alone have no apparent phenotypes, deletion of *HED1* in a *dmc1* diploid allows Rad51 mediated DSB repair between homologs (TSUBOUCHI and ROEDER 2006). A similar phenotype is observed by overexpressing *RAD51* in *dmc1* diploids (TSUBOUCHI and ROEDER 2003). Hed1 interacts with Rad51 in the yeast two-hybrid assay (TSUBOUCHI and ROEDER 2006). Ectopic expression of *HED1* in vegetative growing cells causes MMS sensitivity. Hed1's inhibitory function is likely due to preventing functional interactions between Rad51 and Rad54 (PATRICK SUNG, PERSONAL COMMUNICATION).

C. Suppression of meiotic recombination between sister chromatids.

Inter-homolog bias during meiosis is created both by promoting interhomolog recombination using factors such as Dmc1, as well as suppressing recombination between sister chromatids. Three genes found to suppress meiotic sister chromatid repair are *MEK1* (*MRE4*), *HOP1* and *RED1*. Null mutants of each gene exhibit poor spore viability and are specifically defective in interhomolog recombination (HOLLINGSWORTH and BYERS 1989; ROCKMILL and ROEDER 1988; ROCKMILL and ROEDER 1991; SCHWACHA and KLECKNER 1997). Mutation of each gene in the *dmc1Δ* background allows meiotic DSB repair between sister chromatids, thereby allowing *dmc1Δ* cells to sporulate and produce inviable spores (Figure 4-1A) (BISHOP *et al.* 1999; NIU *et al.* 2005; WAN *et al.* 2004; XU *et al.* 1997). This phenotype is different from suppression of the *dmc1Δ* arrest due to increased Rad51 activity by overexpression of *RAD51* or

deletion of *HED1* which also allows *dmc1* to sporulate but produces viable spores due to DSB repair off homologs (Figure 1-4B). *HOP1*, *MEK1* and *RED1* are therefore required to create a barrier to sister chromatid repair (BSCR) during meiosis.

Hop1, Red1 and Mek1 associate with axial elements (AEs), a cytologically defined structure formed by the condensation of pairs of sister chromatids along protein cores. AEs of homologous chromosomes are then connected by insertion of a central region to form cytologically visible tripartite structures called synaptonemal complexes (SCs). *RED1* is required for AE formation (ROCKMILL and ROEDER 1988; SMITH and ROEDER 1997). In *hop1*, stretches of AEs are formed, but chromosomes fail to synapse (HOLLINGSWORTH *et al.* 1990). In *mek1* mutants, AEs form normally and regions of SC are observed in some strain backgrounds (BAILIS and ROEDER 1998; ROCKMILL and ROEDER 1991).

Hop1, Red1 and Mek1 form a protein complex *in vivo*. Hop1 and Red1 interaction has been demonstrated by both yeast two-hybrid assays and co-immunoprecipitation (co-IP) experiments, as has the Red1/Mek1 interaction (BAILIS and ROEDER 1998; DE LOS SANTOS and HOLLINGSWORTH 1999; WAN *et al.* 2004; WOLTERING *et al.* 2000). The Hop1/Red1 interaction is specifically disrupted in *red1-K348E*, which contains a point mutation in a short conserved region of Red1 (SMITH and ROEDER 2000; WOLTERING *et al.* 2000). Mek1 contains a forkhead associated (FHA) domain at its N-terminus, which is a conserved

phospho-threonine binding domain (DUROCHER *et al.* 1999) that mediates Mek1/Red1 interaction through binding to phosphorylated Red1 (WAN *et al.* 2004). Hop1 and Mek1 interaction has been demonstrated only in yeast two-hybrid assays and depends on the presence of *RED1*, suggesting that Red1 acts as a bridge between Hop1 and Mek1 (BAILIS and ROEDER 1998).

Mek1 is a serine/threonine kinase (BAILIS and ROEDER 1998; DE LOS SANTOS and HOLLINGSWORTH 1999). A point mutation in *MEK1*, *mek1-Q241G*, creates a conditional *mek1* allele, *mek1-as1*, which encodes a mutated Mek1 kinase with an enlarged ATP binding pocket whose kinase activity can be specifically inhibited by the chemicals, 1-NA-PP1 (4-amino-1-*tert*-butyl-3-(1'naphthyl)pyrazolo[3,4-*d*] pyrimidine) (WAN *et al.* 2004). In the absence of the inhibitor, *mek1-as1* complement *mek1Δ* close to wild-type level (WAN *et al.* 2004). Inactivation of Mek1-as in *dmc1Δ* diploids at a time after DSB formation allows DSBs to be repaired off the sisters, thereby producing dead spores (NIU *et al.* 2005; WAN *et al.* 2004). These results demonstrate that Mek1 kinase activity is directly involved in creation of a BSCR. Further studies have shown that Hop1, Red1 and Mek1 complex formation is necessary for wild-type levels of Mek1 kinase activity, suggesting that Mek1 acts downstream of *HOP1* and *RED1* to create the BSCR (WAN *et al.* 2004). Studies on the BSCR can be broken down into two basic questions: 1) how is Mek1 kinase activity regulated to create a BSCR in the vicinity of DSBs? and 2) what is the mechanism by which Mek1-phosphorylated

substrates create a BSCR? My thesis involved experiments designed to address both questions.

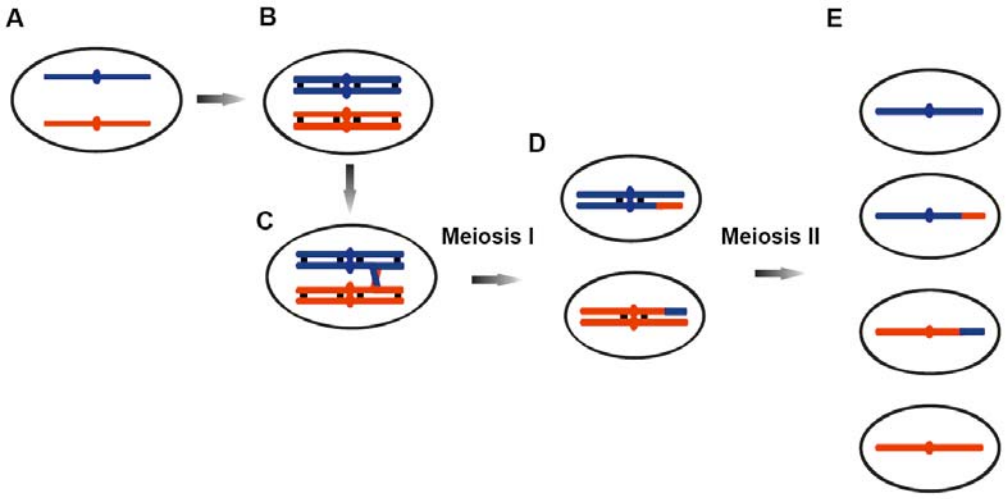

Figure 1-1: **Meiotic chromosome segregation.** A. A diploid cell before entering meiosis containing a single pair of homologous chromosomes (ovals indicate centromeres). B. After pre-meiotic DNA replication, pairs of sister chromatids are connected by sister chromatid cohesion (indicated by black squares). C. Recombination between non-sister chromatids generates crossovers. Crossovers, together with sister chromatid cohesion, physically connect the homologs. D. At MI, arm cohesion is removed allowing homologous chromosomes to segregate to opposite poles of the spindle. E. At MII, centromeric cohesion is removed allowing sister chromatids to segregate. The four meiotic products (called spores) are packaged into a sac called an ascus or a tetrad.

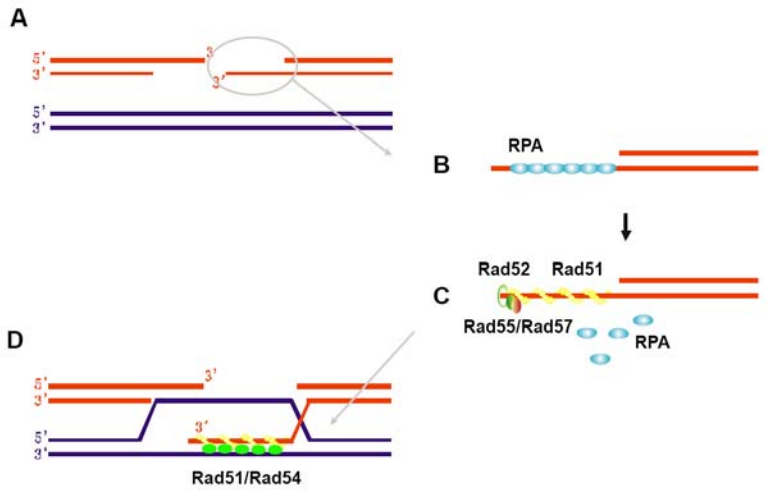

Figure 1-2: **Rad51-mediated strand invasion in mitotic recombination.** A. DSBs get resected to produce 3′ ssDNA. B. ssDNA is coated with RPA. C. Mediator proteins, Rad52, Rad55 and Rad57, promote replacement of RPA with the recombinase, Rad51, thereby enabling Rad51 nucleoprotein filament formation. D. Rad54 interacts with Rad51 to facilitate strand invasion.

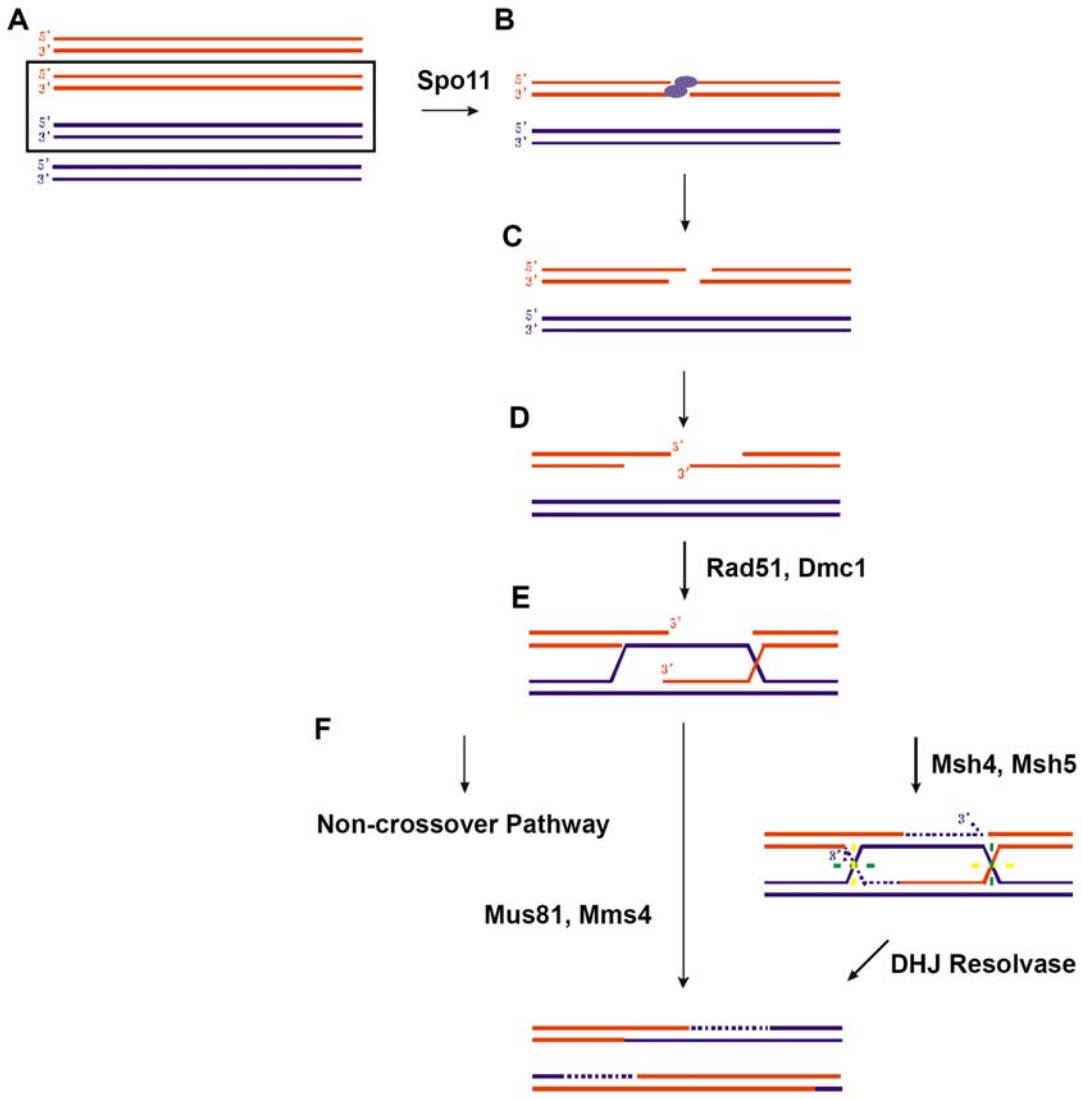

Figure 1-3: **Molecular model for meiotic recombination.** A. Pre-meiotic DNA replication of a pair of homologous chromosomes results in four chromatids. The two non-sister chromatids which are going to recombine are indicated by the black box. Each chromatid is shown as a duplex of DNA. B. DSB formation is catalyzed by Spo11 (represented as purple ovals). C. Spo11 is removed from break ends. D. DSB ends get resected to produce 3′ ssDNA. E. Rad51 and Dmc1 catalyzes strand invasion of non-sister chromatids. F. Recombination intermediates are processed into either non-crossover or crossover products. Crossover formation can result from either resolving dHJs or a Mus81/Mms4 mediated pathway.

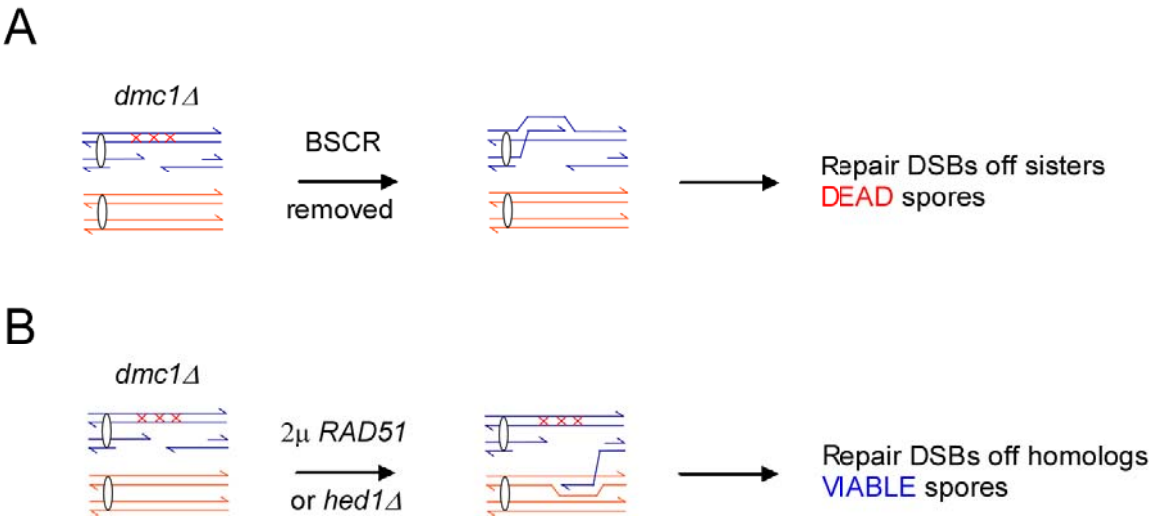

Figure 1-4: **Different phenotypic consequences due to suppression of the dmc1Δ arrest by inactivation of the BSCR or an increase of Rad51 activity.** A. Removing the BSCR allows *DMC1*-independent DSB repair occurs between sisters, which results in dead spores. B. Increasing Rad51 activity allows *DMC1*-independent DSB repair between homologs, which results in viable spores. Red X's indicate the BSCR.

CHAPTER TWO

Partner choice during meiosis is regulated by Hop1-promoted dimerization of Mek1

[The text of this chapter is taken directly from a manuscript published in Molecular Biology of the Cell 16(12): 5804-5818 and represents the work of several people, including myself (NIU *et al.* 2005).]

INTRODUCTION

In mitotically dividing cells, recombination is used to repair lesions in DNA resulting from problems in replication or exogenous DNA damage. Sister chromatids are the preferred templates for DNA repair in these cells and homologous recombination is mediated primarily by the recombinase, Rad51 (KADYK and HARTWELL 1992; SYMINGTON 2002). In contrast, recombination during meiosis is initiated by the deliberate introduction of meiosis-specific double strand breaks (DSBs). The resulting crossovers occur preferentially between non-sister chromatids and are mediated not only by Rad51 but also by the meiosis-specific recombinase, Dmc1 (BISHOP *et al.* 1992; KEENEY 2001; SCHWACHA and KLECKNER 1997). Crossovers between homologs, in combination with sister chromatid cohesion, physically connect homologous chromosomes, thereby allowing them to align properly at Metaphase I (PETRONCZKI *et al.* 2003). Failure to crossover leads to high levels of missegregation and aneuploid gametes.

Many of the molecular details of meiotic recombination have been elucidated in the budding yeast, *Saccharomyces cerevisiae* (HOLLINGSWORTH and BRILL 2004). Recombination begins by the introduction of DSBs catalyzed by the highly conserved, topoisomerase-like protein, Spo11. The 5′ ends on either side

of the break are resected to produce 3′ single stranded (ss) tails. Resection requires both the trimeric complex *MRE11/XRS2/RAD50* as well as *SAE2 (*also known as *COM1)*. After 3′ ss tails are bound by Rad51 and Dmc1, they invade non-sister chromatids to produce D-loops. DNA synthesis extends the D-loops until the displaced strands anneal to the 3′ ss tails on the other side of the breaks. Further DNA synthesis and ligation result in double Holliday junction structures (observed in physical analyses as joint molecules) that may then be resolved to create crossover chromosomes. In addition to this canonical pathway, it has recently been discovered that budding yeast has an additional minor pathway for generating crossovers, mediated by the Mus81/Mms4 structure specific endonuclease, that may not utilize double Holliday junction intermediates (de los Santos *et al*. 2003).

Relatively little is known about the mechanism by which the change in partner choice from sister chromatids in vegetative cells to non-sister chromatids in meiotic cells is accomplished. An important question is whether the interhomolog bias observed in meiosis is due to the active promotion of interhomolog recombination or because sister chromatid recombination is suppressed. Originally, the discovery of a meiosis-specific recombinase, *DMC1*, seemed to support the former idea. In the absence of *DMC1*, meiotic DSBs are resected but fail to invade the homolog and the DSBs remain unrepaired (BISHOP *et al.* 1992; HUNTER and KLECKNER 2001). These persisting DSBs trigger the

meiotic recombination checkpoint and the cells arrest in prophase I (LYDALL *et al.* 1996; XU *et al.* 1997). Therefore the difference between mitotic and meiotic partner choice could be explained by the use of a different strand transfer enzyme, with some property of Dmc1 conferring the ability to discriminate between sister and non-sister chromatids. Recent experiments, however, have indicated that Dmc1 does not itself supply specificity to the strand invasion reaction. Over-expression of *RAD51* largely suppresses the interhomolog recombination defect of *dmc1*, resulting in viable spores (TSUBOUCHI and ROEDER 2003). Therefore while *DMC1* is required for interhomolog recombination in budding yeast, its function may be simply to increase the level of recombinase, rather than to promote strand invasion specifically of non-sister chromatids. Consistent with this idea, organisms such as worms and fruit flies, which, like yeast, undergo *SPO11*-dependent meiotic recombination, contain Rad51, but no Dmc1, orthologs (VILLENEUVE and HILLERS 2001).

The fact that strand invasion occurs preferentially between non-sister chromatids, even when Rad51 is the only recombinase available, suggests that there is a barrier to sister chromatid repair (BSCR) in meiotic cells. One potential component of this barrier is *RED1*, a gene encoding a meiosis-specific component of the chromosome cores formed between sister chromatids (SMITH and ROEDER 1997; THOMPSON and ROEDER 1989). Mutation of *RED1* in a *dmc1* diploid results in the disappearance of DSBs, progression through the meiotic

divisions and the generation of dead spores (BISHOP *et al.* 1999; SCHWACHA and KLECKNER 1997; XU *et al.* 1997). That the disappearance of the breaks is due to repair, as opposed to extensive resection, was demonstrated by the finding that mutation of *spo13* suppresses the spore inviability of *red1 dmc1* diploids (BISHOP *et al.* 1999). *spo13* mutants undergo just a single meiotic division, thereby eliminating the requirement for interhomolog crossovers to produce viable spores, (MALONE and ESPOSITO 1981). Furthermore, the disappearance of the DSBs in *red1 dmc1* strains, as well as the spore viability in *red1 dmc1 spo13* diploids, is dependent upon *RAD54*, a gene required primarily for sister chromatid recombination during meiosis (ARBEL *et al.* 1999; BISHOP *et al.* 1999). *red1* mutants are pleiotropic, displaying a number of mutant phenotypes including defects in chromosome structure and synapsis, as well as DSB formation (Rockmill and Roeder, 1990; Xu *et al.*, 1997). The wide range of processes affected by *red1* has made it difficult to determine the specific function that *RED1* has in establishing interhomolog bias.

During meiosis, sister chromatids condense to form structures called axial elements (AEs). AEs of homologous chromosomes are then connected to form a tri-partite structure called the synaptonemal complex (SC) *RED1* localizes to AEs in budding yeast and is required for their formation (ROCKMILL and ROEDER 1990; SMITH and ROEDER 1997). It was therefore possible that the defect in the BSCR observed in *red1 dmc1* mutants was due to the failure to create the correct

chromosome structure. However, studies involving the meiosis-specific kinase, *MEK1*, suggest that the absence of the BSCR in *red1* cells may be best explained by a failure to localize Mek1 to chromosomes (WAN *et al.* 2004). Like *red1*, *mek1* mutants allow *dmc1* diploids to sporulate and produce inviable spores (WAN *et al.* 2004; XU *et al.* 1997). Unlike *red1*, *mek1* mutants allow AE and even some SC formation, depending upon strain background (ROCKMILL and ROEDER 1990; ROCKMILL and ROEDER 1991). A conditional allele called *mek1-as1* allows inactivation of the Mek1 kinase by addition of a chemical inhibitor to sporulating cells (WAN *et al.* 2004). Inactivation of Mek1 in a *mek1-as1 dmc1* diploid after DSB formation and cell cycle arrest results in the disappearance of DSBs and the production of inviable spores. Given that DSBs were created under wild-type conditions in the presence of Red1, this experiment shows that Mek1 kinase activity acts after *RED1* to prevent DSB repair in *dmc1* strains. Although it was proposed that the disappearance of the DSBs observed in this situation was due to sister chromatid repair, similar to what has been proposed for *red1*, this idea was not proven (WAN *et al.* 2004).

RED1 and *MEK1* are part of a genetic epistasis group that includes a third meiosis-specific gene, *HOP1* (ROCKMILL and ROEDER 1990; ROCKMILL and ROEDER 1991). Mutations in *hop1*, *red1* and *mek1* specifically reduce interhomolog recombination and produce inviable spores (HOLLINGSWORTH *et al.* 1995), suggesting that *HOP1* may play a role in the BSCR along with *RED1* and *MEK1*.

The genetic data suggesting that these proteins work in a common pathway is supported by biochemical experiments showing that Red1/Hop1 and Red1/Mek1 form complexes in meiotic cells (BAILIS and ROEDER 1998; DE LOS SANTOS and HOLLINGSWORTH 1999). Two-hybrid experiments indicate Red1 acts as a bridge to bring Hop1 and Mek1 together (BAILIS and ROEDER 1998). Determining whether *HOP1* plays a role in the BSCR has been complicated, however, because *hop1* mutants have a more severe DSB phenotype than either *red1* or *mek1* in the SK1 background where the *dmc1* arrest is most pronounced (PECINA *et al.* 2002; WOLTERING *et al.* 2000). Therefore, should *hop1Δ* suppress the *dmc1* arrest, it could be an indirect effect due to an insufficient number of DSBs to trigger the meiotic recombination checkpoint.

In this paper we present experiments to demonstrate that Mek1 kinase activity is required in *dmc1* diploids to prevent DSB repair using sister chromatids. Furthermore we describe the characterization of a novel allele of *HOP1*, *hop1-K593A*, that is mutated in a domain specifically required for the BSCR called the C domain. The discovery that the *hop1-K593A* mutant can be suppressed by versions of Mek1 containing ectopic dimerization domains suggests that the function of the C domain is to promote dimerization of Mek1 during meiosis. Finally, we show that Hop1 is phosphorylated in a DSB- and C domain-dependent manner, but is independent of *MEK1*. Based on these results, we propose that the interhomolog bias observed during meiosis is created by the

suppression of inter-sister recombination mediated by Hop1/Red1/Mek1 complexes. This suppression is most likely achieved by the phosphorylation of as yet unidentified proteins by Mek1 that prevent strand invasion. Activation of Mek1 function by dimerization may be coordinated with DSB formation via phosphorylation of the Hop1 C domain.

MATERIALS AND METHODS

Plasmids: Plasmid names, genotypes and sources can be found in Table 2-1. Plasmids for this study were constructed by standard procedures using the *E. coli* strain BSJ72 (MANIATIS *et al.* 1982). Details of plasmid constructions are available upon request. All *MEK1* fusions are expressed under the control of the *MEK1* promoter. The TAP tag was cloned from plasmid pBS1761, obtained from EUROSCARF. Mutations were introduced directly into pLT11 by site-directed mutagenesis (QuikChange kit from Stratagene). The presence of the mutations was confirmed by DNA sequencing (Research Genetics, Huntsville, AL; Center for the Analysis and Synthesis of Macromolecules at SUNY Stony Brook). For *hop1-K593A*, *hop1-K590A*, *hop1-564Δ* and *hop1-585Δ*, the entire sequence of each allele was determined to ensure that no additional mutations were created during the mutagenesis.

Yeast strains and media. Strain genotypes can be found in Table 2-2. NH246 and NH270 are derived from a cross between the slow sporulating BR and A364a genetic backgrounds (WOLTERING *et al.* 2000). All other strains are derived from SK1. Details of strain constructions are available upon request. All experiments were conducted at 30°. Liquid and solid media have been described (DE LOS SANTOS and HOLLINGSWORTH 1999; VERSHON *et al.* 1992). The inhibitor of Mek1-as1, 1-NA-PP1, 4-amino-1-*tert*-butyl-3-(1'naphthyl)pyrazolo [3,4-*d*]pyrimidine, was diluted from a 10 mM stock purchased from Cellular Genomics, Inc. (New Haven, CT).

Antibodies, immunoprecipitations and Western Blots. The G/R antibodies, as well as the IP and Western blot protocols, are described in Wan et al. (2004). The Hop1 antibodies and phosphatase experiment protocol are described in de los Santos and Hollingsworth (1999). To detect phosphorylated Hop1 by SDS-polyacrylamide gel electrophoresis, proteins were fractionated on 8% gels (29:1 acrylamide: bis-acrylamide) 20 cM in length at 15 mAmp for 15 hrs.

Timecourses. Liquid sporulation conditions used were 2% potassium acetate at 30°. Sporulation was monitored by phase contrast microscopy of at least 200 cells per strain. DSB and cytological analyses were as described in Woltering *et al*. (2000) and (LOIDL *et al.* 1998). For experiments in which strains were transformed with plasmids, the cells were grown to stationary phase in SD-ura medium instead of rich medium prior to dilution into YPA. Quantitation of

DSB fragments was performed using a Molecular Dynamics PhosphorImager and Image Quant 1.11 software. The formula used for quantitation was ($DSB_{t=x} - DSB_{t=0}$)/($DSB_{t=x} + P_{t=x}$) X 100 where P represents the parental fragment.

RESULTS

Inhibition of Mek1 kinase activity after DSB formation allows DSB repair and produces viable spores in a *dmc1 spo13* diploid. Previously we showed that inhibition of Mek1 kinase activity after DSB formation in a *dmc1* mutant suppressed the arrest triggered by the meiotic recombination checkpoint, caused DSBs to disappear and produced inviable spores (WAN *et al.* 2004). This result was interpreted to mean that Mek1 kinase activity was necessary to prevent DSB repair using sister chromatids but this experiment did not rule out alternative explanations. For example, degradation of the ends of the DSBs would also result in the loss of detectable DSBs and dead spores. In these two scenarios, however, the spores are dead for different reasons: the lethality that occurs in spores that have undergone DSB repair using sister chromatids is a result of non-disjunction occurring because homologs are not physically connected prior to MI. In contrast, the spore death arising from hyper-resection is due to the irreversible loss of genetic information. These two possibilities can be distinguished by assaying spore viability in the absence of *SPO13*. Spore

inviability arising due to a lack of interhomolog recombination should be suppressed by the single division meiosis conferred by *spo13* (MALONE and ESPOSITO 1981). If, however, spore death is due to DNA degradation, the spores will be dead even in a *spo13* background.

Mek1 kinase activity can be specifically inhibited by the addition of 1-NA-PP1 to strains containing the *mek1-as1* mutant [note that the mutation in *mek1-as1* is Q241G and not Q247G as originally reported in Wan et al. (2004)]. A *mek1-as1 dmc1 spo13* diploid was transferred to sporulation medium, a final concentration of 1 μM 1-NA-PP1 was added to 1 ml aliquots at 0, 2, 4 and 6 hours, and the cells returned to the 30° incubator. After a total of 24 hrs, sporulation was monitored by phase contrast light microscopy. In the absence of inhibitor, the diploid behaved like a *dmc1* mutant with only 4.5% of the cells forming dyads, all of which were immature. In contrast, all of the timepoints to which inhibitor was added exhibited greater than 35% sporulation, similar or better than the 36% sporulation observed for *spo13* alone (Table 2-3). In addition, at the four hour timepoint, 1 μM 1-NA-PP1 was added to one half of the sporulating culture and the cells were returned to the 30° shaker. Cells were then fixed at two hour intervals for analysis of DSBs at the naturally occurring *YCR048w* and *HIS2* DSB hotspots (BULLARD *et al.* 1996; WU and LICHTEN 1994). In the absence of inhibitor, DSBs failed to be repaired and became hyper-resected with increasing time in Spo medium. Within two hours after the addition of I nhibitor, however,

the DSBs were no longer detectable (Figure 2-1A and B; data not shown).

The behavior of the DSBs after addition of inhibitor in the *mek1-as1 dmc1 spo13* diploid is highly similar to what was previously observed for the *mek1-as1 dmc1 SPO13* strain (Wan et al. 2004). A major difference in the two experiments is the spore viability. Whereas only 3% of the spores were viable in the *SPO13* experiment, 46.7% of the spores were viable in the *mek1-as1 dmc1 spo13* mutant (Table 2-3) (Wan et al. 2004). The fact that 32.6% of the dyads contained two viable spores provides strong support for the argument that DSBs are disappearing as a result of repair rather than degradation.

***mek1-as1 dmc1 spo13* mutants are reduced for inter-homolog recombination and increased for inter-sister recombination.** If Mek1 kinase activity is acting to prevent sister chromatid repair in the *mek1-as1 dmc1 spo13* diploid, then inactivation of Mek1 should result in dyads which exhibit reduced levels of interhomolog recombination and increased levels of inter-sister recombination. To monitor both interhomolog and intrachromosomal recombination, a sister chromatid recombination reporter, SCR::*URA3*, was introduced between *LEU2* and *HIS4* on one of the chromosome III homologs (Figure 2-1C) (KADYK and HARTWELL 1992). Interhomolog recombination between *URA3* and *MAT* can be detected by a change in the coupling relationship between the two genes, whereas intersister events can be detected by the generation of a full-length *ADE3* gene (see below).

In *spo13* meioses, chromosomes may segregate either reductionally (homologs segregate to opposite poles), equationally (sisters segregate to opposite poles) or aberrantly (three chromatids go to one pole and one to the other pole) (HUGERAT and SIMCHEN 1993; KLAPHOLZ and ESPOSITO 1980). Defects in interhomolog recombination result in improved spore viability and dyads that display predominantly equational segregation (HOLLINGSWORTH and BYERS 1989; WAGSTAFF *et al.* 1982). The dyads formed by the *mek1-as1 dmc1 spo13* diploid in the presence of inhibitor displayed both of these properties. The spore viability of the *spo13* strain was only 25.5%, while the *mek1-as1 dmc1 spo13* spore viabilities ranged from 38.5 to 61.2%, depending upon when the inhibitor was added (Table 2-3). The highest viability was observed when inhibitor was added at 0 hrs, suggesting that there is a deleterious effect in allowing DSBs to form in the presence of Mek1 kinase activity when *DMC1* is absent. As for segregation, 72.7% of the *spo13* dyads could be unambiguously defined as equational segregants for chromosome III, increasing to 98.4% for *mek1-as1 dmc1 spo13* plus inhibitor. [(To discriminate between reductional and equational segregants in recombinant dyads, a centromere linked marker is necessary but was not available in this strain. Because *MAT* and *URA3* are on different arms of chromosome III, non-recombinant dyads produce distinctive patterns for reductional and equational segregation (Table 2-3)]. These results indirectly support the hypothesis that interhomolog recombination is reduced in *mek1-as1*

dmc1 spo13 diploids lacking Mek1 kinase activity.

To directly examine interhomolog recombination, changes in the coupling relationship between *URA3* and *MAT* were examined. Because the poor spore viability of the *spo13* diploid resulted in a low yield of two viable spore asci, the analysis used spores from both one and two viable spore dyads (Table 2-3). Out of 499 dyads from the *mek1-as1 dmc1 spo13* strain to which inhibitor was added, only 4 (0.8%) were recombinant for *MAT* and *URA3*. In contrast, 35 of the 236 *spo13* dyads were recombinant (14.8%). Therefore, interhomolog recombination is signficantly reduced in the absence of *DMC1* and Mek1 kinase activity (χ^2 analysis; $p < 0.0001$).

Recombination between truncated *ade3* alleles in the *SCR::URA3* reporter was used to determine whether sister chromatid recombination was elevated under these conditions (Figure 2-1C) (KADYK and HARTWELL 1992). To prevent ectopic interactions, *ADE3* was deleted from its normal chromosomal position. *ADE3* is required for the biosynthesis of histidine and the diploid is therefore His^-. Two types of intersister events are detectable by the formation of His^+ recombinants: unequal reciprocal recombination and gene conversion (KADYK and HARTWELL 1992). The frequency of intersister recombination events for the *mek1-as1 dmc1 spo13* diploid was 2.2% (11/499) (Table 2-3). In two viable spore dyads it is possible to discriminate between gene conversion and reciprocal exchange events. All of the His^+ two viable spore dyads resulted from gene

conversion—no reciprocal recombinants were detected. In the *spo13* diploid, no His^+ spore colonies were detected out of 236 *spo13* dyads, although 5 would be expected if the frequency on intersister recombination were the same as *mek1-as1 dmc1 spo13* (Table 2-3). Although the sample size is small, these data suggest there may be a bias towards intersister gene conversion events in the absence of *DMC1* and Mek1 kinase activity.

The *DMC1*-independent DSB repair observed in the absence of *MEK1* requires *RAD54*. To further test the hypothesis that sister chromatid recombination is responsible for DSB repair in *mek1Δ dmc1Δ*, the dependence of this repair on *RAD54* was analyzed. The Rad54 protein stimulates Rad51 activity *in vitro* and is involved primarily in intersister recombination during meiosis (ARBEL *et al.* 1999; BISHOP *et al.* 1999; PETUKHOVA *et al.* 1999). Therefore, if the disappearance of DSBs in *mek1Δ dmc1Δ* strains is due to recombination between sister chromatids, this repair should not occur in a *rad54Δ dmc1Δ mek1Δ* diploid. To compare isogenic strains, a *rad54Δ mek1Δ dmc1Δ* diploid was transformed with *RAD54*, *MEK1*, *DMC1* or vector to generate *mek1Δ dmc1Δ*, *rad54Δ dmc1Δ*, *mek1Δ rad54Δ* and *rad54Δ mek1Δ dmc1Δ* diploids, respectively. The wild-type strain was also included as a control. DSBs at the naturally occurring *YCR048w* hotspot were monitored by Southern blot analysis with a radioactively labeled probe to detect 10.5 kb B*gl*II genomic fragment where DSB formation produces shorter fragments that migrate faster on an agarose gel (WU

and LICHTEN 1994). DSBs appeared in the wild-type diploid by three hours and the bulk of the breaks were gone by 9 hours (Figure 2-2). The kinetics of DSB appearance and disappearance were similar in the *mek1Δ rad54Δ* strain, although there appeared to be significant hyper-resection as indicated by the long smear in the DSB region of the gel (Figure 2-2A). This repair is presumably being mediated by Dmc1, indicating that *MEK1* is not required to promote Dmc1 function. DSBs persisted in the *rad54Δ dmc1Δ* diploid and became hyper-resected (Figure 2-2). Deletion of *RAD54* from the *mek1Δ dmc1Δ* diploid blocked DSB repair, with the DSBs exhibiting even more hyper-resection than the *rad54Δ dmc1Δ* strain (Figure 2-2). There was a delay in the onset of break formation in the triple mutant, raising the possibility that repair might also be delayed. Extending the timecourse to 15 hours gave the identical result, however, making this possibility unlikely (Figure 2-2B). *RAD54* is therefore necessary for *DMC1*-independent repair in the absence of *MEK1*.

Suppression of *dmc1Δ* by over-expression of *RAD51* is dependent upon Mek1 kinase activity. Over-expression of *RAD51* largely suppresses the interhomolog recombination and sporulation defects of *dmc1Δ* during meiosis (TSUBOUCHI and ROEDER 2003). If the ability of Rad51 to promote meiotic inter-homolog recombination is due to a BSCR, then *RAD51* suppression of *dmc1Δ* should be dependent upon Mek1 kinase activity. This hypothesis was tested by transforming a *dmc1Δ mek1-as1* diploid with either vector, *DMC1* or a

plasmid over-expressing *RAD51* and testing the transformants for a variety of meiotic phenotypes in the presence or absence of the 1-NA-PP1 inhibitor. To eliminate any possible negative effects arising from the over-expression of *RAD51* in vegetative cells, *RAD51* was expressed under the control of the meiosis-specific *HOP1* promoter (HOLLINGSWORTH *et al.* 1990).

Meiotic timecourses were performed on *mek1-as1*, *mek1-as1 dmc1Δ*, and *mek1-as1 dmc1Δ*/2μ *RAD51* cultures. The culture over-expressing *RAD51* was split immediately after transfer to sporulation medium and a final concentration of 1 μM 1-NA-PP1 was added to half. The cells were then incubated at 30° for 24 hrs. As expected in the absence of inhibitor, the *mek1-as1* diploid sporulated well (96.0 ± 0.9% asci) and produced viable spores (90.0 ± 5.2%, 72 asci dissected), in contrast to the *mek1-as1 dmc1Δ* strain which failed to sporulate. Consistent with the results of Tsubouchi and Roeder (2003), over-expression of *RAD51* partially rescued the sporulation defect of *mek1-as1 dmc1Δ* (36.6 ± 5.1% asci). The high spore viability of the tetrads produced in the absence of inhibitor in this strain (70.0 ± 13.2% viable spores, 102 asci dissected) indicates that interhomolog recombination is occurring. Measurements of plasmid stability at the time of transfer to Spo medium showed that approximately 70% of the *mek1-as1 dmc1Δ* cells contained the *RAD51* plasmid. Therefore, the observed suppression of sporulation underestimates the amount of possible suppression. Addition of inhibitor to the *RAD51* over-expressing strain resulted in even higher levels of

sporulation (72.6 ± 10.6% asci) but inviable spores (0.8 ± 1.0%, 101 asci dissected).

This experiment provides a unique opportunity to compare the kinetics of meiotic progression in a culture in which Rad51 is being used to repair DSBs either using homologs or sister chromatids as templates. When interhomolog recombination utilizes only Rad51, the onset of MI is delayed, supporting the idea that Dmc1 facilitates this process (Figure 2-3). In contrast, inhibition of *mek1-as1* in the *RAD51* over-expressing *dmc1* diploid allowed even more rapid meiotic progession than wild type (Figure 2-3). Comparison of DSBs in the *RAD51* over-expression strain showed that in the presence of inhibitor, DSBs at the *YCR048w* hotspot were repaired by six hours, whereas in the absence of inhibitor the DSBs did not disappear until 12 hours (some of these persisting DSBs are most likely due to those cells that lost the *RAD51* plasmid prior to the initiation of meiosis). Similar results were obtained looking at the *ARG4* DSB hotspot (data not shown). These results demonstrate that removal of the BSCR in *dmc1* mutants results in a rapid, efficient repair of DSBs. Furthermore the ability of *RAD51* to mediate interhomolog recombination when over-expressed in a *dmc1* mutant is dependent upon the BSCR being present.

Mutagenesis of the C-terminal tail of Hop1 identifies two lysines, K590A and K593A, which are important for *HOP1* function. Intragenic complementation studies using various mutant alleles of *HOP1* indicated that the 605 amino acid protein contains at least two discrete functional domains

(FRIEDMAN *et al.* 1994). One domain consists of the last 20 amino acids of the protein (the C domain), while the other domain is comprised of the rest of the Hop1 protein (the N domain). One of the alleles used by FRIEDMAN *et al.* (1994), *hop1-R6Δ*, resulted not only in the deletion of the last 41 amino acids of Hop1, but also the addition of 18 amino acids as a result of translation of downstream vector sequences. Therefore it was not clear whether the spore inviability observed for *hop1-R6Δ* was due to the loss of the Hop1 C domain or to the insertion of extra amino acids at the end of the protein. To address this question, stop codons were introduced into *HOP1* immediately after codon 564 (*hop1-564Δ*) or 585 (*hop1-585Δ*), thereby truncating Hop1 by 41 and 20 amino acids, respectively. Diploids carrying either *hop1-564Δ* or *hop1-585Δ* produced 0 viable spores out of 22 tetrads dissected, indicating both mutations create null alleles with regard to spore viability. The truncations do not appear to destabilize the mutant proteins, however, as their protein levels are similar to wild-type Hop1 (measured 3 hours after transfer to sporulation medium) (Figure 2-4A). The conclusion therefore, is that the last 20 amino acids of Hop1 are essential for its function.

Assuming that the C domain of Hop1 represents a discrete functional module, it should be possible to isolate point mutations that abolish the function of this domain without affecting activities that are mediated by the rest of the protein. Null alleles of *HOP1* exhibit a number of mutant phenotypes,

including low spore viability, reduced levels of interhomolog recombination and DSBs, as well as a defect in chromosome synapsis (HOLLINGSWORTH and BYERS 1989; WAN *et al.* 2004; WOLTERING *et al.* 2000). In addition, Hop1 is a DNA binding protein that physically interacts both with itself and with Red1 (DE LOS SANTOS and HOLLINGSWORTH 1999; KIRONMAI *et al.* 1998). To generate separation of function alleles, charged residues located between amino acids 567 and 605 were mutated to alanine and assayed for defects in spore viability. Out of 15 amino acids that were mutated, two resulted in a reduction in spore viability. The most severe mutant, *hop1-K593A*, produced <1% viable spores in the SK1 background (36 asci dissected), equivalent to a deletion of *HOP1*. In addition, changing K590 to alanine or methionine reduced spore viability to 42% and 59%, respectively (*hop1-K590A*, 49 asci; *hop1-D584A K590M*, 49 asci). The amino acid substitutions present in *hop1-K590A* and *hop1-K593A* do not appear to decrease protein stability (Figure 2-4A).

***hop1-K593A* mutants exhibit increased levels of crossovers and DSBs compared to a null allele of *HOP1*.** *hop1Δ* and *red1Δ* mutants reduce, but do not eliminate, meiotic recombination (HOLLINGSWORTH and BYERS 1989; MAO-DRAAYER *et al.* 1996; ROCKMILL and ROEDER 1990). *hop1Δ* displays a more severe recombination phenotype than *red1Δ*, with *hop1Δ red1Δ* resembling *hop1Δ* alone, suggesting that *HOP1* has a function in recombination independent of *RED1* (ROCKMILL and ROEDER 1990). To determine whether the C-terminus is

required for this recombination function, the effect of *hop1-K593A* on interhomolog crossing over was measured in *spo13* diploids heterozygous for markers on two different chromosomes. A *hop1Δ* mutation was used as the null control. The *hop1Δ* diploid exhibited a mean 60-fold reduction in crossing over measured in four intervals. In contrast, *hop1-K593A* decreased crossing over on average only 11-fold (Table 2-4). This phenotype is highly similar to that observed for *hop1-R6Δ*, supporting the idea that the K593A mutation abolishes the function of the C domain. Both *hop1-K593A* and *hop1-R6Δ* are phenotypically similar to an isogenic *red1Δ* diploid, which also reduced crossing over on average 11-fold (Table 2-4). These results argue that *HOP1* contains a recombination function that is partially intact in the *hop1-K593A* mutant .

hop1Δ and *red1Δ* mutants exhibit decreased steady state levels of DSBs (MAO-DRAAYER *et al.* 1996; WOLTERING *et al.* 2000; XU *et al.* 1997). In the SK1 background, a fast sporulating strain that is frequenctly used to study meiosis, *red1Δ* mutants exhibit a higher frequency of DSBs compared to *hop1Δ*, even when resection of the ends is prevented by mutation of *SAE2*/*COM1*, a gene that is required for removing Spo11 from DSB ends (Figure 2-5; (PECINA *et al.* 2002; WOLTERING *et al.* 2000). *hop1Δ* is epistatic to *red1Δ* with regard to DSBs, as a *red1Δ hop1Δ sae2Δ* diploid produces a level of DSBs equivalent to *hop1Δ sae2Δ* (data not shown). The amount of DSBs in the *hop1-K593A sae2Δ* diploid resembled that of *red1Δ sae2Δ*, representing a six-fold increase over the *hop1Δ*

sae2Δ strain (Figure 2-5). Similar results were obtained in the *SAE2* strains, although the levels of DSBs in these strains were lower than those in the *sae2Δ* diploids, presumably because DSBs in the *SAE2* diploids are repaired and therefore do not accumulate (Figure 2-5). These results argue that the N domain either promotes initiation of DSBs or prevents DSB ends from being degraded.

The Hop1-K593A protein localizes to chromosomes but *hop1-K593A* mutants are defective in chromosome synapsis. Null mutants of *HOP1* result in the formation of AEs but no SCs (HOLLINGSWORTH *et al.* 1990; LOIDL *et al.* 1994). Electron microscopic analysis of spread chromosomes from *hop1-K593A* revealed a similar phenotype (Figure 2-6). The synapsis defect was also manifested by the failure of Zip1, a component of meiotic chromosomes frequently used as an indicator of synapsis (SYM *et al.* 1993; SYM and ROEDER 1995), to localize along the lengths of chromosomes from both *hop1-K593A* and *hop1Δ* diploids. Localization of the Hop1-K593A protein to unsynapsed chromosomes was unaffected, however, indicating that while the C domain is necessary for synapsis, it is not required for Hop1 to interact with chromosomes (Figure 2-6).

The C domain is not required for interaction with Red1 or Hop1. The fact that over-expression of *RED1* specifically suppresses a mutation at codon 595 in the *HOP1* C domain had suggested that Red1 might physically interact with the Hop1 C-terminus (HOLLINGSWORTH and JOHNSON 1993). This idea was tested by examining the ability of Red1 to co-immunoprecipitate (IP) various

Hop1 tail mutants. For these experiments a polyclonal antibody generated against a fragment of the Red1 protein was used (WAN *et al.* 2004). Co-IP of Red1 with Hop1 is readily detectable using these antibodies (Figure 2-4B). Soluble extracts from isogenic diploids containing various alleles of *HOP1* were used to precipitate either Hop1 or Red1 by addition of the appropriate antibody. After the IPs were fractionated by SDS-PAGE, the filters were probed with α-Hop1 antibodies. As expected, no Hop1 was observed in the strains deleted for *HOP1* (Figure 2-4A). Hop1, Hop1-K590A, Hop1-K593A, Hop1-564, and Hop1-585 all co-IPed with Red1 (Figure 4A). The C-terminus of Hop1 is therefore dispensable for Red1 binding.

Purified Hop1 protein exists as a dimer in solution (KIRONMAI *et al.* 1998). To test whether the C domain affects Hop1 dimerization, Hop1 and Hop1-585 were purified after expression in *E. coli* and analyzed by gel filtration analysis under non-denaturing conditions. Both proteins exhibited the same elution profile, indicating that Hop1 can dimerize in the absence of the C domain (H. Niu and N. M. Hollingsworth, unpublished results). These results are consistent with genetic data showing that mutations in the C domain can intragenically complement mutations in the N domain (FRIEDMAN *et al.* 1994).

C domain mutants in *HOP1* can be bypassed by ectopic dimerization of Mek1. Given that the Hop1 C domain functions downstream of DSBs as well as Red1 and Hop1 binding, we wanted to test whether the C-terminal tail of Hop1

is needed for Mek1 activation. Our standard Mek1 kinase assay uses Gst-Mek1 partially purified from meiotic extracts and monitors Mek1 autophosphorylation (DE LOS SANTOS and HOLLINGSWORTH 1999). A *hop1-K593A GST-MEK1* diploid was therefore constructed (in these experiments all of the *HOP1* and *MEK1* alleles are integrated into the chromosome in single copy, unless otherwise stated). Given that a *hop1-K593A MEK1* diploid produces inviable spores, the finding that *hop1-K593A GST-MEK1* produces nearly the same high level of viable spores as an isogenic *HOP1 GST-MEK1* diploid was unexpected (Table 2-5). Suppression of *hop1-K593A* requires Mek1 kinase activity, as a catalytically inactive mutant, *GST-mek1-K199R*, fails to suppress (Table 2-5). Zip1 staining demonstrated that *GST-MEK1* also suppresses the synapsis defect of *hop1-K593A* (data not shown). These results suggest that the presence of GST in the Mek1 protein is sufficient to bypass the requirement for the Hop1 C domain during meiosis.

It has previously been shown that GST dimerizes in solution (LIM *et al.* 1994; VARGO *et al.* 2004). This observation raised the possibility that the function of the Hop1 C domain is to promote dimerization of Mek1. In this case, the presence of a dimerization domain such as GST in Mek1 could bypass the requirement for the Hop1 C domain by providing an alternative means for dimerization. Two experiments were performed to test this hypothesis. In the first experiment, alternative N-terminal fusions to *MEK1* were assayed for their

ability to complement the spore inviability of *mek1Δ* in a *HOP1* diploid as well as for their ability to suppress *hop1-K593A*. Similar to GST, the lexA protein has been shown to form dimers in solution (MOHANA-BORGES *et al.* 2000). In contrast, the TAP tag contains protein A sequences as well as a calmodulin binding domain, neither of which is known to dimerize (DE *et al.* 1997; PUIG *et al.* 2001). The *TAP-MEK1* and *lexA-MEK1* fusions were transformed into *mek1Δ HOP1* and *mek1Δ hop1-K593A* diploids and assayed for spore viability. In single copy, both *lexA-MEK1* and *TAP-MEK1* complemented well, producing >85.0% viable spores (Table 2-5). *TAP-MEK1* failed to improve the spore viability of *hop1-K593A*, but *lexA-MEK1* conferred partial suppression, producing 23.3% viable spores (Table 2-5). Over-expression of *lexA-MEK1* exhibited better suppression of *hop1-K593A* than single copy *lexA-MEK1*, producing 46.5% viable spores (Table 5), suggesting that the partial suppression exhibited by *lexA-MEK1* may be due to inefficient dimerization within the cell.

The second experiment to test the dimerization hypothesis was to introduce amino acid substitutions into GST that are likely to disrupt dimerization. Using the crystal structure of dimerized GST as a guide for mutagenesis (LIM *et al.* 1994; VARGO *et al.* 2004), proline was substituted for an arginine at position 72 and an arginine was substituted for an aspartic acid at position 76 to disrupt hydrophobic and hydrophilic interactions required for dimerization (*gst-RD-MEK1*). *gst-RD-MEK1* complemented well in the *mek1Δ*

HOP1 diploid, indicating that the *MEK1* in this fusion is functional (Table 2-5). Suppression of the spore viability defect of *hop1-K593A* was greatly reduced in the *gst-RD-MEK1* background, however, dropping from 87.9% for *GST-MEK1 hop1-K593A* to 6.7% (Table 2-5). Furthermore, Zip1 staining revealed that chromosome synapsis was reduced in the *hop1-K593A gst-RD-MEK1* strain, although some nuclei showed partial SC formation indicating that the phenotype was somewhat better than *hop1-K593A* alone (data not shown). Attempts to confirm Mek1 dimerization by co-immunoprecipitation of differentially tagged Mek1 proteins have thus far been unsuccessful. Given the strong genetic evidence for dimerization, this negative result seems likely to be due to technical issues. One possibility is that only a fraction of Mek1 is dimerized during meiosis. If this fraction is small relative to the total amount of Mek1 protein, then detecting the interaction by biochemical methods may be difficult.

GST-MEK1 not only suppresses the K593A point mutant in the *HOP1* C-domain, it also partially suppresses a version of Hop1 in which the tail is deleted (*hop1-585Δ*) (Table 2-4). This result argues that the primary role of the Hop1 C domain is to actively promote dimerization of Mek1.

Dimerization of Mek1 is necessary for preventing *DMC1*-independent repair of meiotic DSBs. We infer that the spore inviability of *hop1-K593A* results from missegregation of chromosomes at Meiosis I due to a failure to prevent recombination between sister chromatids. If true, then the absence of

the BSCR in *hop1-K593A* should allow DSBs in *dmc1Δ* diploids to be repaired and *dmc1Δ hop1-K593A* diploids should sporulate. A *hop1Δ dmc1Δ* diploid was constructed and various alleles of *HOP1* and *MEK1* introduced by transformation. Addition of both *HOP1* and *DMC1* creates a wild-type diploid that sporulates well and exhibits high spore viability (Table 2-6). In the *HOP1 dmc1Δ* diploid, sporulation was reduced to <0.2% as previously reported (BISHOP *et al.* 1992). Deletion of *HOP1* in the *dmc1Δ* background allowed the cells to sporulate, consistent with a role for *HOP1* in the BSCR. The *hop1-K593A dmc1Δ* diploid also sporulated well and produced dead spores, indicating that the Hop1 C domain is required for preventing *DMC1*-independent repair (Table 2-6). The possibility that *hop1-K593A* does not generate sufficient DSBs to trigger the meiotic recombination checkpoint is ruled out by the fact that *GST-MEK1*, while having no effect on sporulation in the *hop1Δ dmc1Δ* strain, restores the meiotic arrest of the *hop1-K593A dmc1Δ* strain (Table 2-6). As with spore viability, the ability of *GST-MEK1* to restore the arrest to the *hop1-K593A dmc1Δ* diploid requires Mek1 kinase activity (Table 2-6).

Hop1 is a DSB-dependent phosphoprotein. Because of the genetic interactions between the Mek1 kinase and Hop1, we tested to see whether Hop1 is a phosphoprotein. Our previous work had detected only a single band on protein gels for Hop1 (e. g., Figure 2-4). We found, however, that running the gels for a much longer period of time enabled the detection of slower migrating

species (Figure 2-7A). The slower migrating forms are eliminated by treatment of IPed Hop1 with λ- protein phosphatase, demonstrating that Hop1 is a phosphoprotein. The absence of *MEK1* did not affect the Hop1 mobility shift, indicating that Mek1 is unlikely to be the kinase that phosphorylates Hop1 (Figure 2-7A). Hop1-585, which is deleted for the Hop1 C doman, exhibits only a single, phosphatase-insensitive form, indicating either that the C-domain is phosphorylated directly or that its presence is required for phosphorylation elsewhere on Hop1 (Figure 2-7A).

To test whether Hop1 phosphorylation is regulated by DSBs, the gel mobility of Hop1 IPed from a *rec104* diploid was examined. *REC104* is one of several meiosis-specific genes required for generating meiotic DSBs (PECINA *et al.* 2002). Whereas the phosphorylated form of Hop1 was present at both 5 and 7 hrs after the induction of meiosis, the bulk of the Hop1 remained unphosphorylated in the *rec104* diploid at both timepoints (Figure 2-7B). Similar results have been obtained with *spo11* mutants (data not shown). Therefore the majority of phosphorylated Hop1 protein present in meiotic cells is dependent upon the formation of DSBs.

DISCUSSION

Previously we proposed that the *DMC1*-independent repair observed in the absence of Mek1 kinase activity utilized sister chromatids, based on the assumption that *MEK1* behaves analogously to *RED1* in this process (Wan et al., 2004). Several pieces of evidence demonstrate that this assumption is correct. First, the spore lethality observed in *mek1-as1 dmc1* is partially suppressed by eliminating the need for interhomolog crossovers for proper segregation using *spo13*. Second, the viable spores formed in *mek1-as1 dmc1 spo13* diploids are decreased for interhomolog recombination and increased for intersister recombination compared to wild type. Third, the DSB repair observed in *mek1Δ dmc1Δ* diploids is dependent upon *RAD54*, a gene required primarily for sister chromatid recombination in meiosis. Finally, Mek1 kinase activity is necessary for the production of viable spores in a *dmc1* diploid over-expressing *RAD51*. Given that in mitotic cells the preferred substrate of Rad51 is the sister chromatid, this observation supports the idea that over-expression of *RAD51* rescues the interhomolog recombination defect of *dmc1* because of a *MEK1*-dependent BSCR.

Our results indicate that meiotic interhomolog bias results from the suppression of intersister recombination created by phosphorylation of target proteins by Mek1. This idea is in contrast to a previous proposal that meiotic interhomolog bias is an active process in which a subset of *RED1*-dependent DSBs become destined for interhomolog recombination (SCHWACHA and KLECKNER 1997). The basis for this idea was the observation that DSBs are

reduced in a *red1* mutant and that the frequency of joint molecules between sister chromatids is not increased, as would be predicted if sister chromatid recombination is suppressed by *RED1* (SCHWACHA and KLECKNER 1997). Consistent with the latter finding, no increase in meiotic unequal sister chromatid exchange was observed for *red1* mutant using a genetic assay (HOLLINGSWORTH *et al.* 1995). However, the interpretation of these experiments is complicated by the pleiotropic phenotypes of *red1*, as well as by the fact that it assumes that sister chromatid recombination utilizes primarily joint molecule intermediates. Our experiments with the chemically inhibitable *mek1-as1* mutant avoid these complications because DSBs can be allowed to form under wild-type conditions (i.e. the presence of Red1 and Mek1 kinase activity). The failure to observe an increase in intersister recombination in *red1* and *mek1* diploids may be because the physical and genetic assays used by Schwacha and Kleckner (1997) and Hollingsworth et al. (1995) measured only crossing over. In fact, an increase in intersister recombination by *red1* and *mek1* was observed by Thompson and Stahl (1999) using a genetic assay that produced a positive signal either by exchange or gene conversion, although they did not discriminate between the two. Thompson and Stahl (1999) proposed that one explanation for the difference between their results and those of Schwacha and Kleckner (1997) could be because sister chromatid repair occurring in *mek1* and *red1* diploids utilizes a pathway that does not generate joint molecules. Our finding that

intersister gene conversion events are specifically increased in the *mek1-as1 dmc1 spo13* dyads supports the idea that DSB repair in this diploid is occurring by a non-crossover recombination pathway such as synthesis-dependent strand annealing (PAQUES and HABER 1999).

The critical step in determining partner choice is at the time of strand invasion. A BSCR is therefore only necessary after a DSB has been generated on one of the two chromatids to ensure that invasion of the homolog occurs. How might the BSCR be regulated so that it is established after DSB formation? This problem could be solved by activating Mek1 function in a DSB-dependent fashion. Our work indicates that Hop1 may be the bridge that connects the creation of a DSB on the DNA with the activation of Mek1 function.

Previous work has indicated that Mek1 must be in a complex with Hop1 and Red1 for the kinase to become activated (Wan et al. 2004). Mek1 binds to phosphorylated Red1 via a conserved protein-protein interaction module in its N-terminus called the FHA domain (Wan et al. 2004). Purified Hop1 exists as a dimer in solution and binds to DNA *in vitro* (KIRONMAI *et al.* 1998). Given that *hop1Δ* has more severe recombination and DSB phenotypes than *red1Δ*, we propose that Hop1 dimers bind directly to the DNA in chromosomes, although this disagrees with cytological studies that indicate that *RED1* is required for Hop1 localization to chromosomes (SMITH and ROEDER 1997). Red1 acts as a bridge between Hop1 and Mek1 in two-hybrid experiments and Hop1 and Red1

are bound to chromosomes in the absence of DSBs (BAILIS and ROEDER 1998; SMITH and ROEDER 1997). These results lead us to propose that inactive complexes of Hop1/Red1/Mek1 are assembled onto DNA prior to DSB formation (Figure 2-8).

Inactivation of the *HOP1* C domain by the point mutation, *hop1-K593A*, creates a protein that is still able to bind Red1, localize to chromosomes and produce higher levels of detectable DSBs than the *hop1Δ*, presumably because the mutant protein is still able to bind DNA. *hop1-K593A* mutants exhibit defects in spore viability and synapsis and allow *dmc1* mutants to sporulate, indicating that the Hop1 C domain has a role in creating the BSCR. This role appears to be enabling Mek1 to dimerize. The need for the C domain can be completely bypassed by providing Mek1 with an alternative means to dimerize such as Gst. Changes in amino acids in Gst-Mek1 that are predicted to disrupt Gst dimerization abolish suppression of *hop1-K593A*, further supporting the idea that the function of the C domain is to mediate Mek1 dimerization.

What role does Mek1 dimerization play in creating the BSCR? One possibility is that dimerization allows two Mek1 proteins to phosphorylate each other at threonine 327, a conserved residue in the activation loop whose phosphorylation is required for kinase activation (WAN *et al.* 2004) (Figure 2-8). In this model, the absence of a functional C domain prevents kinase activation in the *hop1-K593A* mutant, thereby preventing phosphorylation of Mek1 target

proteins to create the BSCR. Ectopically dimerizing Mek1 would allow kinase activation and formation of the barrier. Gst-Mek1 exhibits higher levels of kinase activity in *hop1-K593A* mutants compared to *hop1Δ* (H. Niu and N. M. Hollingsworth, unpublished results), indicating that dimerization is not sufficient to activate the kinase but that it must also be localized to chromosomes. A similar conclusion was drawn from the fact that Gst-Mek1 kinase activity is reduced by mutants in *red1* and the Mek1 FHA domain (Wan et al., 2004). Experiments to test the requirement of the C domain for Mek1 activation require a kinase assay that uses a form of Mek1 that is not ectopically dimerized. Thus far efforts to develop a reproducible kinase assay using a tagged, non-dimerized form of Mek1 have been unsuccessful. A second possible role for Mek1 dimerization may be to facilitate binding to target proteins. In this model, Mek1 is active even in the undimerized state, but is unable to interact with its substrates in the *hop1-K593A* mutant.

Hop1 is a phosphoprotein whose phosphorylation is dependent upon both DSB formation and the presence of the C domain, but is independent of *MEK1*. Deletion of the C domain produces an unphosphorylated, truncated Hop1 protein that is still capable of being suppressed by *GST-MEK1*. Therefore, providing an alternative means for Mek1 to dimerize bypasses not only the requirement for the C domain but also the requirement for Hop1 phosphorylation. It may be that phosphorylation of Hop1 has no functional

role in meiosis, an idea that seems unlikely given its DSB dependence. Alternatively, Hop1 phosphorylation could be directly tied to C domain function. Our model proposes that phosphorylation of the Hop1 C domain in response to DSBs triggers Hop1 to promote dimerization of Mek1, which in turn allows kinase activation or binding to target proteins (Figure 2-8). In this way, barriers to sister chromatid repair can be regulated to occur only after a DSB has occurred on one of the two sisters. Furthermore, by controlling the extent of Hop1 phosphorylation, for example, by modifying only those Hop1 molecules adjacent to DSBs, the BSCR could be localized to the part of the sister chromatid opposite a DSB. Such local control would reduce the risk of overly inhibiting strand invasion, which in excess could inhibit DSB repair even between homologs.

An important question is whether the mechanism for interhomolog bias proposed here for budding yeast is evolutionarily conserved. Comparison of *hop1* mutants in other organisms suggests the answer is yes. In plants, nematodes and fission yeast, meiotic mutants have been found in genes that encode chromosome core components analogous to Hop1 (CARYL *et al.* 2000; LORENZ *et al.* 2004; ZETKA *et al.* 1999). These proteins, HIM-3, ASY1 and SpHop1, respectively, all contain a HORMA domain but lack the C domain of Hop1. In addition, the CT46/HORMAD1 gene from humans encodes a HORMA domain protein that is preferentially expressed in the testis and may represent a mammalian ortholog of Hop1 (CHEN *et al.* 2005). In *him-3* worms, homologs are unsynapsed and fail to

undergo interhomolog recombination, yet Rad51 foci, which are presumed to mark the sites of recombination intermediates, disappear with similar kinetics to wild-type. This observation led the authors to propose that "HIM-3's presence at chromosome axes inhibits the use of sister chromatids as templates for repair" (COUTEAU *et al.* 2004). Fission yeast *hop1* mutants exhibit an increase in meiotic sister chromatid recombination, consistent with a role for Hop1 in creating a BSCR in this organism (V. Latypov and J. Kohli, personal communication). Mek1 and Red1 orthologs have been described in *S. pombe*, but not in any non-yeast species (LORENZ *et al.* 2004). Therefore, while Hop1 may have a conserved role in the formation of a BSCR during meiosis, whether it regulates a kinase to generate a barrier in these organisms is not yet known.

In summary, this work suggests a specific molecular pathway by which the single stranded ends generated by DSBs may be prevented from invading sister chromatids during meiosis, thereby ensuring that crossovers occur between homologs. A number of important questions remain to be answered. For example, is Mek1 activated only in regions adjacent to a DSB, thereby preventing strand invasion in part of the sister opposite the break, or is there a global effect on the recombination? What is the kinase that phosphorylates Hop1 and is this phosphorylation biologically relevant? Is Mek1 dimerization needed for kinase activation or for substrate recognition? Finally, what is the target of Mek1 phosphorylation and how does its phosphorylation prevent

strand invasion? It has recently been shown that the meiotic cohesin, Rec8, may be involved in preventing sister chromatid repair during meiosis (Zierhut *et al.*, 2004). Is Rec8 a target of Mek1 or do Rec8 and Mek1 act independently to suppress recombination between sister chromatids? Having a molecular model for how the BSCR is generated will greatly facilitate finding the answers to these interesting questions.

Table 2-1 Plasmids

Name	*Yeast genotype*	*Source*
pRS402	*ADE2*	Brachmann et al. 1998
YCp50	*URA3 CEN ARS*	Rose et al. 1987
YEp352	*URA3* 2μ	Hill et al. 1986
pRS306	*URA3*	Sikorski and Heiter 1989
YIp5	*URA3*	Parent et al 1985
YIp5-hop1R6Δ	*hop1-R6Δ URA3*	Friedman et al. 1994
pLT11	*HOP1 URA3*	This work
pLT11-K593A	*hop1-K593A URA3*	This work
pLT11-K590A	*hop1-K590A URA3*	This work
pLT11-585	*hop1-585Δ URA3*	This work
pLT11-564	*hop1-564Δ URA3*	This work
pDW39	*HOP1 ADE2*	This work
pDT12	*hop1-K593A ADE2*	This work
pSB3	*RED1 URA3*	Woltering et al. 2000
pLW20	*MEK1 ADE2*	This work
pTS30	*GST-MEK1 ADE2*	de los Santos and Hollingsworth, 1999
pTS31	*GST-mek1-K199R ADE2*	de los Santos and Hollingsworth, 1999
pTS30-R72P, D76K	*gst-RD-MEK1 ADE2*	This work
pHN16	*TAP-MEK1 ADE2*	This work
pHN23	*lexA-MEK1 ADE2*	This work
pHN24	*lexA-MEK1 ADE2* 2μ	This work
pLP37	*MEK1 URA3*	de los Santos and Hollingsworth, 1999
pBL12	*GST-MEK1 URA3*	This work
pHN26	*GST-mek1-K199R URA3*	This work
pLW28	*DMC1 URA3*	This work
pRS316-DMC1	*DMC1 URA3 CEN ARS*	J. Engebrecht
pNRB143	*RAD54 URA3* 2μ	K. Runge
pR4C4	*MEK1 URA3 CEN ARS*	Hollingsworth and Ponte 1997
pNH251	*mek1-as1 ARG4*	This work
pNH255	*HOP1p-RAD51 URA3* 2μ	This work

Table 2-2 Strains

Name	Genotype	Source
NH246	*MATa CDC10 leu2 his4 arg4-8 thr1-1 ura3-1 CAN1 trp1-1 cyh10 ade2-1* *MATa cdc10-2 LEU2 HIS4 ARG4 THR1 ura3 can1 trp1 CYH10 ade2-1* *spo13::ura3-1 CYH2 red1Δ::ADE2* *spo13-1 cyh2 red1Δ::ADE2*	Woltering et al. 2000
NH270	same as NH246 only *RED1 hop1Δ::ADE2*	This work
NH144	*MATa leu2ΔhisG his4-x ARG4 ura3 lys2 hoΔ::LYS2* *MATa leu2-K HIS4 arg4-Nsp ura3 lys2 hoΔ::LYS2*	Hollingsworth et al. 1995
YTS3	same as NH144 only *red1::LEU2*	de los Santos and Hollingsworth 1999
DW10	same as NH144 only *hop1::LEU2*	de los Santos and Hollingsworth 1999
DW11	same as NH144 only *rec104Δ::LEU2*	de los Santos et al. 2001
NH311	same as NH144 only *hop1::LEU2 ade2-bgl sae2Δ::URA3*	Woltering et al. 2000
NH217	same as NH144 only *red1::LEU2 sae2Δ::URA3*	This work
YTS1ade2::pRS402	same as NH144 only *mek1::LEU2 ade2::ADE2*	Wan et al. 2004
NH566	*MATa HIS4 lys2 hoΔ:: LYS2 ura3 ade2 arg4 hop1::LEU2 mek1Δ::LEU2* *MATa HIS4 lys2 hoΔ:: LYS2 ura3 ade2 arg4 hop1::LEU2 mek1Δ::LEU2*	This work
NH601	*MATa leu2::hiG his4-X hoΔ::LYS2 lys2 ura3 dmc1Δ::LEU2 hop1Δ::kanMX* *MATa leu2::hiG his4-X hoΔ::LYS2 lys2 ura3 dmc1Δ::LEU2 hop1Δ::kanMX*	This work
NH624	*MATa leu2 his4 dmc1Δ::LEU2 mek1Δ::kanMX rad54Δ::NAT arg4 ADE2 hoΔ::LYS2 lys2* *MATa leu2 HIS4 dmc1Δ::LEU2 mek1Δ::kanMX rad54Δ::NAT arg4 ade2 hoΔ::LYS2 lys2*	This work
NH639	*MATa leu2::hisG his4-x mek1Δ::kanMX dmc1Δ::NAT hoΔ::LYS2 ura3 can1 ade2-bgl* *MATa leu2::hisG his4-x mek1Δ::kanMX dmc1Δ::NAT hoΔ::LYS2 ura3 CAN1 ade2-bgl* *cyh2 ARG4* *CYH2 arg4*	This work
NH567:: pNH251	*MATa leu2 SCR::URA3 arg4::mek1-as1 ARG4 ade3Δ::kanMX ade2-bgl mek1Δ::LEU2* *MATa leu2 SCR::URA3 arg4 ade3Δ::kanMX ade2-bgl mek1Δ::LEU2* *spo13::hisG ura3 lys2 hoΔ::LYS2* *spo13::hisG ura3 lys2 hoΔ::LYS2*	This work
NH574:: pNH251	same as NH567::pNH251 only *dmc1Δ::NAT* *dmc1Δ::NAT*	This work

Table 2-3. Sporulation, spore viability and recombination in *spo13* and *mek1-as1 dmc1 spo13* diploids in which Mek1 kinase activity is inhibited at different times in meiosis. (Contributed by Nancy M. Hollingsworth)

A. Two viable spore dyads[a]

			% Non-recombinant (# dyads)			% Interhomolog recombinant (# dyads)				% Intersister recomb. (# dyads)
	% spor.	% s. v. (# asci)	Equat.	Red.	Aberrant	Crossover			Gene conv.	Gene conv.
dmc1 mek1-as1[b] *spo13*			NM + -: NM + -	a + -: α - -	a + - :NM + - or α - -: NM + -	NM + - : NM - -	a + -: α + -	a - -:NM +- or α + -: NM + -	NM - -: a + -	NM + +: NM + -
no I[c]	4.5	NA	NA	NA	NA	NA	NA	NA	NA	
I added at 0 hr	44.5	61.2 (183)	93.7 (74)	1.3 (1)	3.8 (3)	0	0	0	0	1.3 (1)
I added at 2 hr	43.0	44.2 (182)	87.7 (50)	3.5 (2)	7.0 (4)	0	0	0	0	1.7 (1)
I added at 4 hr	52.5	46.7 (610)	85.2 (173)	0	9.4 (19)	0.5 (1)	1.0 (2)	0.5 (1)	0	3.4 (7)
I added at 6 hr	38.5	38.5 (183)	77.8 (35)	6.7 (3)	13.3 (6)	0	0	0	0	2.2 (1)
total			86.5 (332)	1.6 (6)	8.3 (32)	0.3 (1)	0.5 (2)	0.3 (1)	0	2.6 (10)
spo13	36.0	25.5 (646)	24.2 (8)	27.3 (9)	24.2 (8)	9.1 (3)	9.1 (3)	0	6.1 (2)	0

B. One viable spore dyads

	% Non-recombinant (# dyads)			% Interhomolog recombinant (dyads)			% Intersister recomb. (# dyads)
	NM + -	a + -	α - -	α + -	a - -	NM - -	
dmc1 mek1-as1 spo13 I added at 4 hr	88.7 (102)	4.3 (5)	6.1 (7)	0	0	0	0.9 (1)
spo13	41.9 (85)	30.5 (62)	12.8 (26)	2.5 (5)	1.0 (2)	11.3 (23)	0

[a]Phenotypes are indicated in the following order: Mat Ura His (*ade3* mutants are His$^-$).

[b]The *mek1-as1 dmc1 spo13* diploid NH574::pNH251 is isogenic with the *spo13* diploid (NH567::pNH250).

[c]I indicates 1 μM 1-NA-PP1.

Table 2-4. Effect on meiotic interhomolog crossing over in *red1 spo13* and various *hop1 spo13* mutants. (Contributed by Bridget Baumgartner)

		Map distance (cM) [a]				
Strain::plasmid	relevant	*HIS4-LEU2*	*LEU2-CDC10*	*CDC10-MAT*	*ARG4-THR1*	Mean fold reduction
NH246::pSB3[b]	*RED1 HOP1*	18.3 (254)	13.1 (245)	22.2 (248)	12.1 (286)	1
NH246::pRS306[b]	*red1*	0.7 (284)	1.6 (286)	1.7 (295)	2.0 (318)	11
NH270::YIp5	*hop1Δ*	0.3 (317)	0 (317)	0.6 (317)	0.2 (324)	60
NH270::YIp-hop1R6Δ	*hop1-R6Δ*	0.6 427)	1.6 (427)	2.8 (427)	0.9 (440)	11
NH270::pLT11-K593A	*hop1-K593A*	0.5 (401)	1.4 (401	2.3 (401)	1.3 (414)	12

[a]Map distances were calculated as described in Hollingsworth, Ponte and Halsey (1995).
[b]Data taken from Woltering et al. (2000).

Table 2-5. Spore viabilities of different *hop1* strains containing various alleles of *MEK1*.

	% viable spores (# asci dissected)			
MEK1 genotype[a]	*HOP1* genotype[a]			
	hop1::LEU2	*HOP1*	*hop1-K593A*	*hop1-585*
mek1Δ	ND[b]	1.0 (25)	<2.0 (13)	ND
MEK1	<1.0 (26)	96.4 (77)	<1.0 (76)	<1.0 (78)
GST-MEK1	1.0 (26)	93.5 (50)	87.9 (128)	47.6 (103)
GST-mek1-K199R	<2.0 (13)	<1.0 (26)	<1.0 (24)	<2.0 (13)
gst-R72P,D76K-MEK1	ND	91.4 (54)	6.7 (104)	ND
lexA-MEK1	ND	86.8 (76)	23.3 (182)	ND
2μ *lexA-MEK1*	ND	89.4 (26)	46.5 (182)	ND
TAP-MEK1	1.9 (26)	87.0 (77)	1.0 (52)	<1.0 (78)

[a]All strains are derived from the same *hop1::LEU2 mek1Δ::LEU2* SK1 diploid, NH566. The *hop1* alleles were introduced by integrating the following plasmids: *hop1::LEU2*, pRS306; *HOP1*, pLT11; *hop1-K593A*, pLT11-K593A; *hop1-585*, pLT11-1-585. The *MEK1* alleles were introduced by integrating the following plasmids into the appropriate *hop1* strain: *mek1Δ*, pRS402; *MEK1*, pLW20; *GST-MEK1*, pTS30; *GST-mek1-K199R*, pTS31; *gst-R72P, D76K-MEK1*, pTS30-R72P, D76K; *lexA-MEK1*, pHN23; 2μ *lexA-MEK1*, pHN24 *TAP-MEK1*, pHN16.
[b]ND, no data.

Table 2-6. Sporulation and spore viability in *dmc1* strains carrying various alleles of *HOP1* and *MEK1*.

Relevant genotype[a]	% spo	viable spores
HOP1 DMC1	78.2	yes
HOP1 dmc1Δ	<0.2	ND
hop1 dmc1Δ	79.8	no
hop1 dmc1Δ GST-MEK1	81.7	no
dmc1Δ hop1-K593A	83	no
dmc1Δ hop1-K593A GST-MEK1	4.2	ND
dmc1Δ hop1-K593A GST-mek1-K199R	77.8	no

All strains were derived by transformation of the *dmc1Δ::LEU2 hop1Δ::kanMX* diploid, NH601. *HOP1* alleles were integrated at ura3 in one haploid parent using the following plasmids: HOP1, pLT11; *hop1-K593A*, pLT11-K593A. *MEK1* alleles and *DMC1* were integrated at ura3 into the other haploid parent using the following plasmids: *DMC1*, pLW28; *MEK1*, pLP37; *GST-MEK1*, pBL12; *GST-mek1-K199R*, pHN26. The resulting transformants were then mated in the appropriate combinations to give the indicated genotypes. ND, no data. Spore viability was determined by tetrad dissection.

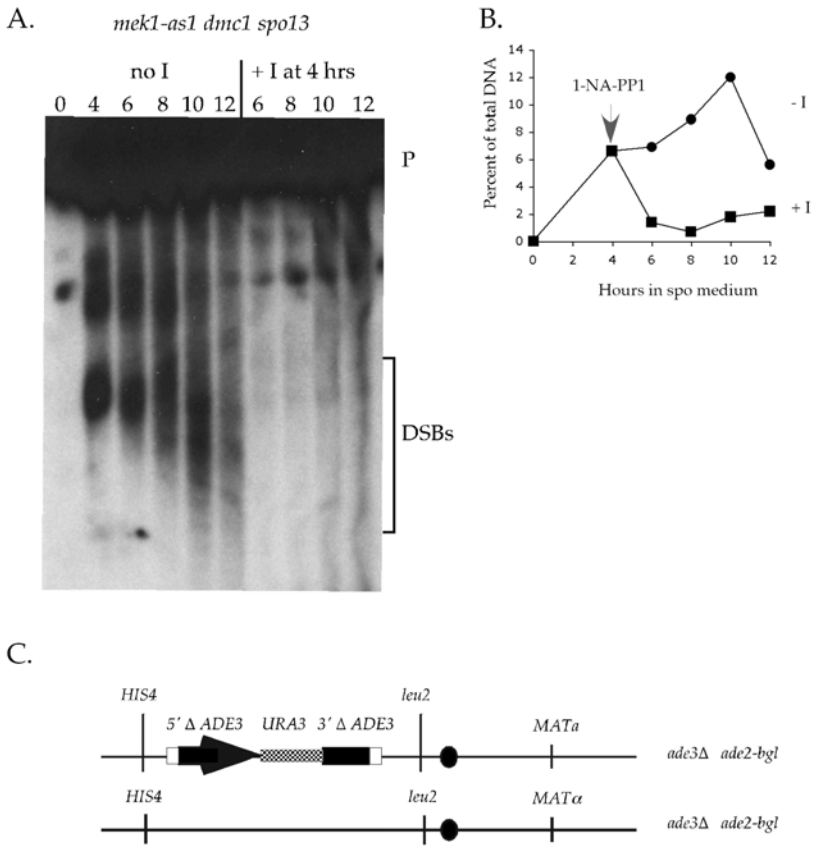

Figure 2-1. Double strand breaks in a *mek1-as1 dmc1 spo13* diploid in the absence of inhibitor and after addition of inhibitor after 4 hours in Spo medium. (Contributed by Nancy M. Hollingsworth) A. The *mek1-as1 dmc1 spo13* diploid, NH574::pNH251, was transferred to sporulation medium and incubated at 30° for 4 hours. At that time, 1 μM 1-NA-PP1 was added to one half of the sporulating cells and returned to the incubator. At two hour intervals, cells were fixed and analyzed for DSB formation at the *YCR048w* hotspot as described in Woltering et al. (2000). Numbers above each lane indicate hours after transfer to sporulation medium. The bracket indicates the DSB fragments. P = parental band. B. Quantitation of the DSBs shown in Panel A. C. Configuration of the sister chromatid recombination reporter present on chromosome III in the isogenic *spo13* (NH567::pNH250) and *mek1-as1 dmc1 spo13* (NH574::pNH251) diploids (KADYK and HARTWELL 1992). The black oval indicates the centromere on chromosome III. The white box indicates the region of shared homology between the 5′Δ*ADE3* and 3′*ADE3* truncations between which recombination can occur.

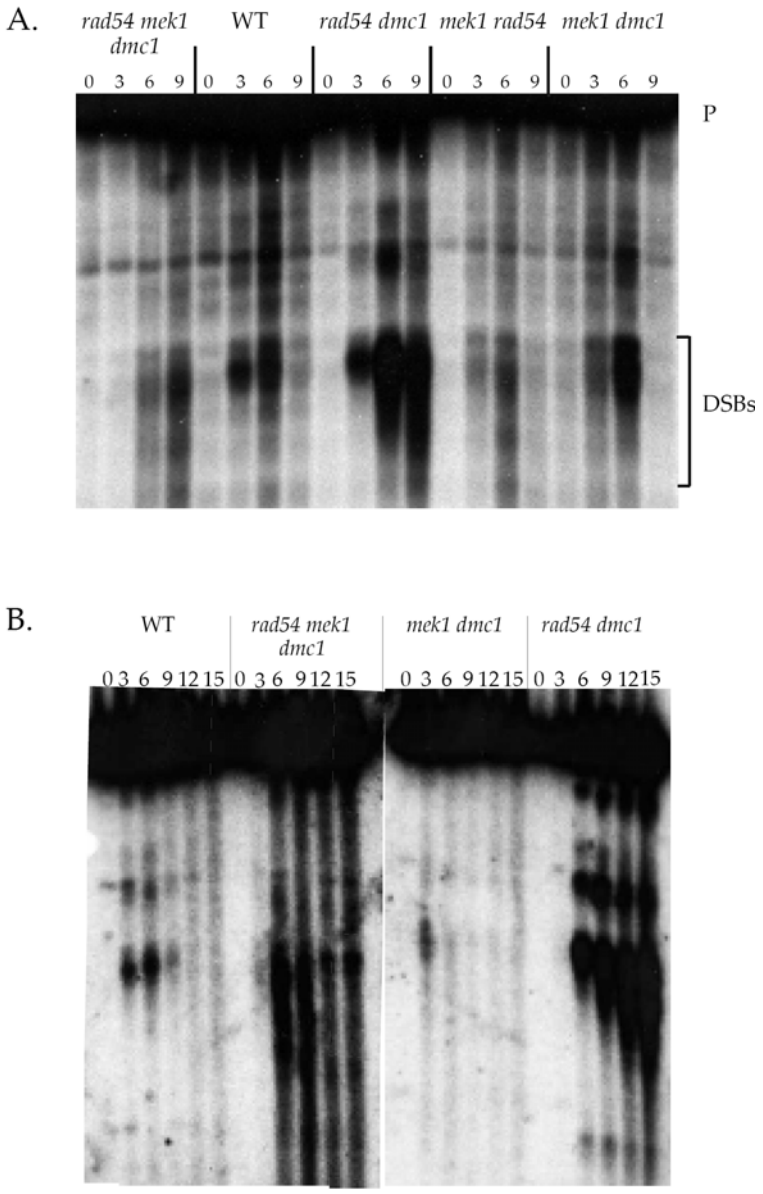

Figure 2-2. DSBs in strains containing various combinations of *mek1Δ*, *dmc1Δ* and *rad54Δ*. (contributed by Dana Schaefer) NH624 was transformed with YCp50 (*rad54Δ mek1Δ dmc1Δ*), pR4C4 (*rad54Δ dmc1Δ*), pRS316-DMC1 (*mek1Δ rad54Δ*) or pNRB143 (*mek1Δ dmc1Δ*). In addition the wild-type diploid, NH144, was transformed with YCp50 so that all of the strains could be grown under selective conditions for the plasmids until they were sporulated at 30°. DSBs at the *YCR048w* hotspot were analyzed by Southern blot as described in Woltering et al (2000). P indicates the parental fragment. The bracket indicates the DSBs. A. Timecourse carried out for nine hours. B. Timecourse carried out for 15 hours.

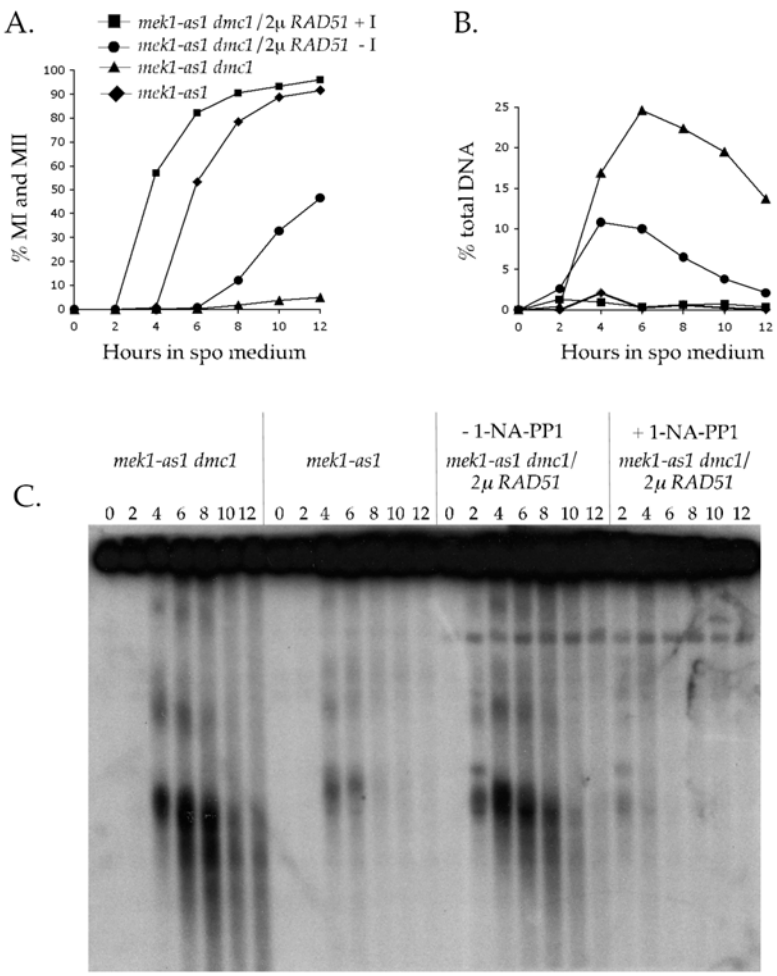

Figure 2-3. Meiotic progression and DSBs in *mek1-as1 dmc1* diploids over-expressing *RAD51* in the presence or absence of 1-NA-PP1. (Contributed by Nancy M. Hollingsworth and Dana Schaefer) NH639 was transformed with pRS306 (*mek1-as1 dmc1Δ*), pLW28 (*mek1-as1*) or pNH255 (*mek1-as1 dmc1Δ*/2μ *RAD51*). A final concentration of 1 μM 1-NA-PP1 was added to half of the pNH255 containing culture immediately after transfer to sporulation medium and the cells were incubated at 30°. A. Meiotic progression was measured by DAPI staining to determine the fraction of bi-nucleate (MI) and tetranucleate (MII) cells. The graph represents the averages of four independent cultures for each strain. B. Quantitation of the percentage of total DNA contained in the DSB fragments shown in Panel C. C. Southern blot exhibiting DSB fragments generated at the *YCR048w* hotspot on chromosome III

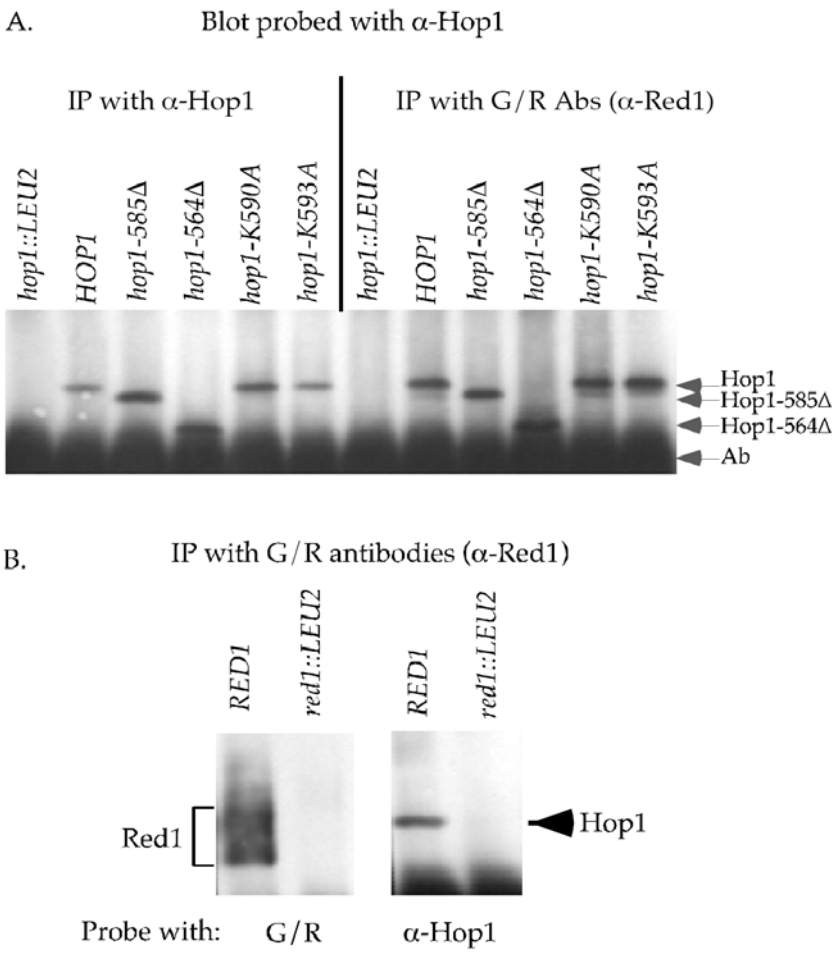

Figure 2-4. Co-immunoprecipitation of various Hop1 mutant proteins with Red1 (Contributed by Dana Schaefer). A. *hop1::LEU2* (DW10::YIp5), *HOP1* (DW10::pLT11), *hop1-585Δ* (DW10::pLT11-585), *hop1-564Δ* (DW10::pLT11-564), *hop1-K590A* (DW10::pLT11-K590A), and *hop1-K593A* (DW10::pLT11-K593A) diploids were sporulated for 3 hr at 30° and soluble yeast extracts used for immunoprecipitation with either α-Hop1 or G/R (α-Red1) antibodies. The IPs were fractionated by SDS-PAGE using 6% gels and probed with either α-Hop1 or G/R antibodies as indicated. B. Red1 was IPed from extracts derived from *RED1* (YTS1::pTS30-Q241G) and *red1::LEU2* (YTS3) diploids using G/R antibodies. The Red1 IPs were then probed with either G/R or α-Hop1 antibodies to detect Red1 or Hop1, respectively.

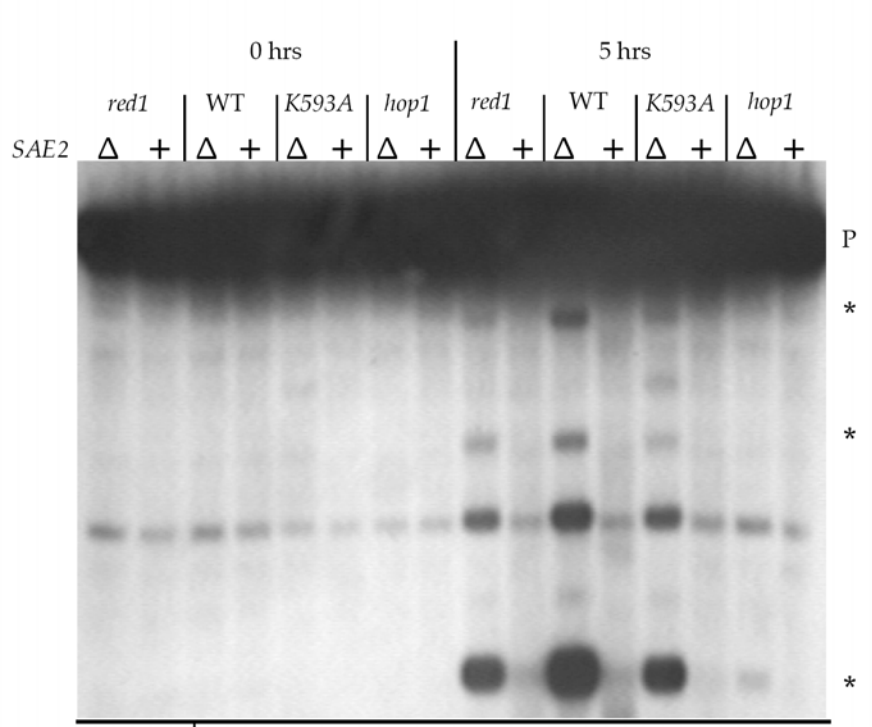

	% of total DNA (% total DNA/% wild type)			
	*red1*Δ	wild type	*hop1-K593A*	*hop1*Δ
SAE2	0.64 (58)	1.1 (100)	0.31 (28)	0.04 (3.6)
*sae2*Δ	1.7 (27)	6.3 (100)	2.0 (32)	0.3 (5)

Figure 2-5. DSB formation at the *YCR048w* hotspot in various *hop1* diploids. (Contributed by Dana Schaefer) Isogenic diploids were transferred to sporulation medium and cells were fixed after 0 and 5 hr at 30°. A Southern blot of digested DNA was probed to detect DSB fragments formed at the *YCR048w* hotspot. P, parental band; asterisks indicate meiosis-specific DSB fragments. *red1::LEU2 sae2Δ* (NH217); *red1::LEU2* (YTS3); *sae2Δ* (NH311::pDW39); wild type (DW10::pLT11); *hop1-K593A sae2Δ* (NH311::pDT12); *hop1-K593A* (DW10::pLT11-K593A); *hop1::LEU2 sae2Δ* (NH311::pRS402); *hop1::LEU2* (DW10::YIp5).

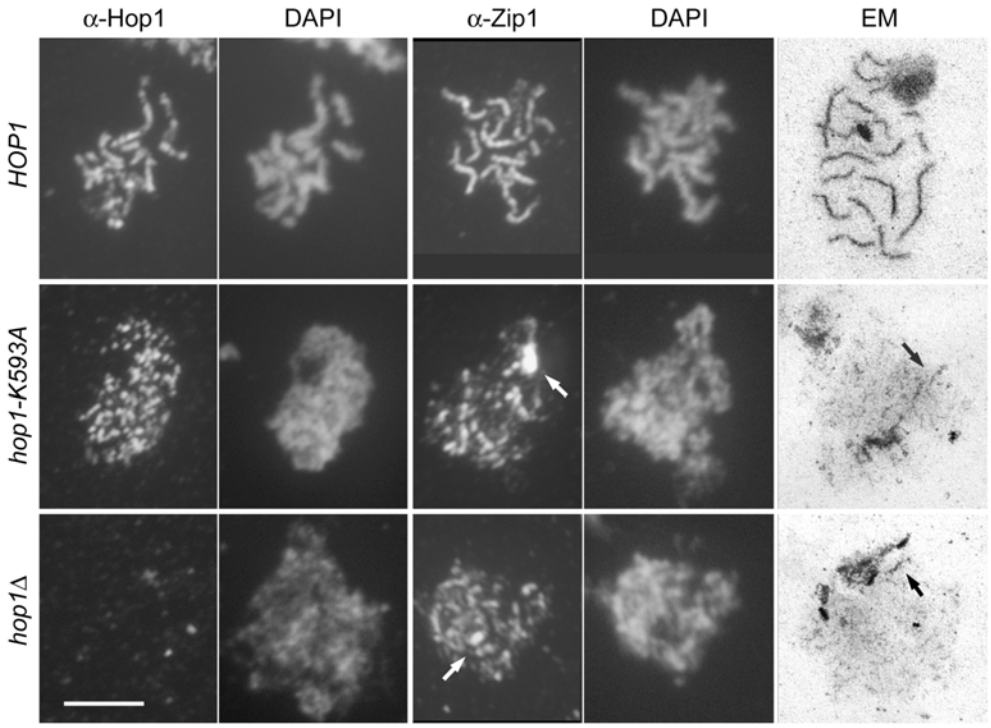

Figure 2-6. Hop1 localization and chromosome synapsis in *hop1-K593A* diploids. (Contributed by Josef Loidl) Preparation of nuclei, immunostaining, and silver staining for electron micrscopy were done as described by Loidl et al. (1998). Hop1 and Zip1 were localized by immunostaining with α-Hop1 and α-Zip1 antibodies. DNA was visualized using DAPI. Silver stained chromosomes were analyzed by electron microscopy (EM). The few thick structures observed by EM are probably polycomplexes (indicated by arrows) that are prominently decorated by Zip1 as well (arrows). Bar = 5μm. *HOP1* (DW10::pLT11); *hop1-K593A* (DW10::pLT11-K593A); *hop1::LEU2* (DW10::YIp5).

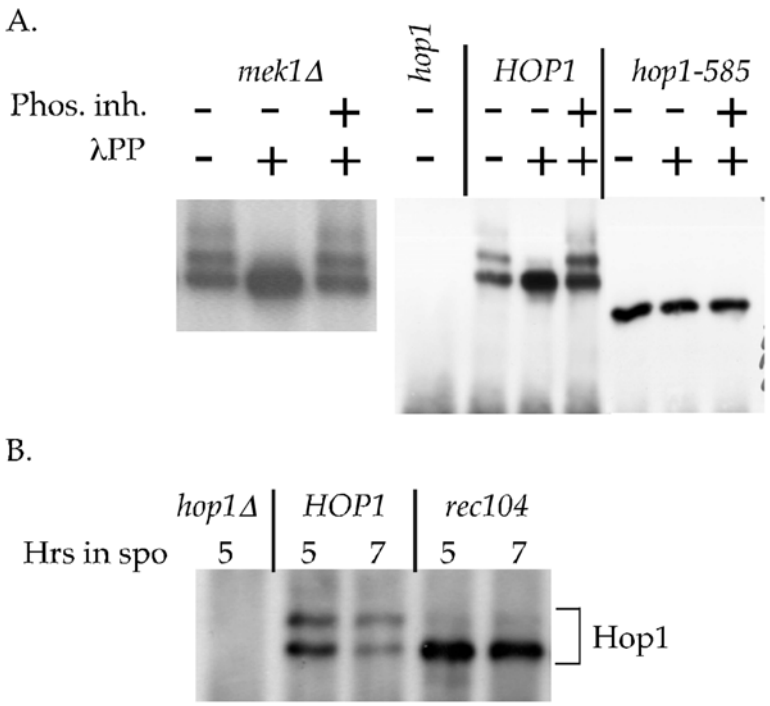

Figure 2-7. Hop1 phosphorylation in *mek1Δ* and *rec104Δ* diploids. (Contributed by Lihong Wan) A. Phosphatase treatment of Hop1 and Hop1-585Δ. Hop1 or Hop1-585Δ was IPed from *mek1Δ* (YTS1ade2::pRS402), *hop1::LEU2* (DW10), *HOP1* (DW10::pLT11) or *hop1-585Δ* (DW10::pLT11-585) extracts using α-Hop1 antibodies. The proteins were fractionated on an 8% SDS-polyacrylamide gel. The IPs were treated with λ protein phosphatase (λPP) as described in de los Santos and Hollingsworth (1999). The phosphatase inhibitors, NaF and $Na_4P_2O_7$, were used at 10 and 1 mM final concentrations, respectively. The Western blot was then probed with Hop1 antibodies. B. Hop1 was IPed and detected as described in Panel A using protein extracts from wild-type (NH144) and *rec104* (DW11) diploids 5 or 7 hours after transfer to sporulation medium as indicated.

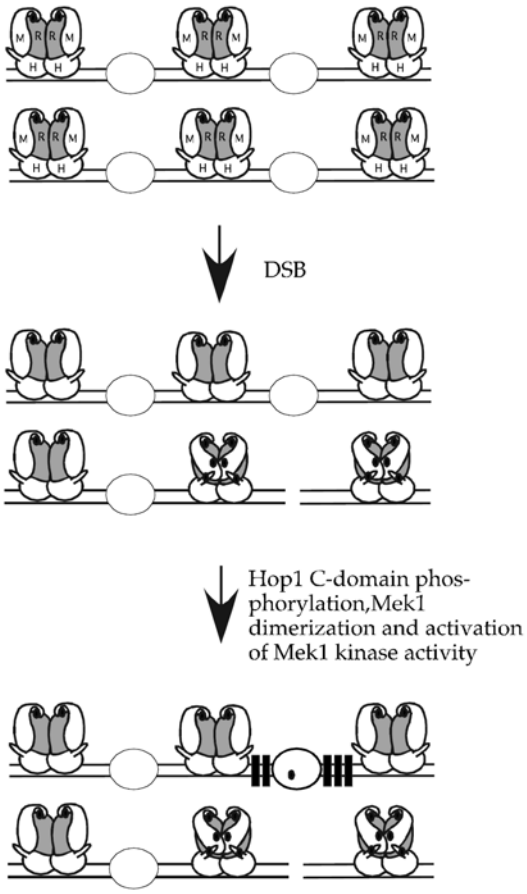

Figure 2-8. Model coordinating DSB formation, Mek1 dimerization and the creation of a BSCR. (Contributed by Nancy M. Hollingsworth) Hop1 (H), Red1 (R), and Mek1 (M) complexes are bound to chromosomes in regions where DSBs are likely to form. A single pair of sister chromatids is shown. Hop1 binding to DNA is mediated by the N domain. Hop1 binds to Red1 and Mek1 binds to phosphorylated Red1 via its FHA domain. Phosphate groups are indicated by black ovals. Large white ovals indicate target proteins for the Mek1 kinase that, when phosphorylated, prevent strand invasion. In this model, introduction of a DSB results in phosphorylation of Hop1 molecules adjacent to the DSB. Phosphorylation of the Hop1 C domain triggers dimerization of Mek1. Dimers of Mek1 become activated by auto-phosphorylation of threonine 327 in *trans*. Activated Mek1 then phosphorylates target proteins that act to prevent strand invasion on the sister chromatid. The BSCR is indicated by black rectangles.

CHAPTER THREE

Mek1 kinase is regulated to suppress double-strand break repair between sister chromatids during budding yeast meiosis

[The text of this chapter is taken directly from a manuscript published in Molecular and Cellular Biology, 27: 5456-5467 and represents the work of several people, including myself (NIU *et al.* 2007).]

INTRODUCTION

During the specialized cell division of meiosis, two rounds of chromosome segregation follow one round of chromosome duplication, thereby creating haploid gametes from diploid cells. In the first meiotic division (Meiosis I), homologous chromosomes segregate to opposite poles, while in the second division (Meiosis II), sister chromatids segregate to opposite poles. Recombination between non-sister chromatids of homologous chromosomes, combined with sister chromatid cohesion, create physical connections that enable homologs to segregate properly at MI (PETRONCZKI et al. 2003). In the absence of these connections, homologous chromosomes disjoin randomly, resulting in chromosomally imbalanced gametes. In humans, the consequences of these non-disjunction events are infertility or birth defects such as Trisomy 21 or Down syndrome (HASSOLD and HUNT 2001). While crossovers must occur between homologs during meiosis to be effective for chromosome segregation, in vegetative cells sister chromatids are the preferred templates for DNA repair (KADYK and HARTWELL 1992). Determining how the bias in recombination partners changes from sister chromatids to homologs is therefore key to understanding meiosis.

In the budding yeast, *Saccharomyces cerevisiae*, meiotic recombination is initiated by double strand breaks (DSBs) catalyzed by a meiosis-specific endonuclease, Spo11 (KEENEY 2001). The 5′ ends of the DSBs are resected to generate 3′ single stranded tails, which then invade homologous non-sister chromatids, displacing strands of like polarity. Extension of the invading 3′ tails by DNA repair synthesis proceeds until the displaced strands anneal with 3′ single stranded tails from the opposite side of the breaks. Further extension and ligation generate double Holliday junction structures that are resolved to make crossovers (ALLERS and LICHTEN 2001; SCHWACHA and KLECKNER 1995). In addition, a subset of crossovers is created by an alternative pathway using the structure-specific Mus81-Mms4 endonuclease [reviewed in (HOLLINGSWORTH and BRILL 2004)].

Strand invasion is the critical step that determines partner choice. In vegetative cells, where recombination occurs preferentially between sister chromatids, the recombinase mediating strand invasion is Rad51 (PAQUES and HABER 1999). In meiotic cells, a meiosis-specific recombinase, Dmc1, is also present (BISHOP *et al.* 1992). Rad51 and Dmc1 co-localize to DSBs and function together in meiotic recombination between homologs (BISHOP 1994; YVES-MASSON and WEST 2001). *RAD51* facilitates Dmc1 localization to breaks, although the reverse is not true (BISHOP 1994; SHINOHARA and SHINOHARA 2004).

In diploids deleted for *DMC1*, there is no strand invasion of homologs and as a result, DSBs are unrepaired and hyper-resected (BISHOP *et al.* 1992; HUNTER and KLECKNER 2001). Furthermore, cells arrest in prophase due to triggering of the meiotic recombination checkpoint (LYDALL et al. 1996). Given that Rad51 is present at breaks in *dmc1Δ* mutants and that Rad51 preferentially utilizes sister chromatids as templates for DSB repair in vegetative cells, the fact that DSBs are unrepaired in *dmc1Δ* meiosis suggests that there is a meiosis-specific "barrier to sister chromatid repair" (BSCR) functioning to suppress Rad51-mediated inter-sister DSB repair.

An important clue to understanding how the BSCR is created came from the discovery that deletion of the meiosis-specific protein kinase Mek1 (also known as Mre4) allows repair of DSBs in *dmc1Δ* diploids (XU *et al.* 1997). Consistent with a role in the BSCR, *mek1Δ* mutants are specifically defective in interhomolog recombination and, in some genetic assays, exhibit increased sister chromatid recombination (HOLLINGSWORTH *et al.* 1995; NIU *et al.* 2005; THOMPSON and STAHL 1999). An analog sensitive allele of *MEK1* (*mek1-as*) allows conditional inhibition of Mek1 kinase activity during meiosis. Using this allele, Mek1 kinase activity was shown to be constitutively required after DSB formation in *dmc1Δ* strains to prevent sister chromatid repair (NIU *et al.* 2005; WAN *et al.* 2004). Increased Rad51 activity, either by over-expression of *RAD51*

or *RAD54* or deletion of a negative regulator of Rad51, *HED1*, suppresses the interhomolog recombination, sporulation and spore viability defects of *dmc1Δ* (BISHOP *et al.* 1999; TSUBOUCHI and ROEDER 2003; TSUBOUCHI and ROEDER 2006). This suppression requires Mek1 kinase activity as inactivation of Mek1-as when *RAD51* is over-expressed in the *dmc1Δ* background results in inter-sister recombination and dead spores (NIU *et al.* 2005). This result indicates that Mek1 does not create a BSCR by directly inhibiting the catalytic activity of Rad51, but is instead preventing active Rad51 from invading sister chromatids.

A BSCR is only necessary when DSBs create 3′ single stranded ends that are faced with the choice of invading either sister chromatids or homologs. Recent experiments suggest that coupling of DSB formation to creation of a BSCR occurs by regulation of Mek1 kinase activity. Mek1 exists in a complex with two other meiosis-specific chromosomal core components, Hop1 and Red1 (BAILIS and ROEDER 1998; SMITH and ROEDER 1997). The last 20 amino acids of Hop1 constitute a functionally distinct region called the C domain that is specifically required for the BSCR (NIU *et al.* 2005). Ectopic dimerization of Mek1 suppresses *hop1-K593A* mutant phenotypes, suggesting that the function of the Hop1 C domain in the BSCR is to dimerize Mek1. The Hop1 C domain is phosphorylated in response to DSBs by a kinase other than Mek1, suggesting a mechanism by which DSB formation may be tied to Mek1 activation (NIU *et al.*

2005).

Mek1 belongs to the RD family of protein kinases, many of which are activated by phosphorylation of conserved threonines in a portion of the protein called the activation loop (JOHNSON et al. 1996; NOLEN et al. 2004). Phosphorylation of the activation loop can create conformational changes that allow substrate binding and/or affect the phosphoryl transfer step (ADAMS 2003). Modification of activation loop threonines can result either from autophosphorylation (e.g.,interleukin-1 receptor associated kinase 4), or by reaction with another kinase (e.g. cyclin-dependent kinase) (CHENG et al. 2006; KALDIS et al. 1996). For kinases activated by autophosphorylation *in trans*, dimerization is one way to bring the kinase molecules together. Mek1 contains two conserved threonines in its activation-loop, T327 and T331. Genetic evidence indicates that T327 phosphorylation is important for Mek1 function during meiosis, but a role for T331 has not been reported (WAN *et al.* 2004).

To determine whether T327 and T331 phosphorylation occur *in vivo*, mass spectrometry was used to identify amino acids that are phosphorylated in Gst-Mek1 purified from *dmc1Δ*-arrested cells where Mek1 kinase activity is constitutively required to prevent inter-sister DSB repair. *In vivo* phosphorylation of T327 and T331 was confirmed. T327 phosphorylation therefore provides a molecular marker for the activation state of Mek1.

Analysis of T327 phosphorylation of Mek1 in various mutant conditions revealed several requirements for Mek1 activation in response to DSBs. In addition, mass spectrometry identified a third amino acid in the activation loop, S320, which is also phosphorylated. Unlike T327 and T331, however, S320 phosphorylation is required specifically in maintaining Mek1 function in *dmc1Δ*-arrested cells.

MATERIALS AND METHODS

Plasmids. Plasmid names, genotypes and sources can be found in Table 3-1. All *MEK1* alleles (including N-terminal fusions) are under control of the *MEK1* promoter. Mutations in T327 and T331 were introduced into *GST-MEK1* by site directed mutagenesis of the *ADE2*-integrating plasmid, pTS30 (Quikchange Kit, Stratagene, La Jolla, California). To create *URA3* integrating plasmids containing the P_{MEK1}-*GST-mek1* alleles (pHN31-pHN35), 3.0 kb Not1/SalI fragments from the corresponding *ADE2* plasmids were subcloned into NotI/SalI digested pRS306. Untagged *mek1* alleles (pTS9, pTS15, pHN36, pHN37) were created by substituting 0.75 kb Spe1/Hpa1 fragments from *GST-mek1* mutant alleles for the corresponding fragment in pLP37. Mutations in S142 and S320 were made by site-directed mutagenesis in untagged and *GST-tagged MEK1* using pLP37 and pBL12 as templates, respectively. *mek1-I459A L460A* (*mek1-IL*)

was created by introducing I459A and L460A into pLP37 to make pLP37-IL. A 0.5 kb HpaI/KpnI fragment from pLP37 was substituted for the analogous fragment in Hpa1/KpnI digested pBL12, thereby making *GST-mek1-IL* in pEJ2. For *gst-R72P D76R-mek1-IL*, a 2.6 kb HpaI/BamHI fragment from pTS30-R72P D76K replaced the analogous fragment in pEJ2 to make pEJ4. Mutations were confirmed by DNA sequencing (Stony Brook University DNA Sequencing Facility). All mek1 alleles exhibiting a mutant phenotype were sequenced in their entirety to ensure that no unintended mutations were created during the mutagenesis. *gst-R72P D76K-mek1-S320A* was constructed by cloning a 1.9 kb SpeI fragment from pEJ4 containing gst-R72P D76K into SpeI-digested pBL12-S320A, thereby creating pHN38.

The *FKBP-MEK1* over-expression plasmid was constructed using the plasmid, pC_4-F_v1E, from the ARGENT Regulated Homodimerization Kit (ARIAD Pharmaceuticals; www.ariad.com/regulationkits/) as a template to amplify FKBP by the polymerase chain reaction (PCR). The fragment was engineered to introduce an NdeI site at the start codon of FKBP and EcoRI-SalI sites immediately downstream of the FKBP coding sequence. After digestion with NdeI and SalI, the PCR fragment was ligated to NdeI/SalI digested pTS25 to fuse FKBP to the *MEK1* promoter and create pHN27. A BamHI/SalI fragment containing the P_{MEK1}-*FKBP* cassette was subcloned into BamHI/SalI cut pRS402 to

make pHN28. The *MEK1* coding sequence was fused in frame to FKBP by ligation of an EcoRI/SalI fragment from pTS3 into EcoRI/XhoI digested pHN28, thereby creating pHN29. In this fusion the methionine of Mek1 is deleted and replaced with the amino acids FPGI. Finally, the P_{MEK1}-*FKBP-MEK1* fusion carried on a NotI/KpnI fragment was subcloned into NotI/KpnI digested pRS422 to make pHN30.

Yeast Strains and Media. Strain genotypes are listed in Table 3-2. All strains are derived from the SK1. The *mek1Δ::kanMX6 rec104Δ::LEU2* diploid, NH561, was constructed by transforming *mek1Δ* haploid strains S2683 mek1Δ::KAN and RKY1145 mek1Δ::KAN with BamHI/XbaI-digested pNH131. The presence of the *rec104Δ::LEU2* mutation was confirmed by Southern blot analysis and the haploids mated to make the diploid. All integrating plasmids were digested with StuI to target integration either to *ADE2* or *URA3* in diploid strains and are presumed to be present in single copy. Liquid and solid media were as described in (DE LOS SANTOS and HOLLINGSWORTH 1999). Cultures were sporulated at a density of 3 X 10^7 cells/ml in 2% potassium acetate at 30°C. The ligand used to induce dimerization of FKBP, AP20187, was obtained from the ARGENT Regulated Homodimerization kit (ARIAD Pharmaceuticals).

Kinase assays and western blots. For Western blots, Gst-Mek1 was partially purified from 50 ml of cells after 4.5 hr in sporulation medium at 30°C

as described in (WAN *et al.* 2004). The precipitates were fractionated on 8% SDS-polyacrylamide gels, transferred to nitrocellulose membranes and blocked with 5% non-fat milk for 1 hour at room temperature. The blots were then incubated in 5% bovine serum albumin (BSA) with a 1:1000 dilution of Akt antibody (Cell Signaling Technology) and incubated at 4° C overnight. The blot was washed with TBS (20 mM Tris-HCl pH7.5, 250 mM NaCl, 0.1% Tween 20) and probed with α-rabbit secondary antibodies (Bio-RAD) for 4 hours before being developed using the Immun-Star HRP kit (Bio-RAD). To determine the relative amounts of Gst-Mek1 in each pulldown, the blots were incubated in stripping buffer (50 mM Tris-HCl pH 6.8, 2% SDS, 50 mM DTT) at 55° C for 30 minutes, then probed with a 1:5000 dilution of α-Gst antibodies (generously provided by Doug Kellogg, University of California, Santa Cruz). Kinase assays using glutathione-precipitated Gst-Mek1 were performed as described in (NEIMAN and HERSKOWITZ 1994) except that 0.2 mM ATP without any radioactivity was used.

Protein purification and mass spectrometry. For mass spectrometry analysis, Gst-Mek1 was purified from the *GST-MEK1 dmc1Δ* diploid, NH520::pBL12. One liter of sporulating culture (~10 g of cell pellet) was collected 5 hours after transfer to Spo medium at 30° C. Soluble extracts were made by resuspending the cells in 10 ml lysis buffer (50 mM Tris 8.0, 10 mM

EDTA 8.0, 300 mM NaCl, 1 mM DTT, 5% Triton X-100, 0.05% SDS, 1 mM PMSF, 1 μg/mL leupeptin, 1 μg/mL aprotinin, 1 μg/mL pepstatin, 10 mM NaF, 10 mM $Na_4P_2O_7$) and 10 g acid washed glass beads and vortexing for 20 seconds 10 times with 2 minutes on ice in between. 500 μL glutathione-S-sepharose (GE Health Science) were added and incubated at 4° C with rotation for 2 hours. Gst-Mek1 was eluted by the addition of 500 μL elution buffer (50 mM Tris-HCl pH7.5, 200 mM NaCl, 1 mM DTT, 10 mM glutathione). The flowthrough was collected and this step was repeated twice. All three flowthroughs were pooled and Gst-Mek1 was precipitated by addition of trichloroacetic acid to a final concentration of 20%, then incubated on ice for 20 min. The precipitate was collected by centrifugation at 16,000 g for 20 min at 4° C. The pellet was washed with 100% acetone and the protein fractionated using a 4-12% Bis-tris NuPAGE gel (Invitrogen).

Proteins were stained in the gel using Gel-code Blue reagent (Pierce) and the Gst-Mek1 band was cut out of the gel. The band was cut into approximately 1-mm cubes, washed with MilliQ water, and destained using 50% CH_3CN/50 mM NH_4HCO_3. Gel pieces were dehydrated with 100% CH_3CN and dried for 30 min under vacuum. For in-gel digestion, dry gel pieces were rehydrated with 10 ng/μL trypsin (50 mM NH_4HCO_3, pH 8) on ice for 2 hour. The digestion was carried out at 37 ^oC overnight. Digests were extracted twice using a solution of

50% CH_3CN /5% HCOOH, dried completely under vacuum, and stored at -80 °C until further analysis.

LC-MS/MS experiments were performed on a LTQ mass spectrometer (Thermo Electron, San Jose, CA). Peptide mixtures were loaded onto a 100-μm i.d. fused-silica microcapillary column packed in-house with C_{18} resin (Michrom Bioresources Inc., Auburn, CA) and were separated using a 40 minute-gradient from 8% to 45% solvent B (0.15% HCOOH/ 97.5% CH_3CN). Solvent A was 0.15% HCOOH/ 2.5% CH_3CN). The LTQ mass spectrometer was operated in the data-dependent mode using the TOP10 strategy (HAAS et al. 2006; LI et al. 2007). In brief, a scan cycle was initiated with a full scan, which was followed by MS/MS scans on the 10 most abundant precursor ions with dynamic exclusion of previously selected ions.

Time courses. Liquid sporulation was performed at 30° C with 2% potassium acetate. Sporulation was monitored using phase contrast light microscopy to count the number of asci present in 200 cells per strain. Meiotic progression was monitored by staining cells with DAPI (4'-6-diamidino-2-phenylindole) using fluorescent microscopy. Binucleate cells have completed MI, while tetranucleate cells have completed MII. DSBs were monitored at the naturally occurring YCR048w hotspot as described in WOLTERING *et al.* (2000) (WU and LICHTEN 1994). DSBs were quantitated using a

Molecular Dynamics PhosphoImager (Amersham, Piscataway, NJ) and Image Quant 1.1 software.

RESULTS

Two conserved threonines in the Mek1 activation domain are important for Mek1 function. Alignment of budding yeast Mek1 with different kinases activated by phosphorylation as well as different fungal orthologs of Mek1 indicates that there are two conserved threonine residues within Mek1's activation domain, T327 and T331 (Figure 3-1A). Although genetic evidence exists for a role of T327 in Mek1 function, a role for T331 has not been reported (WAN *et al.* 2004). Various T327/T331 mutant combinations were therefore introduced by site-directed mutagenesis into *GST-MEK1* and the mutants were tested for complementation of the *mek1Δ* spore viability defect. As was previously observed, mutation of T327 to alanine reduces spore viability, while the presence of a negatively charged amino acid at this position (*GST-mek1-T327D*) creates a more functional allele (WAN *et al.* 2004) (Table 3-3). Substitution of T331 to alanine decreased spore viability significantly to 20.1%, indicating that T331 is also required for Mek1 to function properly during meiosis. In this case, however, the presence of a phosphomimetic amino acid at this position did not improve the phenotype, producing only 12.9% viable spores (Table 3-3). This result could mean either that T331 is not normally

phosphorylated, or more likely, that aspartic acid is not a good mimic for phosphate at this position.

The ability of the activation loop mutants to mediate *dmc1Δ* arrest was also analyzed. *dmc1Δ GST-mek1-T327A* and *dmc1Δ GST-mek1-T327D* both sporulated as well as *dmc1Δ GST-mek1-K199R* (a catalytically inactive version of Mek1) (Table 3-3). DSBs are repaired in these diploids and the spores are inviable (data not shown), indicating that these mutants are defective in the BSCR. These results suggest that *dmc1Δ* arrest requires a higher level of kinase activity than what is required for creating a BSCR in an otherwise wild-type meiosis. This could be because the BSCR functions only transiently in a *DMC1* diploid, whereas it must function constitutively in *dmc1Δ*-arrested cells to prevent repair off sister chromatids and consequently, meiotic progression and sporulation.

Untagged *mek1-T327D* exhibits higher spore viability than *mek1-T327A*, although the absolute number of viable spores is much lower than with *GST-mek1* mutants (Table 3-3). One explanation is that binding of predimerized Gst-Mek1 to phospho-Red1 results in a higher local concentration of the kinase compared to untagged Mek1 (bringing two kinase molecules to Red1 instead of one). Consistent with the low level of activity in the untagged activation domain mutants, no *dmc1Δ* arrest was observed (Table 3-3).

Examination of various double mutant combinations suggests that phosphorylation of T327 and/or T331 occur during meiosis. Although neither the T327A nor T331A single mutant decreases spore viability to the null level, *mek1-T327A T331A* produced 6.5% viable spores, equivalent to the catalytically inactive *mek1- K199R* mutant (Table 3-3) (DE LOS SANTOS and HOLLINGSWORTH 1999). Therefore, some functional redundancy exists between these two sites. If the presence of a negative charge at T327 is sufficient for Mek1 kinase activation, then aspartic acid at this position should bypass the requirement for phosphorylation at T331. However, this is not the case as *mek1-T327D T331A* resembles *mek1-T331A*, not *mek1-T327D* (Table 3-3). Therefore the function of T331 phosphorylation is not simply to promote phosphorylation of T327. *mek1-T327D T331D* generates significantly more viable spores than either *mek1-T327D T331A* or *T327A T331D*, as well as exhibiting partial *dmc1Δ* arrest, suggesting that negative charges at both positions promote Mek1 activation (Table 3-3).

Mek1 is phosphorylated on T327 and T331 in meiotic cells. To obtain direct biochemical evidence that T327 and/or T331 are phosphorylated on Mek1 during meiosis, mass spectrometry was used to map phosphorylation sites on Gst-Mek1 purified after 5 hours in Spo medium. A *dmc1Δ* diploid was used because Mek1 is constitutively active during *dmc1Δ* arrest to prevent

DMC1-independent repair of DSBs (WAN *et al.* 2004). Therefore *dmc1Δ* provides a way of synchronizing meiotic cells at a time after Mek1 has been activated. After glutathione sepharose precipitation and elution, Gst-Mek1 was fractionated by SDS-PAGE and the protein cut out of the gel and digested with trypsin. The Mek1 peptides were subjected to phosphorylation analysis by LC-MS/MS techniques (PENG and GYGI 2001). Phosphopeptides were identified by database searching using the Sequest algorithm. A doubly-phosphorylated peptide was identified with the sequence, MHT*VVGT*PEYCSPEVGFR. The phosphorylated threonines in this peptide are T327 and T331, respectively. Both monophosphorylated forms of the peptide were also found (Figure 3-1B). A tandem mass spectrum for each event is shown in Figure 3-1C and D. Combining the genetic and biochemical data, these experiments demonstrate that phosphorylation of the Mek1 activation domain is essential for accurate chromosome segregation during meiosis.

Phosphorylation of T327 is dependent upon DSBs and Hop1/Red1/Mek1 complexes. T327 is contained within the peptide KXRXXT, which after being phosphorylated, matches the recognition site of the commercially available phospho-(Ser/Thr) Akt Substrate Antibody (MARTE and DOWNWARD 1997). Gst-Mek1 was partially purified from meiotic cells and probed on immunoblots with the Akt antibodies. A strong signal was detected

from the strain carrying *GST-MEK1* but not from *mek1Δ* (Figure 3-2). The blot was stripped and then reprobed with α-Gst antibodies to confirm that the protein being analyzed is Gst-Mek1 (Figure 3-2). No signal was detected for either *Gst-mek1-T327D* or *Gst-mek1-T327A*, indicating that the antibody is specifically recognizing phosphorylation at T327 (Figure 3-2, data not shown). The Akt antibodies therefore provide a means of probing the activation state of Mek1 *in vivo* under various mutant conditions.

REC104 encodes a meiosis-specific protein that is required to generate DSBs (PECINA et al. 2002). No phospho-T327 was detected in Gst-Mek1 partially purified from a *rec104Δ* diploid after 4.5 hr in Spo medium (Figure 3-2). [(In strains that reduce or abolish T327 phosphorylation, a faint band is sometimes observed that migrates slightly faster than Gst-Mek1 (Figure 3-2). However, because this band is not reproducibly observed in other experiments, it is unlikely to be phosphorylated Gst-Mek1 (data not shown)]. The failure of Gst-Mek1 to be phosphorylated at T327 in *rec104Δ* diploids indicates that DSBs are required for Mek1 activation.

Hop1/Red1/Mek1 complexes can be disrupted by a variety of mutations. Deletion of either *HOP1* or *RED1* destroys the complex, and Gst-Mek1 fails to undergo T327 phosphorylation in both cases (Figure 3-2). In addition there are mutants that interfere with specific parts of the complex. For example,

GST-mek1-R51A contains a point mutation in the Mek1 FHA domain that specifically disrupts the interaction of Mek1 with phospho-Red1 (WAN *et al.* 2004). This mutation prevents T327 phosphorylation, indicating that Mek1 cannot be activated unless it is bound to Red1 (Figure 3-3). *red1-K348E* is specifically defective for interaction with Hop1 and this mutant exhibits a reduced amount of phospho-T327 (WOLTERING *et al.* 2000) (Figure 3-2). Finally, T327 is phosphorylated in *GST-MEK1::hop1-K593A* diploids, where the Hop1 C domain requirement for Mek1 dimerization has been bypassed by Gst, while other functions remain intact (Figure 3-2).

T327 phosphorylation requires Mek1 kinase activity. No *in vivo* T327 phosphorylation is observed when Mek1 is catalytically inactive (*GST-mek1-K199R*), indicating that Mek1 activates itself by autophosphorylation (Figure 3-2). Further evidence for this idea comes from the finding that Gst-Mek1 can phosphorylate T327 *in vitro*. To show this, Gst-Mek1 lacking *in vivo* T327 phosphorylation was first purified from *hop1Δ* and *rec104Δ* diploids. The beads containing the precipitated kinase were then split into two tubes containing kinase assay buffer. ATP was added to one tube and the proteins were incubated at 30° C for 30 min. The kinase incubated without ATP exhibits the *in vivo* phosphorylation state of Mek1, whereas the presence of ATP allows Mek1 phosphorylation to occur *in vitro*. Gst-Mek1 from wild-type is

phosphorylated *in vivo* on T327 but the Akt signal is increased after incubation with ATP, suggesting that additional phosphorylation of T327 is occurring *in vitro* (Figure 3-3). This idea was confirmed by observing that T327 is phosphorylated in the kinase purified from the *hop1Δ* and *rec104Δ* diploids only after incubation with ATP (Figure 3-3). No T327 phosphorylation was observed with *Gst-mek1-K199R* with or without ATP, demonstrating that both *in vivo* and *in vitro* T327 phosphorylation require Mek1 kinase activity, and are not due to a co-purifying kinase. These results suggest that Mek1 activates itself by autophosphorylation of T327.

The Akt antibodies were used to directly examine whether phosphorylation of T331 is required for T327 phosphorylation. *Gst-mek1-T331A* exhibited autophosphorylation of T327 *in vitro*, although the amount of phosphorylated kinase was less than that observed with *Gst-mek1-T331D*, which, in turn, was less than Gst-Mek1 (Figure 3-3B). Therefore it appears that a negative charge at T331 enhances the ability of Mek1 to phosphorylate itself at T327 but is not absolutely required.

***MEK1* function in *hop1-K593A* mutants is dependent upon dimerization.** A variety of correlative data from genetic experiments indicates that Mek1 dimerization mediated by the Hop1 C domain is important for kinase function. However biochemical experiments to detect Mek1 dimers by

co-immunoprecipitation experiments have thus far been unsuccessful. To confirm that dimerization is the critical function conferred by Gst when *GST-MEK1* suppresses *hop1-K593A*, a version of *MEK1* was created in which dimerization can be regulated. Addition of the human FK506 binding protein, FKBP, to a protein enables conditional dimerization by addition of a ligand containing two FK506 moieties (AP20187) to the medium (e. g., (WILTZIUS et al. 2005). Over-expression of *FKBP-MEK1* partially complements *mek1Δ* in either the absence or presence of ligand (76% and 70% viable spores, respectively), indicating that FKBP does not interfere with Hop1 C-domain promoted dimerization of Mek1. However, in the *hop1-K593A* background, *FKBP-MEK1* produced only 2% viable spores (65 tetrads) in the undimerized form. Addition of AP20187 to the culture increased spore viability to 40% (87 tetrads), demonstrating that dimerization of Mek1 enhances kinase function under these conditions.

The Mek1 C terminus contains a putative homo-dimerization domain. The Mek1 protein can be divided into three distinct domains: an FHA domain in the N terminus, a catalytic domain in the middle of the protein and a functionally uncharacterized 50 amino acid C terminal tail (pfam domain analysis, http://www.sanger.ac.uk/Software/Pfam/) (Figure 3-4A). Alignment of the C-terminal domains of Mek1 proteins from different fungal species reveals a

conserved sequence of approximately 20 amino acids located immediately downstream of the catalytic domain (Figure 3-4B). If this region allows *HOP1*-mediated dimerization of Mek1, then mutation of conserved amino acids within this domain should disrupt Mek1 function, and these defects should be suppressed by ectopic dimerization of Mek1 by Gst. Substitution of two conserved amino acids within the Mek1 C terminal tail with alanine (*mek1-I459A L460A*, hereafter referred to as *mek1-IL*) creates an allele of *MEK1* that is nearly null for both spore viability and *dmc1Δ* arrest (Table 3-4; Figure 3-5A). Furthermore, *mek1-IL* is defective in the BSCR, as evidenced by the repair of DSBs in the *dmc1Δ* background (Figure 3-5B and C). The IL mutations do not interfere with the catalytic activity of Mek1 as the spore viability and *dmc1Δ* arrest defects of *mek1-IL* are suppressed if the allele is fused to *GST* (Table 3-4; Figure 3-5A). DSBs are unrepaired in *dmc1Δ GST-mek1-IL* diploids, indicating that the BSCR has been restored (Figure 3-5B and C). Ectopic dimerization mediated by Gst is required for suppression of the *mek1-IL* mutant. Mutations in *GST* that disrupt dimerization (*gst-RD-mek1-IL*) abolish suppression of *mek1-IL*, producing inviable spores and failing to arrest in the *dmc1Δ* background (NIU *et al.* 2005) (Table 3-4). Direct proof that this region of Mek1 confers dimerization awaits the development of a biochemical assay that can detect Mek1 oligomers.

Phosphorylation of an amino acid within the Mek1 activation domain is

required to maintain *MEK1* function in *dmc1Δ*-arrested cells. Mass spectrometry of Gst-Mek1 not only confirmed that T327 and T331 are phosphorylated *in vivo*, it also revealed two previously unknown phosphorylation sites: serine 142 (S142) and serine 320 (S320). S142 is located between the FHA and catalytic domains of Mek1 while S320 resides within the activation loop (Figures 3-1 and 3-4). These serines were mutated in *MEK1* both individually (*mek1-S142A* and *mek1-S320A*) and in combination (*mek1-S142A S320A*) and tested for their ability to complement the spore inviability of *mek1Δ*. All three mutant alleles complemented nearly as well as *MEK1*, producing ≥ 93% viable spores, indicating that phosphorylation of these amino acids does not play a critical role in wild-type meiosis (Table 3-5). Given that the Gst-Mek1 protein used for mass spectrometry was purified from a *dmc1Δ* mutant, one possibility is that phosphorylation of S142 and/or S320 is specifically required in *dmc1Δ*-arrested cells. Therefore, the ability of the three mutants to maintain *dmc1Δ* arrest was also examined. *mek1-S142A* behaves like wild type in that it fails to sporulate in the *dmc1Δ* background (Table 3-5). The failure to identify a phenotype for the S142A mutation makes the functional significance of this phosphorylation unclear. In contrast, *mek1-S320A* and *mek1-S142A S320A* are partially defective in *dmc1Δ* arrest, allowing 58% and 56% sporulation, respectively (Table 3-5). Meiotic progression in the *mek1-S320A dmc1Δ* diploid

is nearly as efficient as the catalytically inactive *mek1-K199R dmc1Δ* diploid (Figure 3-6A). Mimicking the phosphorylated state by substitution of S320 with aspartic acid restores Mek1 function, as a *mek1-S320D dmc1Δ* mutant exhibits prophase arrest and only 4% sporulation (Table 3-5, Figure 3-6A). These experiments demonstrate that phosphorylation of S320 is important for Mek1 function specifically during *dmc1Δ* arrest.

To see what effect S320 phosphorylation has on inter-sister DSB repair, DSBs at the *YCR048w* recombination hotspot were monitored in *dmc1Δ*, *mek1-K199R dmc1Δ* and *mek1-S320A dmc1Δ* diploids up to 12 hr after transfer to Spo medium. As expected, DSBs were hyper-resected and unrepaired in the *dmc1Δ* diploid and the cells arrested in prophase (Figure 3-6). In contrast, DSBs were rapidly repaired in the *mek1-K199R dmc1Δ* and *mek1-S320A dmc1Δ* diploids (Figure 3-6C). Substitution of S320 with aspartic acid prevented *DMC1*-independent DSB repair (Figure 3-6B and C), indicating that a negative charge at this position is sufficient for Mek1 function. Because S320A has no phenotype in otherwise wild-type diploids, S320 phosphorylation appears only to be required to keep Mek1 functional and the BSCR active when resected DSBs are unable to invade homologous chromosomes.

Ectopic dimerization suppresses *mek1-S320A*. Fusion of *GST* to *mek1-S320A* restores *MEK1* function, reducing sporulation in the *dmc1Δ*

background (Table 3-5). Preventing Gst dimerization eliminates this suppression: *gst-RD-mek1-S320A* exhibits 64% sporulation in the *dmc1Δ* background and the spores are inviable, as expected if repair is occurring using sister chromatids as templates. Therefore one possible function for S320 phosphorylation is to stabilize Mek1 dimers when cells are arrested by the meiotic recombination checkpoint.

DISCUSSION

Mek1 function requires phosphorylation of conserved threonines in the Mek1 activation loop. Phosphorylation of specific conserved amino acids within the activation loops of protein kinases such as Protein Kinase A (PKA) and insulin receptor kinase (IRK) plays a crucial role in kinase activation. PKA and IRK are members of the RD family of protein kinases, in that they contain an arginine immediately upstream of an invariant catalytic aspartic acid residue within the kinase domain (JOHNSON et al. 1996). Structural studies of active and inactive forms of PKA and IRK have shown that phosphorylation of the activation loop can promote conformational changes that allow proper substrate recognition as well as facilitating the phosphoryl transfer step (HUSE and KURIYAN 2002; JOHNSON et al. 1996). Although in many cases, phosphorylation of a single amino acid within the activation loop is sufficient, there are examples

where two to three phospho-residues are required for maximum kinase activity (LI and MILLER 2006; PROWSE and LEW 2001).

Mek1 is a member of the RD kinase family. Alignment of the Mek1 activation domain sequences with other RD protein kinases identified two conserved threonines, T327 and T331. Phosphorylation of the equivalent threonines in many kinases is required for activation. Mutations in *MEK1* that prevent phosphorylation of T327 and/or T331 reduce spore viability, abolish *dmc1Δ* arrest and allow DSB repair in *dmc1Δ* diploids, indicating that these amino acids are functionally important during meiosis. Substitution of phospho-mimetic amino acids for T327 and T331 partially complements a *mek1Δ*, providing further support that the negative charge conferred by phosphorylation at these positions is important for kinase activation. Mass spectrometry analysis confirmed that T327 and T331 are phosphorylated *in vivo*. We conclude that Mek1 kinase activity is positively regulated by phosphorylation of the activation domain during meiosis.

Mek1 activation occurs by autophosphorylation. Mek1 kinase activity is required to suppress Rad51-mediated DSB repair between sister chromatids during meiosis, thereby promoting recombination between homologs (NIU *et al.* 2005; WAN *et al.* 2004). This suppression is only necessary where DSBs are created, when the choice of whether to invade the sister chromatid or the

homolog must be made. Because Mek1 kinase activity is required constitutively after DSB formation to prevent *DMC1*-independent repair, creation of a BSCR could be regulated at the level of Mek1 kinase activation. Hop1 is a DSB-dependent phosphoprotein and the C domain of Hop1 promotes Mek1 dimerization (NIU *et al.* 2005). Therefore DSB formation and Mek1 kinase activation could be coupled by Hop1-induced dimerization of Mek1, where dimerization enables kinase activation by phosphorylation of T327/T331 *in trans*. Attempts to test this idea using *in vitro* Mek1 autophosphorylation as the assay for kinase activation have been unsuccessful, however, in that mutants predicted to prevent kinase activation such as *rec104Δ* or *hop1Δ* exhibit little to no reduction in Gst-Mek1 kinase activity compared to wild-type (WAN *et al.* 2004) (data not shown). The Akt antibodies specifically detect phosphorylated T327 and therefore provide an alternative method for monitoring Mek1 kinase activation. Use of these antibodies revealed that Mek1 is able to phosphorylate itself on the activation loop during *in vitro* kinase reactions. The high levels of *in vitro* kinase activity observed for Gst-Mek1 purified from mutant strains can therefore be attributed, at least in part, to activation of the kinase in the test tube after being isolated from the cell extract. Gst-mek1 with alanine substitutions at both T327 and T331 exhibits ~ 60% of the kinase activity of wild-type Gst-Mek1 *in vitro* (C. Park and N. M. Hollingsworth, unpublished results). This result suggests that

the unactivated enzyme has some basal activity which may allow significant levels of autophosphorylation when concentrated by the Gst pulldown. Furthermore, at least *in vitro*, Mek1 is able to phosphorylate amino acids other than T327 and T331. For Mek1, therefore, *in vitro* kinase assays measuring autophosphorylation are not a good measure of kinase activation *in vivo*. The Akt antibodies circumvent this problem. The fact that both *in vivo* and *in vitro* T327 phosphorylation requires Mek1 catalytic activity indicates that Mek1 kinase activation is due to autophosphorylation.

***MEK1* function is dependent upon dimerization.** Autophosphorylation can occur either intramolecularly (*in cis*) or between different Mek1 molecules (*in trans*). Autophosphorylation *in trans* could explain the role that Mek1 dimerization plays in creating the BSCR. Although a physical interaction between Mek1 molecules has yet to be demonstrated biochemically, a large body of genetic evidence exists to support this idea. First, when protein fusions are generated between Mek1 and different affinity tags such as Gst, lexA or TAP, a correlation is observed between the ability of the fusion protein to suppress the *HOP1* C domain mutant, *hop1-K593A*, and the ability of the tag to dimerize. Second, mutations that disrupt Gst dimerization fail to suppress *hop1-K593A* but do not interfere with *MEK1* function (NIU *et al.* 2005). Third, *FKBP-MEK1* suppresses *hop1-K593A* only when dimerization is induced by addition of ligand.

This experiment indicates that dimerization is the function directly responsible for bypassing the requirement of the Hop1 C domain in the BSCR. Fourth, a *HOP1*-dependent putative dimerization domain within Mek1 has been identified in a conserved region of the kinase located immediately downstream of the catalytic domain. Mutations within this domain are non-functional in untagged Mek1, but can be suppressed by ectopic dimerization conferred by Gst.

Although our interpretation has focused on dimerization as a requirement for activation, an alternative possibility is that ectopic dimerization mediated by Gst or FKBP raises the threshold concentration of the kinase above the level required for autophosphorylation to occur. This idea is supported by the observation that pre-dimerized Gst-mek1 activation domain mutants exhibit higher levels of spore viability than untagged activation domain mutants. Biochemical detection of untagged Mek1 oligomers is necessary to distinguish between these two possibilities.

A model for Mek1 activation. Gst-Mek1 exhibits T327 phosphorylation in a *hop1-K593A* mutant, indicating that ectopic dimerization can bypass the requirement for the Hop1 C domain. Dimerization alone, however, is insufficient for Mek1 kinase activation. Although Gst-Mek1 is presumably constitutively dimerized in strains lacking DSBs, Hop1/Red1 or Red1/Mek1 complexes, no T327 phosphorylation is observed. Therefore dimerized Mek1 must be properly

localized to Hop1/Red1 complexes to become activated and this activation still requires DSBs. To explain these results, the following model for the regulation of Mek1 kinase activation is proposed. Hop1/Red1 complexes are bound to chromosomes prior to DSB formation, consistent with cytological data showing that both proteins localize to chromosomes in a *spo11Δ* mutant (SMITH and ROEDER 1997) (Figure 3-7-1). DSBs result in phosphorylation of both Red1 and Hop1 (Figure 3-7-2). Although DSB-dependent phosphorylation of Hop1 has been demonstrated (NIU *et al.* 2005), Red1 is already phosphorylated in the absence of breaks (L. Wan and N. M. Hollingsworth, unpublished results) and therefore DSB-dependent hyperphosphorylation of Red1 may be difficult to detect. Mek1 is then recruited to hyperphosphorylated Red1 via the Mek1 FHA domain (Figure 3-7-3). Cytological experiments indicate that Mek1 co-localization with Red1 is dependent upon *SPO11* (and therefore DSBs), consistent with this idea (B. Rockmill, personal communication). Once bound, phosphorylated Hop1 C domains promote Mek1 dimerization (Figure 3-7-4). Dimerization enables Mek1 kinase activation by autophosphorylation of T327 and T331 *in trans* (Figure 3-7-5). The Mek1 FHA-phospho-Red1 interaction may be necessary to position the kinase molecules for autophosphorylation in the dimerized state. Once activated, the kinase must still be properly localized to function. *GST-mek1-R51A-T327D*, a constitutively active allele of Mek1 that is

unable to bind to phospho-Red1, produces inviable spores (C. Park and N. M. Hollingsworth, unpublished results). Proper Mek1 localization may be necessary for phosphorylation of target proteins.

Our model for Mek1 activation in response to DSBs shares similarities with activation of the checkpoint kinase, Rad53, in response to DNA damage (PELLICIOLI and FOIANI 2005). Mek1 resembles Rad53 in being a kinase with an FHA domain (although Rad53 has two). When DNA damage occurs in vegetative cells, Mec1 kinase is activated and phosphorylates Rad9 (SCHWARTZ et al. 2002). FHA domains on Rad53 bind to phospho-threonines on Rad9, which serves as an adaptor protein that allows Mec1 phosphorylation of Rad53 (SWEENEY et al. 2005). Binding to Rad9 increases the local concentration of Rad53, thereby allowing auto-phosphorylation in trans (GILBERT et al. 2001). The *S. pombe* ortholog of Rad53, Cds1, similarly requires multiple steps for activation. In this case, Cds1 is recruited to DNA damage by binding Mrc1, after Mrc1 has been phosphorylated by Rad3 (the *S. pombe* Mec1) ortholog. Both phosphorylation of Cds1 by Rad3 and dimerization-induced autophosphorylation *in trans* of threonines in the activation domain are then required for Cds1 activation (XU et al. 2006). Unlike Rad53 and Cds1, however, phosphorylation by other kinases outside of the activation segment does not appear to be necessary for Mek1 activation. Mass spectrometry of Mek1 purified from meiotic cells detected

only four phospho-amino acids. Of these, phosphorylation of T327 and T331 are required for activation, S320 is required only under *dmc1Δ*-arrested conditions and S142 has no obvious phenotypes. Nevertheless, it is intriguing to note that similar mechanisms for kinase activation may either promote repair of DNA damage in vegetative cells (Rad53 and Cds1) or suppress inter-sister recombination in meiotic cells (Mek1).

Additional phosphorylation of the activation domain is required to maintain the BSCR in *dmc1Δ*-arrested cells. Mass spectrometry revealed an additional phosphorylation site with a previously unsuspected role in meiosis. S320 is located within the Mek1 activation domain (Figure 3-1). Substitution of Mek1 S320 with alanine results in no apparent phenotypes in an otherwise wild-type diploid, but allows *dmc1Δ* diploids to sporulate. The failure of *mek1-S320A dmc1Δ* cells to arrest could result from bypassing the need for *DMC1* in interhomolog recombination, as has been observed either when *RAD51* or *RAD54* is over-expressed or *HED1* is deleted (BISHOP *et al.* 1999; TSUBOUCHI and ROEDER 2003; TSUBOUCHI and ROEDER 2006). In these situations, interhomolog recombination enables proper meiotic chromosome segregation and the production of viable spores. The spores produced in *dmc1Δ* strains containing *mek1-S320A* are dead, however, ruling out this explanation. Alternatively, phosphorylation of S320 could be required for *MEK1* to function in the meiotic

recombination checkpoint (ROEDER and BAILIS 2000; XU *et al.* 1997). In this case, disruption of the checkpoint would allow meiotic progression without DSB repair, producing dead spores as a result of broken chromosomes. However, DSBs are efficiently repaired in *mek1-S320A dmc1Δ* diploids, indicating that the meiotic progression observed in this strain is not due to a defect in Mek1's checkpoint function but instead to the failure of Mek1 to create a BSCR. The *dmc1Δ* arrest and unrepaired breaks are restored if S320 is substituted with a phospho-mimetic amino acid, demonstrating that a negative charge at this position is necessary for *MEK1* function under these conditions. *mek1-S320A* is therefore defective in suppressing inter-sister DSB repair, but only when cells are arrested by the absence of *DMC1*.

Ectopic dimerization bypasses the need for S320 phosphorylation, as addition of *GST* to *mek1-S320A* restores the *dmc1Δ* arrest. Phosphorylation of S320 could promote the initial dimerization of Mek1 in response to DSBs. However this seems unlikely given that *mek1-S320A* alone produces highly viable spores and therefore must be capable of generating a BSCR in otherwise wild-type cells. A more likely explanation is that phosphorylation of S320 is required to maintain Mek1 in the dimerized state after a BSCR has been established. Inactivation of Mek1-as by addition of inhibitor to a *mek1-as dmc1Δ* diploid results in a rapid repair of DSBs, indicating that Mek1 must be

constitutively active to prevent Rad51-mediated strand invasion of sister chromatids during meiosis (WAN *et al.* 2004). The requirement for dimerized, active Mek1 may be relatively brief in wild-type cells, where the need for a BSCR is removed once strand invasion of the homolog has occurred. In contrast, the prolonged arrest triggered by *dmc1Δ* may require continuous reinforcement of the dimerized and active state for Mek1, a process facilitated by phosphorylation of S320. Consistent with this idea, *GST-mek1-T327D* has sufficient activity to create viable spores in an otherwise wild-type meiosis, but has a level of activity insufficient to maintain *dmc1Δ* arrest. The maintenance of the dimerized state may be necessary either because phosphatase removal of the T327 and T331 phosphates requires continuous autophosphorylation to keep Mek1 activated or because dimerized Mek1 is necessary for efficient phosphorylation of the target proteins that create the BSCR.

In summary, phosphorylation plays a key role in suppressing DSB repair between sister chromatids during meiosis. Hop1 is a DSB-dependent phospho-protein and Mek1 recruitment to Hop1/Red1 complexes requires phospho-Red1. Once dimerized, Mek1 activates itself by autophosphorylation of conserved residues in the activation loop. Maintenance of the dimerized state may require additional phosphorylation of the activation loop, whether by Mek1 or another kinase is not yet clear. Finally, Mek1 phosphorylation of unknown

proteins specifically suppresses inter-sister DSB repair in meiosis.

Table 3-1. Plasmids.

Name	Yeast genotype	Source
pRS402	*ADE2*	(Brachmann *et al.* 1998)
pTS30	*GST-MEK1 ADE2*	(de los Santos and Hollingsworth
pTS31	*GST-mek1-K199R ADE2*	(de los Santos and Hollingsworth
pTS32	*GST-mek1-T327A ADE2*	(Wan *et al.* 2004)
pTS33	*GST-mek1-T327D ADE2*	(Wan *et al.* 2004)
pTS30-T331A	*GST-mek1-T331A ADE2*	This work
pTS30-T331D	*GST-mek1-T331D ADE2*	This work
pTS30-AA	*GST-mek1-T327A T331A ADE2*	This work
pTS30-AD	*GST-mek1-T327A T331D ADE2*	This work
pTS30-DA	*GST-mek1-T327D T331A ADE2*	This work
pTS30-DD	*GST-mek1-T327D T331D ADE2*	This work
pHN26	*GST-mek1-K199R URA3*	(Niu *et al.* 2005)
pHN31	*GST-mek1-T327A URA3*	This work
pHN32	*GST-mek1-T327D URA3*	This work
pHN33	*GST-mek1-T331A URA3*	This work
pHN34	*GST-mek1-T331D URA3*	This work
pHN35	*GST-mek1-T327D T331D URA3*	This work
pTS30-R51A	*GST-mek1-R51A ADE2*	(Wan *et al.* 2004)
pTS30-R72P D76K	*gst-R72P D76K-MEK1 ADE2*	(Niu *et al.* 2005)
pRS306	*URA3*	(Sikorski and Hieter 1989)
pBL12	*GST-MEK1 URA3*	(Niu *et al.* 2005)
pBL12-S320A	*GST-mek1-S320A URA3*	This work
pHN38	*gst-R72P D76K-mek1-S320A URA3*	This work
pLT11-K593A	*hop1-K593A URA3*	(Niu *et al.* 2005)
pSB3-K348E	*red1-K348E URA3*	(Woltering *et al.* 2000)
pLP37	*MEK1 URA3*	(de los Santos and Hollingsworth
pLP36	*mek1-K199R URA3*	(de los Santos and Hollingsworth
pTS9	*mek1-T327A URA3*	This work
pTS15	*mek1-T327D URA3*	This work
pHN36	*mek1-T331A URA3*	This work
pHN37	*mek1-T331D URA3*	This work
pLP37-S142A	*mek1-S142A URA3*	This work
pLP37-S320A	*mek1-S320A URA3*	This work
pLP37-S142A S320A	*mek1-S142A S320A URA3*	This work
pLP37-S320D	*mek1-S320D URA3*	This work
pLP37-IL	*mek1-I459A L460A URA3*	This work
pEJ2	*GST-mek1-I459A L460A URA3*	This work
pEJ4	*gst-R72P D76K-mek1-I459A L460A URA3*	This work
pNH131	*rec104Δ::LEU2*	(Hollingsworth and Johnson 1993)
pHN30	*FKBP-MEK1 ADE2 2m*	This work

Table 3-2. Strains.

Strain	Genotype	Source
YTS1	*MATa leu2DhisG his4-X ARG4 ura3 lys2 hoD::LYS2 mek1D::LEU2* *MATa leu2-K HIS4 arg4-Nsp ura3 lys2 hoD::LYS2 mek1D::LEU2*	(de los Santos and Hollingsworth 1999)
YTS1ade	Same as YTS1, only *ade2-Bgl*	(de los Santos and Hollingsworth 1999)
NH520	*MATa leu2::hisG his4-X dmc1Δ::LEU2 hoΔ::LYS2 lys2 ura3 mek1Δ::kanMX6* *MATa leu2::hisG his4-B dmc1Δ::LEU2 hoΔ::LYS2 lys2 ura3 mek1Δ::kanMX6*	(Wan *et al.* 2004)
NH561	*MATa leu2-K HIS4 hoΔ:: LYS2 lys2 ura3 arg4-Nsp mek1Δ::kanMX6 rec104Δ::LEU2* *MATa leu2DhisG his4-x hoDLYS2 lys2 ura3 ARG4 mek1D::kanMX6 rec104Δ::LEU2*	This work
NH566	*MATa leu2 HIS4 lys2 hoΔ::LYS2 ura3 ade2 arg4 hop1::LEU2 mek1Δ::LEU2* *MATa leu2 his4 lys2 hoΔ::LYS2 ura3 ade2 arg4 hop1::LEU2 mek1Δ::LEU2*	(Niu *et al.* 2005)
NH423	*MATa leu2-k HIS4 hoΔ::LYS2 lys2 ura3 arg4-Nsp ade2-Bgl mek1Δ::LEU2 red1Δ::kanMX6* *MATa leu2ΔhisG his4x hoΔ::LYS2 lys2 ura3 ARG4 ade2-Bgl mek1Δ::LEU2 red1Δ::kanMX6*	(Wan *et al.* 2004)

Table 3-3. Spore viability of various mutants in the Mek1 activation loop. (Some data contributed by Caroline Park.)

MEK1 genotype[a]	% spore viability (#asci)[b]	% sporulation in *dmc1Δ* [c]
mek1Δ	6.8 (108)	70.7 ± 8.6
GST-mek1-K199R	7.4 (91)	ND
GST-MEK1	87.8 (39)***	0 ± 0
GST-mek1-T327A	35.5 (105)***	69.2 ± 16.3
GST-mek1-T327D	73.3 (104)***	72.2 ± 15.8
GST-mek1-T331A	20.1 (108)***	71.8 ± 16.4
GST-mek1-T331D	12.9 (101)*	73.7 ± 12.4
GST-mek1- T327A T331A	6.5 (106)	ND
GST-mek1-T327D T331A	6.8 (96)	ND
GST-mek1-T327A T331D	6.6 (102)	ND
GST-mek1-T327D T331D	15.4 (117)**	51.3 ± 11.5
MEK1	96.2 (26)***	1.3 ± 1.1
mek1-K199R	<1.0 (26)	65.5 ± 0.5
mek1-T327A	<0.3 (104)	80.0 ± 4.3
mek1-T327D	4.3 (104)***	80.3 ± 4.6
mek1-T331A	2.9 (104)**	81.0 ± 0.5
mek1-T331D	2.4 (104)	71.3 + 6.4

[a]For spore viability of *GST-mek1* mutants, *ADE2* plasmids were integrated into YTS1ade. For untagged mek1 alleles, *URA3* plasmids were integrated into YTS1. For analysis of *dmc1Δ* arrest, *URA3 GST-mek1* and *URA3 mek1* plasmids were integrated into NH520.

[b]To assess spore viability, transformants were patched onto minimal medium lacking either adenine or uracil, replicated to Spo plates, incubated at 30o for 24 hr and then dissected. Asterisks indicate spore viability values that are statistically significantly increased compared to *mek1*Δ based on χ2-analysis. * = $p < 0.01$; ** = $p < 0.001$; *** = $p < 0.0001$. χ2 analysis was performed using software present at http::://faculty.vassar.edu/lowry/tab2X2.html. For *mek1-T331D*, there were insufficient data to perform the χ2-analysis.

[c]To monitor sporulation, transformants were patched onto SD-uracil plates, replica plated to Spo medium for 24 hr at 30^{o} and 200 cells were assayed for asci formation by phase contrast light microscopy. Three transformants were analyzed for each plasmid. ND = no data.

Table 3-4. Spore viability and *dmc1Δ* arrest phenotypes of *mek1-IL* in the presence or absence of *GST.* (Contributed by Emily Job)

MEK1 genotype[a]	% spore viability (# asci)	% sporulation in *dmc1Δ* [b]
MEK1	97.9 (48)	1.8 ± 1.7
GST-MEK1	94.5 (50)	0.7 ± 0.8
mek1Δ	1.1 (44)	95.9 ± 2.3
mek1-IL	4.4 (120)	82.5 ± 11.6
GST-mek1-IL	67.2 (122)	1.6 ± 0.8
gst-RD-mek1-IL	2.1 (24)	88.4 ± 2.2

[a] Plasmids containing the indicated *MEK1* alleles were integrated either into YTS1 (*mek1Δ*) to measure spore viability or NH520 (*mek1Δ dmc1Δ*) to measure *dmc1Δ* arrest. *gst-RD* contains the R72P D76K mutations in *GST* that disrupt dimerization.

[b] Four independent transformants were transferred to Spo plates and incubated at 30^{o} for at least 24 hr. Asci formation was measured for 200 cells/transformant by phase contrast light microscopy.

Table 3-5. Spore viability and *dmc1Δ* arrest phenotypes of additional Mek1 phosphorylation site mutants

MEK1 genotype[a]	*DMC1*		*dmc1Δ*	
	% spore viability (#asci)	% sporulation[b]	% spore viability (#asci)	% sporulation[b]
MEK1	100.0 (13)	87.2 + 2.6	ND[c]	0.0 + 0.0
mek1-K199R	<2.0 (13)	89.8 + 1.8	<2.0 (13)	81.7 + 6.3
mek1-S142A	100.0 (13)	88.8 + 0.3	ND	0.5 + 0.5
mek1-S320A	93.6 (39)	85.7 + 5.5	3.9 (26)	58.0 + 5.3
mek1-S142A S320A	95.2 (79)	88.2 + 2.0	2.0 (13)	56.3 + 4.7
mek1-S320D	94.9 (39)	76.0 + 11.9	ND	4.1 + 3.2
GST-mek1-S320A	100.0 (13)	86.5 + 2.6	ND	1.3 + 1.4
gst-RD-mek1-S320A	89.4 (26)	82.2 + 8.4	4.8 (26)	63.7 + 5.3

[a] Plasmid containing the indicated *MEK1* allele were integrated into either YST1 (*mek1Δ*) or NH520 (*mek1Δ dmc1Δ*). *gst-RD* contains the R72P D76K mutations in *GST* that disrupt dimerization.

[b] Sporulation was measured by counting the number of asci present in 200 cells/transformant using phase contrast light microscopy. Three independent transformants were measured for all the alleles except *mek1-S320D* where six transformants were analyzed for each strain.

[c] ND, no data.

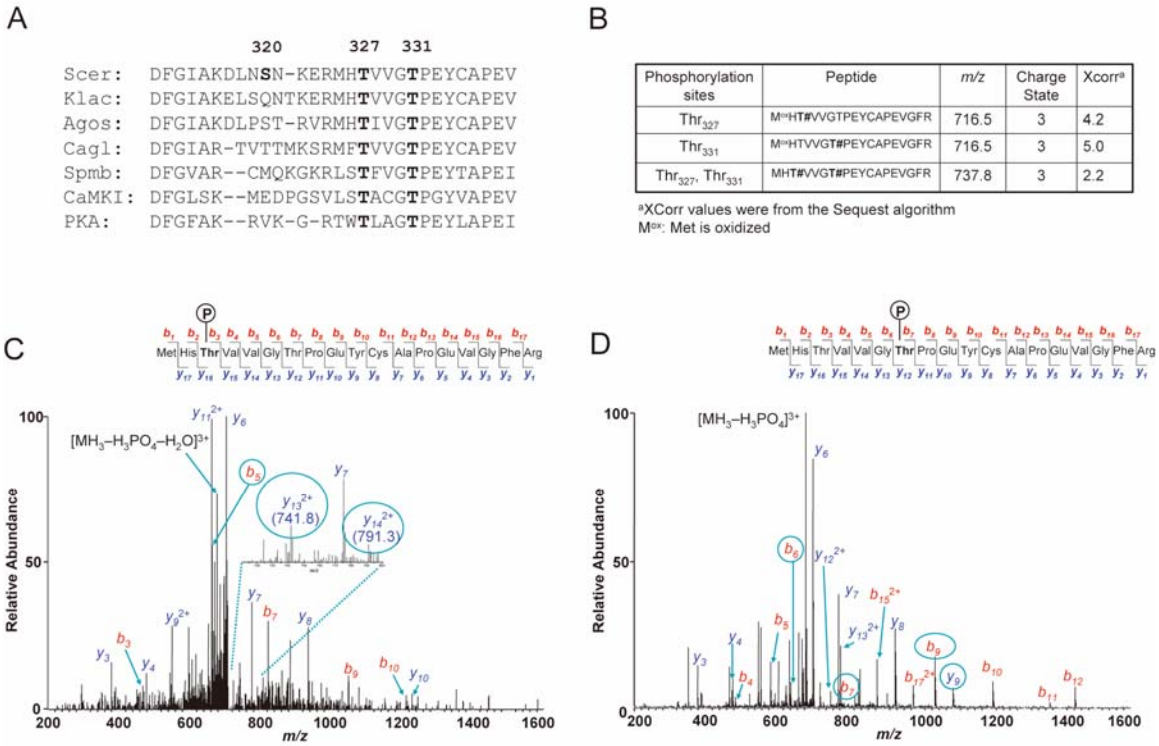

Figure 3-1. Mass spectrometry analysis of phosphorylated threonines in the Mek1 activation domain. (Contributed by Xue Li and Steven Gygi) A. Alignment of the T-loop region in Mek1 proteins from different fungal species. Bold letters indicate conserved threonines. Numbers indicate amino acid position in *S. cerevisiae* Mek1. Scer, *S. cerevisiae*; Scas, *S. castellii*; Agos, *Ashbya gossypii*; Klac, *K. lactis;* Cagl, *Candida gilbrata*; Spmb, *S. pombe*; CaMKI, calcium/calmodulin-dependent protein kinase I (from rat); PKA, cAMP-dependent protein kinase (from mouse). B. Summary of peptides detected phosphorylated at T327 and/or T331. "T#" indicates phosphorylated threonine. C – D. MS/MS spectra of monophosphorylated phosphopeptides showing site localization to either T327 (Panel C) or T331 (Panel D). These two phosphopeptides had different retention times and their fragmentation spectra were also different. Fragment ions used to determine site localization are circled. Cysteine residues were found as carboxyamidomethylated products and methionines were found in their oxidized state.

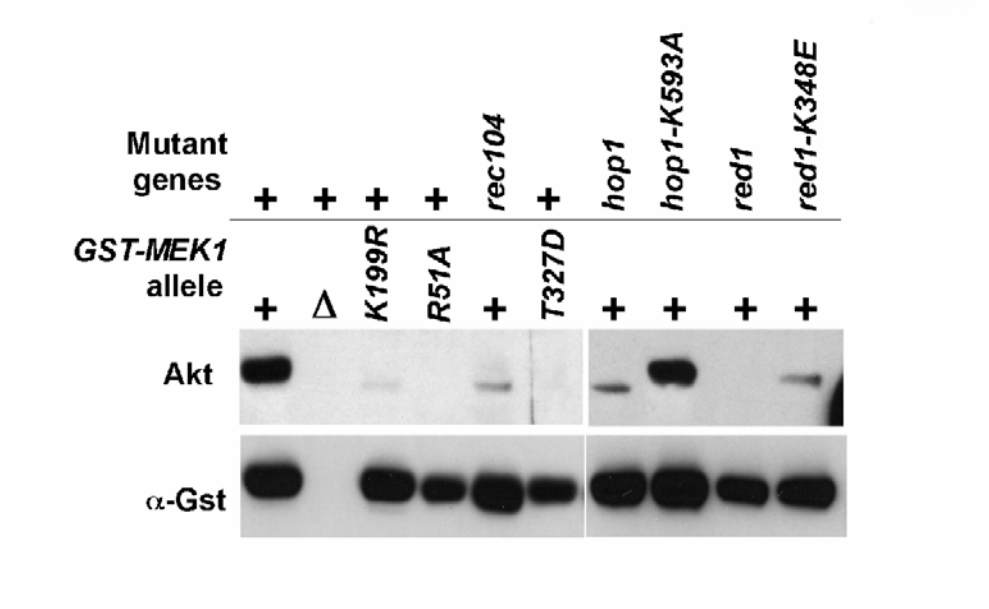

Figure 3-2. Mek1 T327 phosphorylation under different mutant conditions. Gst-Mek1 was partially purified from the indicated diploids after 4.5 hr in Spo medium at 30°. *GST-MEK1* (YTS1ade::pTS30), *mek1Δ* (YTS1ade::pRS402), *GST-mek1-K199R* (YTS1ade::pTS31), *GST-mek1-R51A* (YTS1ade::pTS30-R51A), *GST-mek1-T327D* (YTS1ade::pTS33), *GST-MEK1 rec104Δ* (NH561::pBL12), *GST-MEK1 hop1Δ* (NH566::pRS306::pTS30), *GST-MEK1 hop1-K593A* (NH566::pLT11-K593A::pTS30), *GST-MEK1 red1Δ* (NH423::pTS30::pSB3), *GST-MEK1 red1-K348E* (NH423::pTS30::pSB3-K348E). Proteins were fractionated by SDS-PAGE and probed with AKT antibodies, which specifically recognize phosphorylated consensus Akt kinase substrate sites ([R/K]X[R/K]XX[S/T]), to detect T327 phosphorylation. The blot was then stripped and reprobed with α-Gst antibodies to detect total Mek1 protein.

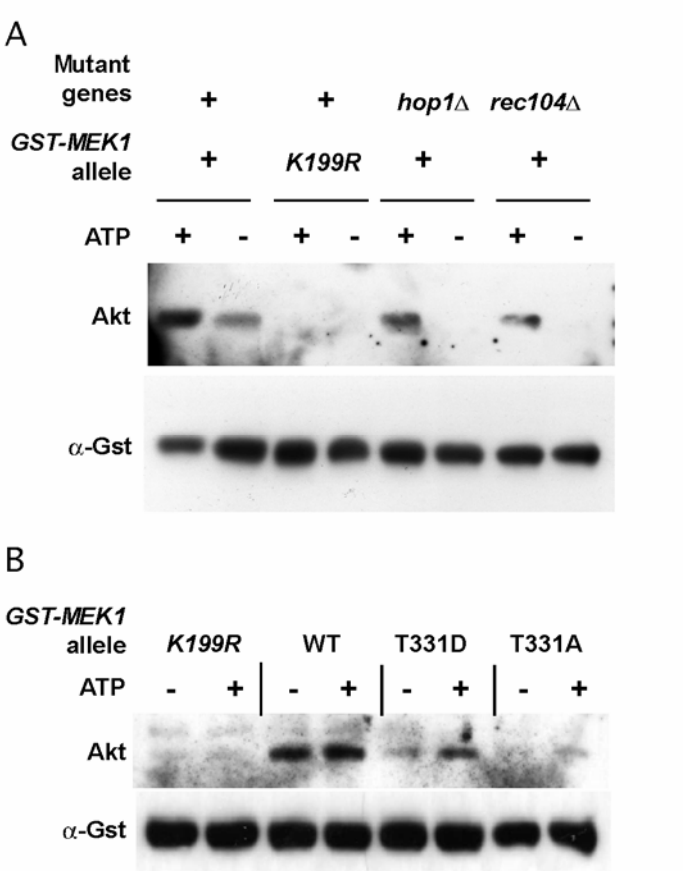

Figure 3-3. Comparison between *in vivo* and *in vitro* T327 phosphorylation of Gst-Mek1 isolated from different mutant diploids. A. Gst-Mek1 was partially purified from wild-type (YTS1ade::pTS30), *hop1Δ* (NH566::pRS306::pTS30) or *rec104Δ* (NH561::pBL12) diploids sporulated for 4.5 hr at 30°. As a control, Gst-mek1-K199R was purified from a wild-type strain (YTS1ade::pTS31) under the same conditions. The beads containing the precipitated kinase were washed, split in half and resuspended in kinase assay buffer at 30° for 30 min in the presence (+) or absence (-) of ATP. Phosphorylated T327 and total Gst-Mek1 were detected as described in Figure 2. B. Gst-Mek1 was partially purified from wild type (YTS1::pBL12), *GST-mek1-K199R* (YTS1::pHN26), *GST-mek1-T331D* (YTS1::pHN34) and *GST-mek1-T331A* (YTS1::pHN33) and processed as described in Panel A.

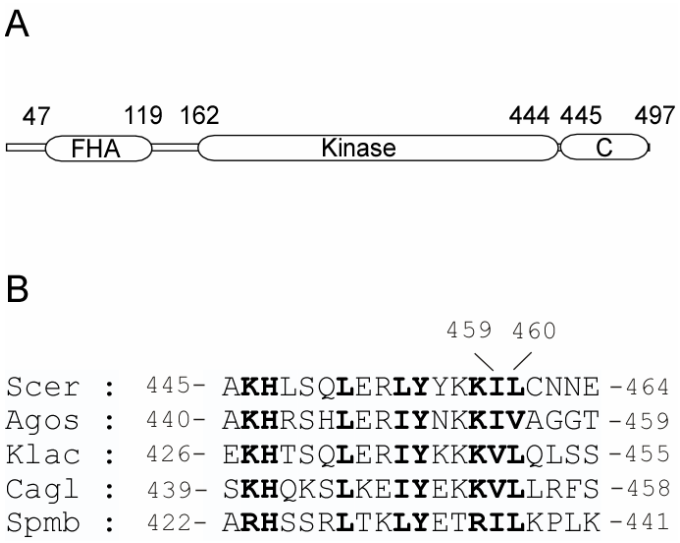

Figure 3-4. Functional domains of Mek1. A. Diagram indicating the positions of the FHA, catalytic and C terminal domains. B. Alignment of the sequences of the C terminal tails of Mek1 proteins from different fungal species. Bold letters indicate conserved residues. Asterisks mark I459 L460.

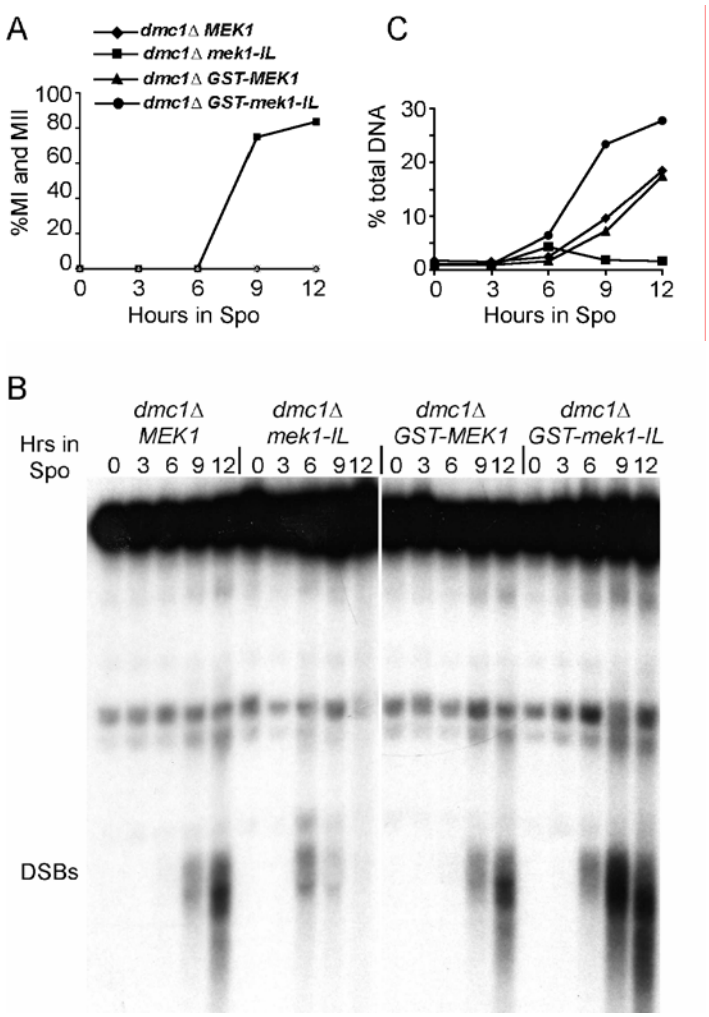

Figure 3-5. Meiotic timecourse analysis of *mek1-IL dmc1Δ* and *GST-mek1-IL dmc1Δ*. (Contributed by Emily Job) *MEK1 dmc1Δ* (NH520::pLP37), *mek1-IL dmc1Δ* (NH520::pLP37-IL), *GST-MEK1 dmc1Δ* (NH520::pBL12) and *GST-mek1-IL dmc1Δ* (NH520::pEJ2) were transferred to Spo medium at 30° C and timepoints were taken at 3 hr intervals. A. Meiotic progression measured by DAPI staining of cells to determine the fraction of binucleate (MI) and tetranucleate (MII) cells. 200 cells were counted for each strain at each timepoint. B. DSBs detected at the YCR048w hotspot on chromosome III. C. Quantitation of the DSB gel shown in B.

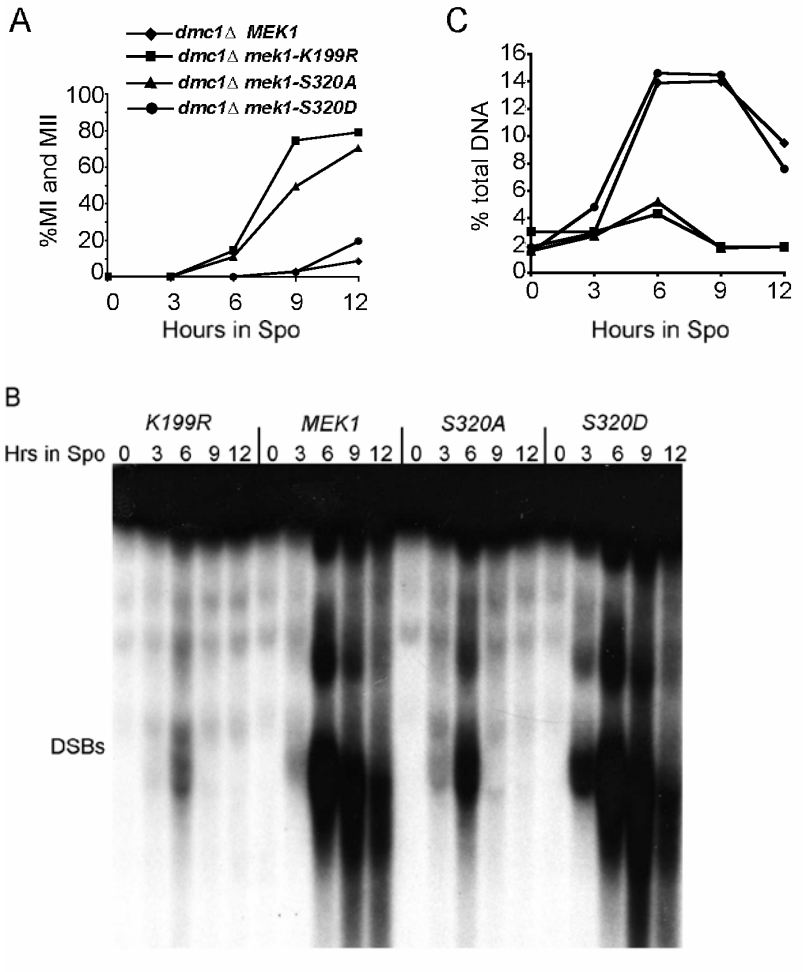

Figure 3-6. Meiotic timecourse analysis of *mek1-S320A dmc1Δ* and *mek1-S320D dmc1Δ*. *MEK1 dmc1Δ* (NH520::pLP37), *mek1-K199R dmc1Δ* (NH520::pLP36), *mek1-S142AS320A dmc1Δ* (NH520::pLP37-S320A) and *mek1-S320D dmc1Δ* (NH520::pLP37-S320D) were transferred to Spo medium at 30° C and timepoints were taken at 3 hr intervals. A. Meiotic progression measured by DAPI staining of cells to determine the fraction of binucleate (MI) and tetranucleate (MII) cells. 200 cells were counted for each strain at each timepoint. B. DSBs detected at the *YCR048w* hotspot on chromosome III. C. Quantitation of the DSB gel shown in B.

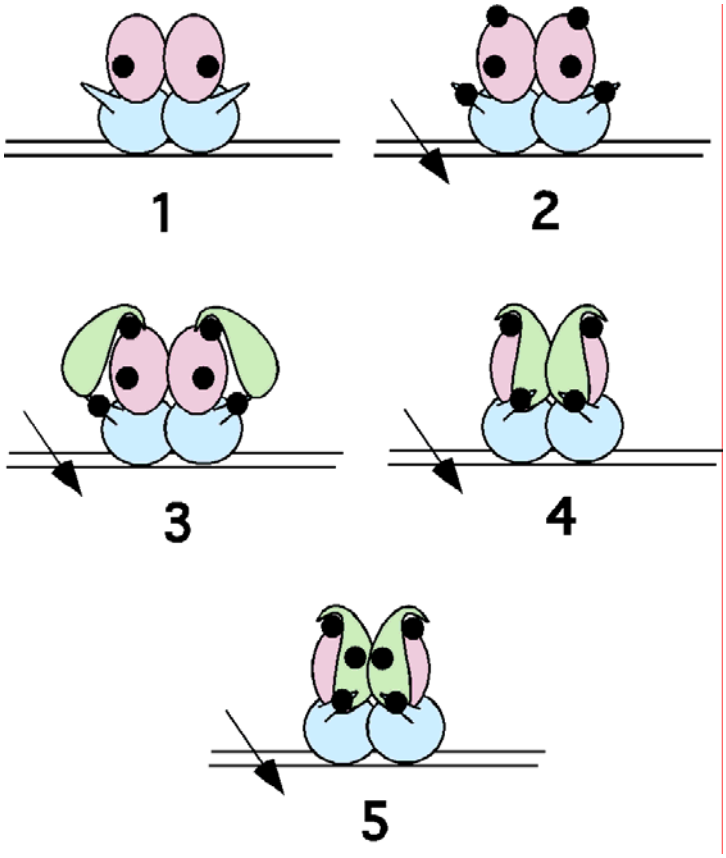

Figure 3-7. Model for Mek1 activation in response to meiotic DSBs. (Contributed by Nancy M. Hollingsworth) (1) Hop1/phospho-Red1 complexes are assembled onto chromosomes prior to DSB formation; (2) introduction of a DSB results in phosphorylation of the C domains of Hop1 molecules in the region of the breaks and additional phosphorylation of Red1; (3) DSB-specific phospho-amino acids on Red1 allow recruitment of Mek1 via the FHA domain; (4) phosphorylated Hop1 C domains promote dimerization of Mek1 (5) Mek1 is activated by autophosphorylation *in trans* of the activation-loop. Blue = Hop1, green = Mek1, red = Red1. Arrow indicates a DSB. Black circles indicate phosphates. Double line indicates DNA duplex of a chromatid.

CHAPTER FOUR

Identification of Mek1 Substrates

INTRODUCTION

Since Mek1 kinase activity is required for partner choice during meiotic recombination, identification of Mek1 substrates may elucidate how inter-sister DSB repair is suppressed during meiosis. I tried two approaches to identify Mek1 substrates. One was a candidate approach, where putative Mek1 targets were assayed for changes in protein mobility in the presence or absence of *MEK1* or for radioactive labeling of purified proteins in *in vitro* kinase reactions using soluble Gst-Mek1. In addition, I tried a more open-ended approach which was to identify proteins that co-purify with Mek1.

For the candidate approach, two categories of protein were selected:

1) Cohesion and recombination proteins: This category contains proteins that are important for mitotic inter-sister DSB repair, including cohesin subunits and recombination proteins that function during or before strand invasion. The interhomolog bias created during meiosis could be achieved if phosphorylation by Mek1 changes a property of one of the proteins.

When a DSB occurs during vegetative growth, the Rad50/Mre11/Xrs2 (MRX) complex gets loaded onto the break first. The break is then resected to generate 3' single strands of DNA (ssDNA) (SUN *et al.* 1991; WANG and HABER 2004). This

resection depends upon MRX complex (IVANOV *et al*. 1994; TSUBOUCHI and OGAWA 1998). ssDNA is coated by the trimeric replication protein A complex (RPA) which removes the secondary structures from ssDNA. The RPA complex is then replaced by recombinase Rad51. This replacement process requires Rad52 and two Rad51 related proteins, Rad55 and Rad57 (SONG and SUNG 2000; SUNG 1997b). Rad51 mediated strand invasion then occurs between sister chromatids in a process that also requires the SNF/SWI chromatin remodeling family protein Rad54 (JASKELIOFF *et al.* 2003; PETUKHOVA *et al*. 1998; VAN KOMEN *et al.* 2002). The break is then repaired either by synthesis dependent strand annealing (SDSA) which results in gene conversion or by a pathway that results in crossover (KROGH and SYMINGTON 2004). Mek1 could create a barrier by interfering with Rad51 function although recent experiments suggest that the BSCR is not that simple (see discussion).

Cohesin, a protein complex that mediates sister chromatid cohesion, contains four subunits, two structural maintenance of chromosome (SMC) family proteins - Smc1 and Smc3, together with two non-SMC family proteins – Scc3 and Mcd1 (Scc1). Smc1 and Smc3 form a heterodimer, which binds to Scc3 and Mcd1 to form a ring structure and hold sister chromatids together (GRUBER *et al.* 2003; HAERING *et al.* 2002). During meiosis, Mcd1 is replaced by a related protein Rec8 (BUONOMO *et al.* 2000; ZIERHUT *et al.* 2004). Normally, cohesin is loaded onto

centromere regions and chromosome arms during S phase and is maintained until anaphase, when Mcd1 is cleaved by separase to allow proper segregation of sister chromatids to opposite poles of the spindle (UHLMANN *et al.* 1999). The importance of cohesin in promoting intersister DSB repair was elucidated recently by the discovery that cohesin complexes load onto the ends of DSB in G2 arrested cells and promote inter-sister repair (STROM *et al.* 2004; UNAL *et al.* 2004). Besides the requirement for the cohesin loading Scc2/Scc4 complex, the DSB cohesin loading also requires Mre11, Rad53 and Mec1/Tel1 dependent H2A-S129 phosphorylation (STROM *et al.* 2004; UNAL *et al.* 2004). Given that cohesin has a role in intersister DSB repair in vegetative cells, one possibility is that Mek1 suppresses intersister recombination during meiosis by interfering with DSB cohesin-loading and/or function.

2) Condensins and Histones: These candidates are based on the idea that meiotic interhomolog bias might be established by forming a localized chromosome structure that prevents strand invasion of sister chromatids, thereby resulting in resected 3′ ends invading non-sister chromatids.

Histones are extensively modified and these modifications are important in regulating chromatin dynamics, so as to form euchromatin or heterochromatin (STRAHL and ALLIS 2000). During meiosis, when chromosomes undergo huge morphological changes, histone modifications are highly dynamic and closely

associated with different stages (IVANOVSKA and ORR-WEAVER 2006). Most histone phosphorylation is associated with chromosome condensation, such as H2A-S1, H2A-T119, H3-T3, H3-S10 and H3-S28 (AIHARA *et al.* 2004; GUO *et al.* 1995; HENDZEL *et al.* 1997). Through phosphorylation of one or multiple histones, Mek1 might promote local condensation of sister chromatids which is inhibitory to strand invasion.

Condensin contains five subunits - Smc2, Smc4, Ycg1, Ycs4 and Btn1 (Haering and Nasmyth 2003). Similar to cohesin complexes, the two SMC family condensin subunits Smc2 and Smc4 form a heterodimer and then bind to non-Smc subunits Ycg1, Ycs4 and Btn1 to form a ring structure (Haering and Nasmyth 2003). Besides directly functioning in chromosome condensation, the condensin complex promotes rDNA segregation during mitosis by resolving a cohesin-independent form of sister chromatid cohesion (D'AMOURS *et al.* 2004; SULLIVAN *et al.* 2004). Targeting of condensin also helps to maintain a balance of Sir2 between telomeres and nucleolus (MACHIN *et al.* 2004). Sir2 is relocalized from telomeres to nucleoli in condensin mutants, suggesting that condensin helps to arrange rDNA repeats into a heterochromatic-like structure. Similar structures could perhaps form on sister chromatids opposite to DSBs upon phosphorylation of condensin by Mek1 to prevent strand invasion.

MATERIALS AND METHODS

Plasmids. Plasmid names, genotypes and sources are listed in Table 4-1. Both *GST-MEK1* fusion and *TAP-MEK1* fusions are under the *MEK1* promoter. Details of plasmid construction are described as follows:

pHN10: A 0.5 kb fragment containing the tandem affinity purification (TAP) tag was amplified by PCR using pBS1761 (Euroscarf) as template and the primers TAP-NDE-5′ and TAP-RI-SAL-3′. The fragment has *Nde*I site and *Eco*RI, *Sal*I, *Xho*I sites engineered into the 5′ and 3′ ends, respectively. After digestion with *Nde*I/*Xho*I, the fragment was ligated to the 6.0 kb *Nde*I/*Xho*I pTS25 backbone to create pTS25-TAP. This ligation puts the TAP-tag under the control of *MEK1* promoter. A 1.3 kb *Not*I/*Xho*I fragment containing P_{MEK1}-TAP fusion from pTS25-TAP was subcloned into *NotI*/*Xho*I digested pRS306, generating pHN9. A 1.5 kb *Eco*RI/*Sa*lI fragment from pTS3-3 containing the *MEK1* coding sequence was then ligated with *Eco*RI/*Sal*I digested pHN9 to fuse *MEK1* inframe with P_{MEK1}-TAP (pHN10). Digestion of pHN10 with *Pst*I targets the plasmid to integrate at *ura3*.

pHN26: A 3.0 kb *Bam*HI/*Sal*I fragment from pTS31 containing *P_{MEK1}-GST-mek1-K199R* was ligated to *Bam*HI/*Sal*I digested pRS306 to make pHN26.

Primers: Primer sequences are listed in Table 4-2

Yeast strains. Strain genotypes are listed in Table 4-3.

NH678: *(YCG1-3HA mek1Δ)***:** S2683 mek1 b was mated to BLY09 to generate the diploid NH674 which has the relevant genotype (*leu2/leu2 HIS3/his3 YCG1/YCG1-HA3::his5*$^{+}$*(Sp) mek1::LEU2/MEK1*). NH674 was sporulated, dissected and the asci were screened for the presence of 2His^{+}:2His^{-} spores. These asci are non-parental ditypes (NPDs) and the His^{+} spores have the genotype *HIS3 YCG1-HA3::his5*$^{+}$*(Sp)*. From these His^{+} spores, *MATa* and *MATα leu*$^{+}$ containing *mek1Δ::LEU2* were selected and mated to give NH678.

NH629: *(YCS4-3HA mek1Δ)***:** S2683mek1ade was mated to 2892-1C to generate the diploid NH622 which has the relevant genotype (*leu2/leu2 HIS3/his3 YCS4/YCS4-HA3::his5*$^{+}$*(Sp) mek1::LEU2/MEK1*). NH622 was sporulated, dissected and the asci were screened for the presence of 2His^{+}:2His^{-} spores. These asci are non-parental ditypes (NPDs) and the His^{+} spores have the genotype *HIS3 YCS4-HA3::his5*$^{+}$*(Sp)*. From these His^{+} spores, *MATa* and *MATα* Leu^{+} containing *mek1Δ::LEU2* were selected and mated to give NH629.

NH680: *(SMC2-8myc mek1Δ)***:** S2683 mek1 b was mated to 2933-2C to generate the diploid NH675 which has the relevant genotype (*leu2/LEU2 SMC2/SMC2-8myc:KanMX4 mek1::LEU2/MEK1*). NH622 was sporulated, dissected and the asci were screened for the presence of 2 Leu^{+}: 2 Leu^{-} spores. These asci are non-parental ditypes (NPDs) and the Leu^{+} spores have the

genotype *LEU2 mek1Δ::LEU2*. From these leu$^+$ spores, *MATa* and *MATα* G418 resistant spores containing *mek1Δ::LEU2* were selected and mated to give NH680.

NH682: *(SMC4-3HA mek1Δ)***:** S2683 mek1 b was mated to BLY08 to generate the diploid NH673 which has the relevant genotype (*leu2/leu2 HIS3/his3 SMC4/SMC4-HA3::his5$^+$(Sp) mek1::LEU2/MEK1*). NH673 was sporulated, dissected and the asci were screened for the presence of 2 His$^+$:2 His$^-$ spores. These asci are non-parental ditypes (NPDs) and the His$^+$ spores have the genotype *HIS3 SMC4-HA3::his5$^+$(Sp)*. From these His$^+$ spores, *MATa* and *MATα mek1Δ::LEU2* strains were selected and mated to give NH682.

NH683: *(SMC1-3HA mek1Δ)***:** S2683 mek1 b was mated to 2823 to make diploid NH676, which has the relevant genotype (*leu2/leu2 SMC1/SMC1-3HA mek1Δ::LEU2/MEK1*) NH676 was sporulated, dissected and the asci containing four viable spores were screened for the presence of 2 Leu$^+$:2 Leu$^-$ spores. These asci are non-parental ditypes (NPDs) and Leu$^+$ segregants have the genotype *LEU2 mek1Δ::LEU2*. These Leu$^+$ spores were screened for *SMC1-3HA* by colony PCR using the primer pair Smc1F1/Smc1R1, which gives a product of ~500 bp for untagged haploids or an ~800 bp fragment for *SMC1-3HA* haploids. From these spores *MATa* and *MATα* strains were selected and mated to give NH683.

NH621: *(REC8-3HA mek1Δ)***:** RKY1145mek1Δade2 was mated to 4739 to generate diploid NH620 which has relevant genotype (*leu2/leu2*

REC8/REC8-3HA::KanMX4 mek1Δ::LEU2/MEK1). NH620 was sporulated and dissected. Spore colonies that were both Leu$^+$ and G418 resistant, *MATa* and *MAT*α strains were selected and mated to give NH621.

Purified proteins. Purified yeast histones (5 μg/μL) and yeast H2B (1 μg/μL) were provided by Dr. Xiaorong Wang from Dr. Rolf Sternglanz' lab. Recombination proteins purified from vegetative yeast cells, RPA (10 μg/μL), Rad51 (10 μg/μL), Rad52 (1.5 μg/μL) and Rad54 (4 μg/μL), were provided by Dr. Patrick Sung. Recombinant Rad54 (13 μg/μL) purified from *E.coli* was also provided by Dr. Sung. As a negative control, recombinant His_6-Hop1 (4.5 μg/μL) was affinity purified from bacteria (see below).

Site-directed mutagenesis of *RAD54*. Rad54 phosphorylation sites were mutated by site-directed mutagenesis (Quickchange kit, Strategene) using pNRB143 (*2*μ *RAD54*) as the template. **pNRB143-T58A** was made using the primer pair, RAD54-T58A-5'/RAD54-T58A-5'r (3') and the presence of the mutation was confirmed by sequencing using primer RAD54-T58SEQ. **pNRB143-T132A** was made using the primer pair, RAD54-T132A-5'/RAD54-T132A-5'r and the presence of the mutation was confirmed by sequencing using the primer RAD54-T132SEQ. **pNRB143-T132D** was made using the primer pair, RAD54-T132D-5'/RAD54-T132D-5'r and the presence of the mutation was confirmed by sequencing using the primer

RAD54-T132SEQ. **pNRB143-T231A** was made using the primer pair, RAD54-T231A-5′/RAD54-T231A-5′r and the presence of the mutation was confirmed by sequencing using primer RAD54-T231SEQ.

Primers for mutagenesis were diluted to a final concentration of 125 ng/μL. For each mutation, two to three reactions were set up independently. Each reaction contained 1 μL (100 ng) pNRB143, 5 μL 10 X Pfu buffer, 5 μL 2 mM dNTP, 1 μL 5′ primer, 1 μL 3′ primer and 37 μL dH_2O and 1 μL of Pfu turbo polymerase (Stratagene). The PCR cycle was: 95° C, 5 min; 16 cycles of 95° C, 40 sec; 55° C, 1 min and 68° C, 22 min. 3 μL were run on 0.8% TBE agarose gel to confirm the PCR had worked. 1 μL of *Dpn*I was added to each reaction to destroy the template plasmid. Then, 3 μL PCR product was transformed into DH5α. For each mutagenesis, plasmids were isolated from two or three Transformants (Qiagen Miniprep kit) and sent for sequencing to confirm mutations (DNA sequencing facility, Stony Brook University).

Purification of soluble Gst-Mek1. Gst-Mek1 was purified from the *dmc1Δ* diploid NH520::pBL12 (*GST-MEK1*) or NH520/pLW1 (*2μ GST-MEK1*). Each strain was sporulated for 5 hours at 30° C and then 50 mL were collected, washed once with 10 mL 25% glycerol, resuspended in 800 μL 25% glycerol, and frozen at -80° C. To make a lysate, cells were washed once with lysis buffer (50 mM Tris·HCl pH 7.5, 10 mM EDTA pH 8.0, 300 mM NaCl, 1 mM DTT, 1 mM PMSF, 1 μg/mL

Leupeptin, 1 μg/mL aprotinin, 1 μg/mL pepstatin, 10 mM NaF, 10 mM $Na_4P_2O_7$), resuspended in 1mL lysis buffer and transferred to a 12 mL Falcon tube. ~800 μL glass beads were added and the cells were vortexed at maximum speed for 30 sec intervals with 1 min incubation on ice for 6 times. After a 3-5 min incubation on ice, a further 6 rounds of vortexing were performed. The lysate was then transferred to a 2 mL microfuge tube and 10% Triton X-100 and 10% SDS were added to a final concentration of 0.5% (~ 80 μL) and 0.05% (~ 8 μL), respectively. The extract was incubated on a rotating platform at 4° C for 15 min and then clarified by centrifugation in a microfuge for 10 min at maximum speed at 4° C. 50 μL of glutathione S sepharose beads (1:1 slurry, GE Health Sciences) were equilibrated by washing once with lysis buffer and added to the lysate. After an additional 1.5 hour at 4° C on the rotating platform, the beads were pelleted, washed twice with lysis buffer and three times with elution buffer lacking glutathione (50 mM Tris-HCl pH 7.5, 200 mM NaCl, 1 mM DTT). Excess liquid was removed using a $30_{1/2}$ gauge needle. The beads were resuspended in 50 μL of elution buffer (50 mM Tris-HCl pH7.5, 200 mM NaCl, 1 mM DTT, 10 mM glutathione) and incubated for 10 min at room temperature. During this incubation, the beads were gently resuspended every 2 min by flicking. After pelleting the beads, the eluate containing soluble Gst-Mek1 was transferred to a new tube and used immediately for *in vitro* kinase assays.

***In vitro* kinase assays using soluble Mek1**. Three types of *in vitro* kinase experiments using soluble Mek1 were performed: 1) Mek1 autophosphorylation; 2) Radioactive assays monitoring Mek1 phosphorylation of candidate proteins; 3) Non-radioactive reactions used for mapping *in vitro* Mek1 phosphorylation sites on recombinant Rad54. The compositions of the 24 μL reaction system in each experiment are slightly different as described in Table 4-4. In the radioactive candidate tests, substrate proteins were diluted to 1 μg/μL with buffer containing 50 mM Tris-HCl pH 7.5, 200 mM NaCl and 1 mM DTT. In non-radioactive Rad54 labeling experiments, Rad54 purified from *E. coli* was diluted to 2.5 μg/μL with the same buffer as above. After addition of ATP, the reactions were incubated at 30° C for 30 min. Reactions involving radioactivity were stopped by adding 6 μL of 5 X protein sample buffer and heating the samples at 95° C for 5 min. 25 μL of reaction were then loaded onto an 8 % SDS-polyacrylamide gel, run at 6 mA for 14 hours, transferred to a nitrocellulose membrane and exposed to film or a phospho-imager screen. For non-radioactive Rad54 labeling experiments, kinase reactions were stopped by adding 10 μL of 3 X protein sample buffer [1:100 TCEP-HCl, Tris(2-Carboxyethyl) phosphine Hydrochloride, Pierce] to 10 μL kinase reaction and heating the samples at 95° C for 5 min. 10 μL of 50 mM Tris-HCl, pH 8.0, 100 mM iodoacetamide were added and the sample was incubated at room temperature for 30 min for reduction and alkylation of

cystidine residues. 15 μL sample containing ~500 ng phosphorylated Rad54 was fractionated using a 4-12% Bis-Tris NuPAGE gel (Invitrogen). The remainder was frozen at -80° C. After Gel-Code Blue straining (Pierce), the Rad54 band was cut out of the gel and sent to Dr. Gygi's lab for mass spectrometry analysis.

Purification of TAP-Mek1. The TAP-Mek1 purification was done under the supervision of Dr. Danesh Moazed in his lab at Harvard Medical School. One liter of NH520::pHN10 (*dmc1Δ TAP-MEK1*) cells were sporulated for 5 hours at 30° C. The cells were harvested by centrifugation for 10 min at 5,000 rpm using a GSA rotor (Sorvall) at 4° C, resuspended in 5 mL of 25% glycerol and frozen at -80° C. After thawing, the cells were resuspended in 10 mL of Buffer L (6 mM Na_2HPO_4, 4 mM $NaH_2PO_4.H_2O$, 1 % NP-40, 150 mM NaCl, 2 mM EDTA, 1 mM EGTA, 50 mM NaF, 4 μg/mL leupeptin, 0.1 mM Na_3VO_4 with freshly added 1 μg/mL each pepstatin, bestatin and aprotinin, 1 mM benzamidine, 1 mM PMSF) and then moved to a 50 mL chamber (BioSpec). Glass beads were added to fill up the chamber (around 10 mL). The cells were lysed by bead beating using 20 sec pulses with 1 min rests on ice for ten times. The lysate was transferred to a 40 mL Oakridge centrifuge tube. The beads were washed with 5 mL 1 X buffer L and the wash was pooled with the lysate. The extract was centrifuged at 15,000 rpm in a SS-34 rotor (Sorvall) for 25 min at 4° C. The supernatant was transferred to a 50 mL Falcon tube. 5 M NaCl was used to increase the NaCl concentration to 300

mM. After addition of 200 μL IgG-Sepharose beads (Amersham) which are pre-equilibrated with 1 X buffer L, the extract was incubated on a rotating platform at 4° C for 2 hours. The lysate with IgG beads was poured into a Biorad polyprep column with a reservoir. The beads were packed by gravity, washed three times with 10 mL buffer W (10 mM Tris-HCl, 150 mM NaCl, 0.1 % NP-40), and once with 10 mL TEV-C buffer (10 mM Tris-HCl, pH 8.0, 150 mM potassium acetate, 0.1 % NP-40, 0.5 mM EDTA, 5 % glycerol, 1 mM DTT). Column flow was blocked with a stopper and 1 mL TEV-C buffer containing 20 μL/mL of His_6-TEV (gift of Dr. Moazed) was added. The column was allowed to stand at room temperature for 1 hour and the eluate was collected into a new column that was sealed at the bottom. The beads in the original column were washed with 0.5 mL TEV-C and the wash was added to the original eluate. Three mL of CAM-B (10 mM Tris-HCl pH 8.0, 150 mM NaCl, 1 mM $Mg(OAc)_2$, 1 mM imidazole, 2 mM $CaCl_2$, 0.1 % NP-40, 5 % Glycerol, 10 mM 2-mercaptoethanol) and 3 μL of $CaCl_2$ per mL of TEV elution were added before adding 150 μL Calmodulin Sepharose beads. The column was then sealed at the top and incubated on a rotating platform at 4° C for 1 hour, drained by gravity and washed twice with 10 mL CAM-B. Mek1 calmodulin binding domain fusion product (CBP-Mek1) was serially eluted with 100 μL, 500 μL and 500 μL CAM-E (10 mM Tris-HCl pH 8.0, 150 mM NaCl, 1 mM $Mg(OAc)_2$, 1 mM Imidazole, 10 mM EGTA, 0.05 % NP-40, 5

% glycerol, 10 mM 2-mercaptoethanol). The second elution (500 μL) was split into half and 100% TCA (trichloroacetic acid) was added to final concentration of 20% (around 65 μL into 250 μL eluate) to precipitate CBP-Mek1 and any co-purifying proteins. After spinning in a microfuge at maximum speed (13,000 rpm) for 20 min at 4° C, the pellet was washed once with 100 % cold acetone and air dried. One sample was sent to Dr. Gygi's lab for mass spectrometry and the other half was resuspended in 1 X Protein Sample Buffer, fractionated on a 4-12% Bis-Tris NuPAGE Gel and silver stained to detect proteins.

Purification of recombinant His_6-Hop1 from *E.coli*. An overnight culture BL21 codon plus RIL (Stratagene) containing pET15b-HOP1 (*His_6-HOP1*), a fusion that is unlikely to be biologically active as other N-terminal tags of *HOP1* fail to complement *hop1Δ* (Dr. Nancy Hollingsworth, personal communication), was diluted 1:50 in 2 liter LB with 100 mg/L ampicillin and incubated on a shaker at 37° C until the OD_{660} of the culture reached 0.8. The culture was then cooled down to room temperature and *His_6-HOP1* expression was induced by adding 1 M IPTG to a final concentration of 0.3 mM and the culture was incubated on a shaker for 14 hours at room temperature. Cells were harvested and resuspended in 20 mL lysis buffer (20 mM Tris-HCl pH 7.5, 1 mM EDTA pH 8.0, 500 mM NaCl, 1 % Glycerol, 1 mM DTT, 1 μg/mL each pepstatin, bestatin and aprotinin, 1 mM benzamidine, 1 mM PMSF). A lysate was made using a French Pressure Cell

Press (SIM-AMINCO Spectronic Instrument.) at pressure between 1000 and 1500 psi and clarified by centrifugation at 15,000 rpm in a SS-34 rotor at 4° C for 20 min. 500 μL Ni-NTA sepharose beads, after equilibration with lysis buffer, were added to the supernatant, which then was incubated on a rotating platform for 1.5 hr at 4° C. The lysate with Ni-NTA beads was poured into a Biorad polyprep column with a reservoir. The beads were packed by gravity and washed 5 times with 10 mL lysis buffer. His_6-Hop1 was eluted with 5 mL elution buffer (20 mM Tris-HCl pH 7.5, 1 mM EDTA pH 8.0, 500 mM NaCl, 1 mM DTT, 200 mM imidazole). The eluate was dialysed using buffer containing 20 mM Tris-HCl pH 7.5, 1 mM EDTA pH 8.0, 100 mM NaCl, 1 mM DTT overnight and then loaded onto a Heparin column using an Akta purifier FPLC (Fast Protein Liquid Chromatography) (GE Health Science). His_6-Hop1 was eluted using 100 mL elution buffer (20 mM Tris-HCl pH 7.5, 1 mM EDTA pH 8.0, 1 mM DTT, 100-500 mM NaCl) with a NaCl gradient from 100 mM to 500 mM. Fractions containing His_6-Hop1 were collected and the presence of His_6-Hop1 was confirmed with western blot using α-Hop1 antibody (DE LOS SANTOS and HOLLINGSWORTH 1999). His_6-Hop1 was then concentrated to 4.5 mg/mL using a Centricon-30 column (Millipore).

Antibodies and Western blots. To make polyacrylamide gels for assaying mobility shifts of condensin and cohesin subunits, Tris-Acetate buffer was used

instead of Tris-HCl buffer. To detect HA tagged proteins, a 1:5000 dilution of purified 12CA5 monoclonal α-HA antibodies was used. To detect Myc tagged proteins, a 1:10 dilution of serum containing 9E10 monoclonal α-myc antibodies was used. To detect His_6-Hop1, a 1:5000 dilution of α-Hop1 antibodies was used.

RESULTS

A. Assaying candidate proteins for *MEK1*-dependent protein mobility shifts.

***MEK1* does not affect the protein mobility of several condensin and cohesin subunits.** To determine whether various condensin and cohesin subunits might be Mek1 substrates, protein mobilities of immuno-precipitated (IPed) target proteins were compared between *MEK1* and *mek1Δ* diploids using SDS-PAGE. Tagged proteins were IPed from 50 mL of culture collected at 4 hrs after transfer to Spo medium at 30° C, except for the condensin subunit Ycs4-3HA which was analyzed at three different time points. The IPed samples were fractionated using 8% tris-acetate SDS-PAGE, transferred onto nitrocellulose membranes and the tagged proteins were detected using either α-HA or α-Myc monoclonal antibodies. Mutation of *MEK1* has no effect on the mobility of the cohesion subunits, Smc1 and Rec8, nor on the condensin subunits Smc2, Smc4 and Ycg1 (Figure 4-1). A slight effect of *mek1Δ* on Ycs4 was seen at

eight hours (Figure 4-1), however, the significance of this shift is unclear since it occurs well after the time which Mek1 is required to function to produce viable spores (WAN *et al.* 2004). Rpa1, Rpa2, Mre11-13myc and Pds1-18myc were also examined, but no differences were observed for any of these proteins (Figure 4-1 and data not shown).

B. Assaying candidate proteins for *in vitro* phosphorylation using soluble Mek1.

Gst-Mek1 *in vitro* kinase assays are usually performed with precipitated Gst-Mek1 on glutathione sepharose beads (WAN *et al.* 2004). To assay whether purified candidate proteins are *in vitro* substrates of Mek1, a protocol was developed for obtaining soluble Gst-Mek1 (See Materials and Methods). *In vitro* autophosphorylation experiments confirmed soluble Gst-Mek1 is active (Figure 4-2A).

Yeast histones H2B and H4 are phosphorylated *in vitro* by Mek1. To test whether histones are Mek1 substrates, *in vitro* kinase assays were performed using 20 μL soluble Gst-Mek1 obtained from 50 mL sporulating culture and purified yeast histones. Phosphorylation of yeast histone H2B was individually tested by adding the same amount of soluble Gst-Mek1 and 1 μg purified H2B. After the kinase reaction, samples were fractionated on 15% SDS polyacylamide gels, transferred onto nitrocellulose membranes and exposed to film. To detect

the purified proteins on the blot, the membrane was subsequently stained with Ponceau S. Radioactive labeling of histones H2B and H4 was observed (Figure 4-2B). Purified histone H2B exhibited a radioactive doublet, despite the fact that no protein was detectable for the slower migrating species by Ponceau S staining. A band in this position was also observed with total histones. However, whether this is H3 and/or a modified form of H2B is not clear. To confirm that phosphorylation is due to Gst-Mek1 and not a co-purifying kinase, the *in vitro* kinase assay with purified H2B was repeated with a catalytically inactive version of Gst-Mek1, Gst-Mek1-K199R. The two phosphorylated bands observed in the H2B reaction are specific for active Mek1 and H2B (Figure 4-2C). Therefore, histones H2B and H4 are candidates for Mek1 phosphorylation *in vivo*.

Recombination proteins Rad52 and Rad54 are phosphorylated *in vitro* by Gst-Mek1. In collaboration with Dr. Patrick Sung's lab, I surveyed homologous recombination proteins for *in vitro* phosphorylation by Mek1. Hop1 is a *MEK1*-independent phospho-protein *in vivo* and I therefore purified His_6-tagged Hop1 as a negative control. Radioactive labeling of Rad52 and Rad54, but not Hop1, Rpa1 or Rad51 was detected in this assay (Figure 4-3A). Because of relatively strong signal obtained with Rad54, the experiment was repeated using Rad54 purified from bacterial cells. In this experiment, no phosphorylation was observed with Gst-Mek1-K199R, demonstrating that Mek1 is the responsible

kinase, rather than a kinase that either co-purifies with Gst-Mek1 or the Rad54 from yeast cells (Figure 4-3B). In addition, increasing the amount of Gst-Mek1 increased the amount of Rad54 phosphorylation (Figure 4-3B).

Threonines 58, 132 and 231 of Rad54 are phosphorylated by Gst-Mek1 *in vitro*. To determine whether Mek1 phosphorylation of Rad54 *in vitro* is functionally important, the phosphorylated residues on the bacterially purified Rad54 were first mapped by mass spectrometry. Gst-Mek1 was affinity purified from sporulating cells carrying either an integrated copy of *GST-MEK1* or a muticopy *GST-MEK1* plasmid. Soluble Gst-Mek1 was used in *in vitro* kinase assays containing Rad54 and non-radioactive ATP. The proteins were fractionated on a 4-12% Bis-Tris Novex Gel (Invitrogen) and stained with Gel-code Blue straining reagent (Pierce) (Figure 4-3C). The Rad54 band from the kinase reaction containing the highest level of Gst-Mek1 was cut out and sent to our collaborator, Dr. Xue Li in Dr. Gygi's lab (Harvard Medical School). The Rad54 band was digested with trypsin and the Rad54 peptides were subjected to phosphorylation analysis by LC-MS/MS techniques. Phosphopeptides were identified by database searching using the SEQUEST algorithm (PENG and GYGI 2001). Three phosphorylation sites were found: T58, T132 and T231. Given that the Rad54 used in this experiment was purified from bacteria and therefore starts out unphosphorylated and that Gst-Mek1-K199R exhibits only a background

level of Rad54 labeling (Figure 4-3B), the Rad54 phosphorylation sites identified by mass spectrometry must be due to Mek1.

Overexpression of *rad54-T132A* partially bypasses the requirement for *DMC1* in interhomolog repair of meiotic DSBs. To see whether Mek1 phosphorylation of either Rad54 T58, T132 or T231 is important during meiosis, these amino acids were mutated individually to alanine using a 2μ *RAD54* plasmid. The plasmids were transformed into *rad54Δ* diploid strain, NH460, already existing in the lab, for complementation tests. Wild type *RAD54* in this strain produces mostly a 2+ : 2- pattern of spore viability, indicating that the strain does not behave properly. A new *rad54Δ* diploid strain is therefore being constructed. Overexpression of *RAD54* has previously been shown to weakly suppress the interhomolog recombination, sporulation and spore viability defects of *dmc1Δ* diploids (BISHOP *et al.* 1999). In contrast, overexpression of *RAD51* strongly suppresses these phenotypes (Tsubouchi and Roeder 2003). We infer that the weak *RAD54* phenotype is an indirect effect of Rad54 stimulation of Rad51 activity (PETUKHOVA *et al.* 1999). The ability of the *rad54* phosphorylation mutants to suppress *dmc1Δ* was therefore tested. Consistent with the literature, overexpression of *RAD54* weakly suppresses the sporulation defect of *dmc1Δ* (Table 4-5). The phenotype of *rad54-T231A* is similar to *RAD54* making the *in vivo* relevance of this phosphorylation site unclear. *rad54-T58A* sporulates at the same

level as the vector control, suggesting that phosphorylation of this threonine may be necessary for Rad54 activity, but further experiments need to be done to reach a firm conclusion about this site. Overexpression of *rad54-T132A* allows *dmc1Δ* to sporulate to 51.2% (Table 4-5). In contrast, overexpression of *rad54-T132D*, a mutant allele that mimics phosphorylation at T132, restores the *dmc1Δ* arrest, reducing sporulation to 8.3%, which is close to the value observed for *RAD54*. These results provide genetic support for an *in vivo* role of phosphorylation at T132 during meiosis.

The ability of the *rad54-T132A dmc1Δ* cells to sporulate could be due to: 1) repair of DSBs using sister chromatids as templates; 2) interference with the meiotic recombination checkpoint; 3) repair of DSBs using non-sister chromatids as templates. The latter possibility can be distinguished because interhomolog repair should result in the production of viable spores. Asci produced by overexpressing *RAD54*, *rad54-T132A* and *rad54-T132D* all exhibited a frequency of viable spores of ~50%. In this way, *rad54-T132A* acts similarly to other situations that boost Rad51 activity, such as overexpression of *RAD51* or deletion of *HED1*. The high percentage of viable spores suggests that DSBs are being repaired using non-sister chromatids, suggesting that the *MEK1*-dependent BSCR is still functional. To test this hypothesis, the *rad54* mutants were overexpressed in a *dmc1Δ mek1Δ* diploid. Dissection of sporulated cells revealed

that all of the spores are dead (Table 4-5). Therefore Mek1 phosphorylation of Rad54-T132 *in vivo* may act to down-regulate Rad54 during meiosis, independent of Mek1's function in the BSCR.

C. Identification of TAP-Mek1 co-purifying proteins.

To affinity-purify Mek1, I used the tandem affinity purification (TAP) tag method, which was first published in 1999 as a tool to perform large scale proteomic analyses (RIGAUT *et al.* 1999). I obtained a plasmid, pBS1761, containing a TAP tag for making N-terminal fusions from Euroscarf. This TAP tag carries a calmodulin-binding peptide next to Protein A with a TEV protease cleavage site in between (Figure 4-4A). Protein A allows a first step purification with IgG resin (Figure 4-4B). TEV protease treatment releases the bound protein still fused to calmodulin binding domain (CBP-Mek1) (Figure 3-1C,D). The eluate containing CBP-Mek1 is then passed over a column containing calmodulin resin in the presence of calcium for a second step purification (Figure 3-1E,F). The TAP tag method has been successfully used to purify protein complexes from the budding yeast *S. cerevisiae* (GAVIN *et al.* 2002; LI *et al.* 2002; MILLER *et al.* 2001).

Rim4 co-purifies with TAP-Mek1 from meiotic cells. As an alternative approach for identifying putative Mek1 substrates, I looked for proteins that co-purify with Mek1 from meiotic yeast cells. A fully functional N-terminal *TAP-MEK1* fusion was generated in an integrating plasmid named pHN10. pHN10 was transformed into *dmc1Δ mek1Δ* strain, NH520. One liter of

sporulating cells was collected 5 hours after transfer to Spo medium and TAP-Mek1 was purified as described in the Materials and Methods. The final elution product was split into half, precipitated with TCA and washed once with 100% cold acetone. After drying, one sample was loaded onto a 4-12% Bis-tris NuPAGE gel to visualize the proteins (Figure 4-5), while the other half was sent to Dr. Xue Li in Dr. Gygi's lab for mass spectrometry. After trypsin digestion, the peptides were subjected to LC-MS/MS analysis on a LTQ mass spectrometer (Thermo Electron, San Jose, CA). The MS/MS of precursor ions was used to scan predicted mass spectra of trypsin digested budding yeast proteins to match the peptides and further identify the co-purified proteins. The copurified proteins with at least one peptide match are listed in table 4-6 and ranked by number of matched peptides. Most of them are ribosomal proteins, which are common contaminants of TAP purification. One protein, Rim4, is specifically expressed in meiosis (SOUSHKO and MITCHELL 2000). Mutation of *RIM4* leads to a meiotic arrest that can be partially suppressed by overexpression of hyperactive *IME2* kinase (Soushko and Mitchell 2000). Besides *MEK1*'s function in BSCR, *MEK1* is also an important checkpoint factor, which is required for meiotic arrest in various mutants that are defective in recombination or SC formation like *dmc1*, *zip1*, etc (XU *et al.* 1997). Therefore, *RIM4* could be a downstream *MEK1* effector to control meiotic progression.

DISCUSSION

Identification of Mek1 substrates in the BSCR by studying TAP-Mek1 co-purifying proteins. Characterization of TAP-Mek1 co-purifying proteins was not successful in identifying Mek1 substrates involved in establishing the BSCR. In our TAP-Mek1 purification, the soluble fraction was taken after making the cell lysate to continue. However, the BSCR protein, which is likely to be associated with chromatin may be largely present in the pellet fraction, therefore missed by our search. In addition, the failure to identified Mek1 substrates by looking for co-purified proteins with TAP-Mek1 could due to the fact that most kinase-substrate interactions are short-lived. Moreover, our current model predicts that Mek1 is activated only near DSBs (Niu *et al*. 2007). Therefore having only a relatively small fraction of Mek1 activated might lower the chances of identifying Mek1 substrates from co-purifying proteins. Being able to stabilize kinase-substrate interactions might greatly facilitate further attempts with this type of approach. Recently, mutations have been found in yeast cAMP dependent protein kinase (Tpk1) that stabilize interactions between Tpk1 and its substrates both in biochemical and yeast two-hybrid assays (DEMINOFF *et al.* 2006). These mutations are located near the C-terminus of Tpk1. One of these amino acids, *TPK1-R324*, is conserved in a large number of kinases, including Mek1 (data not

shown). If the corresponding mutation in *MEK1*, *mek1-R432A*, has the same effect of stabilizing interaction between Mek1 and its substrates, the *mek1-R432A* mutant could be used for TAP purification or a two-hybrid screen to isolate potential targets.

Cohesin and Condensin subunits as potential Mek1 substrates. Besides the affinity purification approach, several condensin and cohesion subunits were tested for *MEK1*-dependent mobility shifts, but this approach was not successful. Mobility shift experiments can be hard to interpret, especially for large proteins where a change in mobility may be difficult to detect. In addition, not all phosphorylation events cause changes in protein mobility. Therefore, it is hard to draw any firm conclusions from negative results using this approach. Another drawback with the candidate approach is that one must guess the right protein. One additional condensin subunit (Brn1) and three additional cohesin subunits (Smc3, Scc3 and Scc1/Mcd1) were not analyzed. Recent data suggest that Mcd1 might be a target of Mek1 in making BSCR. When DSBs are generated in G2, cohesin subunits are recruited to DSBs and facilitate efficient DSB repair using sister chromatids in *Saccharomyces cerevisiae* (STROM *et al.* 2004; UNAL *et al.* 2004). Interhomolog bias during meiosis may be established in part, therefore, by preventing cohesin loading at meiotic DSBs. Rec8 can substitute for Mcd1's S phase cohesion function, but not DSB repair function (Dr. Douglas Koshland,

personal communication). One possibility is that Mek1 kinase actively prevents the localization of Mcd1 cohesin complexes to DSBs. Up to now, several factors have been found to be required for cohesin loading at DSBs, the Scc2/Scc4 complex, Mec1/Tel1 dependent H2A-S129 phosphorylation, Rad53 checkpoint kinase and Mre11 (UNAL *et al.* 2004). The Scc2/Scc4 complex and Mre11 both function during meiosis. In mammals, an H2A isoform H2AX gets phophorylated upon DSB formation, which is analogous to H2A-S129 phosphorylation in yeast. It has been shown that H2AX phosphorylation occurs during mouse meiosis (MAHADEVAIAH *et al.* 2001). *RAD53* is not required for normal meiotic DSB repair, as *rad53* mutants do not show any meiotic phenotypes. Mek1 has been proposed to be the meiotic paralog of Rad53 (USUI *et al.* 2001). Therefore, Mek1 may create a BSCR by failing to activate cohesin loading. A second possibility is that Mek1 can actively prevent cohesin loading by phosphorylating a cohesion subunit, such as Mcd1.

Histones as potential Mek1 substrates. Yeast histone H2B and H4 are phosphorylated *in vitro* by Gst-Mek1. Purified H2B from vegetatively growing yeast cells exhibits a radioactive doublet in Gst-Mek1 *in vitro* kinase assays. The slower migrating band in the H2B doublet is especially interesting in that it is undetectable by ponceau S staining. There are at least four possibilities to explain the slower migrating species: 1) Given the fact that H2B is highly modified *in vivo*

by acetylation, methylation, phosphorylation and/or ubiquitination, the slower migrating band could be an isoform of H2B generated by post-translational modifications; 2) H2B migrates more slowly after Mek1 phosphorylation on particular sites; 3) The slower migrating band migrates at the same position of H3, so there could be contaminating H3 in the H2B fraction. If so, however, Mek1 must have a high affinity for H3, given that it is not detectable by Ponceau S staining; 4) It could be an unknown protein that co-purifies with histones. These possibilities can be distinguished by *in vitro* kinase assays using H3 and H2B purified from bacteria.

H2B is phosphorylated at S10 in budding yeast during meiosis. However, this phosphorylation does not depend on DSB formation as it is detected in a *spo11Δ* strains during meiosis (AHN *et al.* 2005), while Mek1 is activated in a DSB-dependent manner (NIU *et al.* 2007). Furthermore, deletion of the H2B N-terminus does not decrease spore viability in budding yeast (WALLIS *et al.* 1983). Therefore, if Mek1 produces a BSCR by phosphorylation of H2B, the critical phosphorylation sites will likely be located outside of the N-terminus. Histone H3 is phosphorylated at many sites including T3, S10, T11 and S28, which mostly correlate with chromosome condensation, although this varies in different species (DAI and HIGGINS 2005; GOTO *et al.* 1999; HSU *et al.* 2000; PREUSS *et al.* 2003). In the histone fraction that I used in the *in vitro* kinase assay, there is a

truncation of H3, H3', which lacks the first 21 amino acids. H3' is not phosphorylated by Mek1 *in vitro*. Therefore, if the slower migrating band in the H2B kinase assay is H3, the phosphorylation sites must located within the first 21 amino acids of H3. Up to now, only H3-S10 phosphorylation has been reported in budding yeast meiosis and requires the aurora kinase, *IPL1* (AHN *et al.* 2005; HSU *et al.* 2000). As with H2B-S10, the H3-S10 phosphorylation during yeast meiosis is independent of DSB formation (AHN *et al.* 2005), which excludes H3-S10 being a Mek1 phosphorylation site. H3-T3 is phosphorylated in mammalian cells by the kinase Haspin which is required for metaphase chromosome alignment (Dai and Higgins 2005). H3-T11 has been reported to be phosphorylated in mammalian cells by the death-associated protein-like kinase (Dlk) and is exclusively located at centromeres during mitosis where recombination is highly suppressed (PREUSS *et al.* 2003). Both of these sites are interesting candidates for further characterization.

Rad54 as a potential *in vivo* Mek1 target. In my survey of recombination proteins phosphorylated by Mek1 *in vitro*, Rad54 produced the strongest signal, being phosphorylated at three different places, T58, T132 and T231. All three amino acids phosphorylated by Mek1 are located on the N-terminus of Rad54, outside of its conserved catalytic core region. Yeast two-hybrid analysis has shown that the N-terminal 1-327 amino acids of Rad54 are both necessary and

sufficient to interact with Rad51 (JIANG *et al.* 1996). Recent biochemical studies show that deletion of the first 129 amino acids of Rad54 significantly attenuates its functional and physical interactions with Rad51 under physiological ionic strength, but maintains functional interactions with Rad51 under less stringent conditions (RASCHLE *et al.* 2004). Therefore, the N-terminus of Rad54 could play a regulatory role in Rad51/Rad54 cooperative functions.

During yeast meiosis, Rad51 activity is suppressed by a meiosis-specific inhibitor, *HED1* (Tsubouchi and Roeder 2006). Increasing Rad51 activity, either by overexpression of *RAD51* or deletion of *HED1* allows DSB repair in *dmc1Δ* diploids using non-sister chromatids (Tsubouchi and Roeder 2003; Tsubouchi and Roeder 2006). One of Dmc1's functions may therefore be increasing the level of recombinase activity in cells during meiosis as overexpression of *RAD51* or deleting *HED1* allows *dmc1Δ* diploids to progress through meiosis and produce viable spores. Overexpression of *RAD54* weakly suppresses *dmc1Δ* arrest and produces viable spores (BISHOP *et al.* 1999), as might be expected given that Rad54 stimulates Rad51 strand exchange activity *in vivo* (PETUKHOVA et al. 1998). The discovery that mutation of a putative *in vivo* Mek1 phosphorylation site also suppresses the interhomolog recombination defect of *dmc1Δ* suggests that one function of Mek1 during meiosis may be to down-regulate Rad51 activity via Rad54. When Rad54 orthologs from different model organisms are aligned, the

N-terminal sequences of Rad54 are not very conserved (data not shown), except for a few regions located between amino acids 120 and 250. The sequence near T132 is one of the relatively conserved regions (Figure 4-6) (RASCHLE *et al.* 2004), which might contribute to the Rad51/Rad54 interaction. Interestingly, in higher eukaryotes, *Homo sapiens, G. gallus* and *D. melanogaster*, the amino acid corresponding to T132 position is a positively charged lysine, where as in *C. elegans*, *S. pombe* and *S. cerevisiae*, it is either serine or threonine which may be subjected to phosphorylation. Introducing a phosphate at this position by Mek1 may inactivate the function of this motif since a positively charged residue at this position may allow its proper functioning in higher eukaryotes. The fact that *rad54-T132A* produces viable spores in *dmc1Δ* diploids indicates that the BSCR is intact in this mutant. This idea was confirmed by showing that deletion of *MEK1* in *rad54-T132A dmc1* diploids results in dead spores. These results suggest that Mek1 influences recombination in two ways: 1) inhibiting strand invasion of sister chromatids by creation of a BSCR and 2) reducing Rad51 activity, thereby allowing Dmc1 to function as an alternative recombinase during interhomolog recombination.

In summary, to achieve proper DSB repair using non-sister chromatids during meiosis, multiple processes are regulated. First, the bias for using sister chromatids is removed, perhaps by failing to load cohesins to DSBs during

meiosis. Second, activity of mitotic recombination factors, such as Rad51 and Rad54, are suppressed. Third, introducing meiosis specific recombination factors, such as Dmc1, may promote interhomolog recombination.

Table 4-1. Plasmids

Name	Yeast genotype	Source
pRS306	*URA3*	Sikorski and Hieter (1989)
pRS402	*ADE2*	Brachmann *et.al.* (1998)
pLP37	*URA3 MEK1*	de los Santos and Hollingsworth (1999)
pBL12	*URA3* P_{MEK1} *-GST-MEK1*	Niu *et.al.* (2005)
pTS30	*ADE2* P_{MEK1} *-GST-MEK1*	de los Santos and Hollingsworth (1999)
pHN10	*URA3* P_{MEK1} *-TAP-MEK1*	Niu *et.al.* (2005)
pNRB143	2 µ *URA3 LEU2d RAD54*	Bishop *et.al.* (1999)
pNRB143-T58A	2 µ *URA3 LEU2d rad54-T58A*	This study
pNRB143-T132A	2 µ *URA3 LEU2d rad54-T132A*	This study
pNRB143-T132D	2 µ *URA3 LEU2d rad54-T132D*	This study
pNRB143-T231A	2 µ *URA3 LEU2d rad54-T231A*	This study
yEplac195	2 µ *URA3*	Gietz and Sugino (1998)
pHN26	*URA3* P_{MEK1} *-GST-mek1-K199R*	Niu *et.al.* (2005)
pLW1	2 µ *URA3* P_{MEK1} *-GST-MEK1*	Wan *et.al.* (2004)
pET15b-HOP1	His_6 *-HOP1*	C&P Biotech
pBS1761	*TRP1 TAP*	Euroscarf
pTS25	*URA3 CEN* P_{MEK1} *-GST-MEK1*	This study
pTS25-TAP	*URA3 CEN* P_{MEK1} *-TAP*	This study
pHN9	*URA3* P_{MEK1} *-TAP*	This study
pTS3	2 µ *TRP1 ADE2* P_{ADH1} *-LexA-MEK1*	This study

Table 4-2. Strains

Strain	Genotype	Source
NH144	*MATa leu2Δ::hisG his4-x ARG4 ura3 lys2 ho::LYS2* *MATα leu2-k HIS4 arg4-Nsp ura3 lys2 ho::LYS2*	Hollingsworth et al. 1995
DKB201	*MATa leu2::hisG his4-X dmc1Δ::LEU2 hoΔ::LYS2 lys2 ura3* *MATα leu2::hisG his4-B dmc1Δ::LEU2 hoΔ::LYS2 lys2 ura3*	Bishop et al. 1999
NH520	*MATa leu2::hisG his4-X dmc1Δ::LEU2 hoΔ::LYS2 lys2 ura3 mek1Δ::KanMX4* *MATα leu2::hisG his4-B dmc1Δ::LEU2 hoΔ::LYS2 lys2 ura3 mek1Δ:: KanMX4*	Wan et al. 2004
NH678	*MATa leu2Δ ura3 lys2 ade2-10ochre trp1Δ63 arg4-Nsp mek1Δ::LEU2 YCG1-* *MATα leu2Δ ura3 lys2 ADE2 TRP1 ARG4 mek1Δ::LEU2 YCG1-*	This study
NH629	*MATa leu2 ho::LYS2 lys2 ura3 arg4-Nsp ADE2 mek1Δ::LEU2 YCS4-HA3::* *MATα leu2 ho::LYS2 lys2 ura3 ARG4 ade2 mek1Δ::LEU2 YCS4-HA3:: his5+(Sp)*	This study
NH680	*MATa his4 lys2 hoΔ::LYS2 arg4 ura3 SMC2-8myc-KanMX4 mek1Δ::LEU2* *MATα HIS4 lys2 hoΔ::LYS2 arg4 ura3 SMC2-8myc-KanMX4 mek1Δ::LEU2*	This study
NH682	*MATa lys2 hoΔ::LYS2 arg4-Nsp trp1 ura3 mek1Δ::LEU2 SMC4-HA3::his5+(Sp)* *MATα lys2 hoΔLYS2 ARG4 TRP1 ura3 mek1Δ::LEU2 SMC4-HA3::his5+(Sp)*	This study
NH699	*MATa his4-x leu2 hoΔ::LYS2 lys2 ura3 ADE2 mek1Δ::KAN PDS1-* *MATα HIS4 leu2 hoΔ::LYS2 lys2 ura3 ade2-Bg mek1Δ::KAN PDS1-MYC18::LEU2*	This study
NH621	*MATa his4 leu2 ura3 ade2 mek1Δ::LEU2 Rec8-HA::URA3 NDC10* *MATα his4 leu2 ura3 ade2 mek1Δ::LEU2 Rec8-HA::URA3 Ndc10-myc13::KANMX6*	This study
NH683	*MAT a lys2 ura3 mek1Δ::LEU2 ARG4 SMC1-HA3* *MATα lys2 ura3 mek1Δ::LEU2 arg4 SMC1-HA3*	This study
S2683 mek1 b	*MATα hoΔLYS2 ura 3 leu2-K arg4-Nsp mek1Δ::LEU2*	This study
RKY1145mek1ade2	*MATa hoΔLYS2 lys2 ura3 leu2Δ::hisG his4x mek1::LEU2 ade2-BglII*	This study
BLY09	*MATa ura3-52 lys2-801amber ade2-10ochre trp1Δ63 leu2Δ1 his3Δ200 YCG1-HA3::his5+(Sp)*	D. Koshland
BLY08	*MATa ura3-52 lys2-801amber ade2-10ochre trp1Δ63 leu2Δ1 his3Δ200 SMC4-HA3::his5+(Sp)*	D. Koshland
2892-1C	*MATa leu2 ura3 lys2 ho::LYS2 his3::KAN arg4-Nsp YCS4-3HA-his5+ (Sp)*	D. Koshland
2933-2C	*MATa ura3 lys2 ho::LYS2 SMC2-8myc-KanMX4*	D. Koshland
2823	*MATa leu2 ura3 arg4-Nsp SMC1-HA3*	D. Koshland
4739	*MATa lys2 leu2::hisG ura3 trp1::hisG his4 REC8-3HA::URA3 NDC10-13MYC::KANMX6*	A.Amon

Table 4-3. Primers

Name	Seqences
TAP-NDE-5′	5′- GCATACATTATACGAAGTTACATATGGCAGGCCTTGCG -3′
TAP-RI-SAL-3′	5′- GGGTACCGGGCCCCCCCTCGAGGTCGACGAATTCGATAAGC -3′
Smc1F1	5′- AGCCCTAGACATTACTAACGTC -3′
Smc1R1	5′- GCTACAATATTCAATGTTCTTC -3′
RAD54-T58A-5′	5'- CCCGCTGCTGGTAGAATCGCCGCCGGGTCTGATAATATCGTAGG -3'
RAD54-T58A-3′	5′- CCTACGATATTATCAGACCCGGCGGCGATTCTACCAGCAGCGGG -3′
RAD54-T132A-5′	5′- CCAGTACACTTTGAGAAGATCTTTCGCTGTGCCAATCAAGGG -3'
RAD54-T132A-3′	5′- CCCTTGATTGGCACAGCGAAAGATCTTCTCAAAGTGTACTGG -3′
RAD54-T231A-5′	5'- GGACGCCATCCAGCTTTGATGGCAAATGGTGTGAGAAACAAACCG -3'
RAD54-T231A-3′	5′- CGGTTTGTTTCTCACACCATTTGCCATCAAAGCTGGATGGCGTCC -3′
RAD54-T132D-5′	5′- CCAGTACACTTTGAGAAGATCTTTCGATGTGCCAATCAAGGG -3'
RAD54-T132D-3′	5′- CCCTTGATTGGCACATCGAAAGATCTTCTCAAAGTGTACTGG -3′
RAD54-T132K-5′	5' - CCAGTACACTTTGAGAAGATCTTTCAAGGTGCCAATCAAGGG -3'
RAD54-T132K-3′	5′ - CCCTTGATTGGCACCTTGAAAGATCTTCTCAAAGTGTACTGG -3′
RAD54-T58SEQ	5' - CCCTTGATTGGCACAG -3'
RAD54-T132SEQ	5' - CCCGCCCGCTGCTGG -3'
RAD54-T231SEQ	5' - CCAGAACCTCGACCTC - 3'

Table 4-4 *In vitro* kinase reactions with soluble Gst-Mek1.

	Gst-Mek1 autophosphoryation (μL)	Radioactive candidate test (μL)	Non-radioactive Rad54 labeling (μL)
Gst-Mek1 eluate	20	20	20
ATP (2 mM)	1	1	2
^{32}P-γ-ATP (6000 Ci/mmol)	1	1	0
$MgCl_2$ (250 mM)	1	1	1
Substrate proteins	0	1 (1 μg/μL)	1 (2.5 μg/μL)
dH_2O	1	0	0
Total volume	24	24	24

Table 4-5 Spore viability and suppression of *dmc1*Δ arrest by *RAD54* phosphorylation site mutants

RAD54	*dmc1* Δ		*dmc1* Δ *mek1* Δ	
Genotype[a]	% Spo[b]	% S.V. (# asci)[c]	% Spo[b]	% S.V. (# asci)[c]
2 μ	0.8 ± 0.3	ND	73.2 ± 8.4	< 2 (13)
2 μ *RAD54*	4.0 ± 1.7	56.8 (12)	80.7 ± 9.4	< 2 (13)
2 μ *HOP1p-RAD51*	36.6 ± 5.1	70.0 (102)	72.6 ± 10.6	0.8 (101)
2 μ *rad54-T58A*	1.3 ± 1.2	ND	ND	ND
2 μ *rad54-T231A*	5.7 ± 2.4	ND	ND	ND
2 μ *rad54-T132A*	51.2 ± 11.3	57.3 (65)	86.3 ± 3.2	< 2 (13)
2 μ *rad54-T132K*	51.2 ± 11.3	ND	ND	ND
2 μ *rad54-T132D*	8.3 ± 2.6	46.2 (13)	81.0 ± 3.5	< 2 (13)
URA3	0.0 ± 0.0	ND	ND	ND
RAD54	0.0 ± 0.0	ND	ND	ND
rad54-T132A	1.8 ± 1.9	ND	ND	ND
rad54-T132K	18.7 ± 2.8	ND	ND	ND
rad54-T132D	0.7 ± 0.3	ND	ND	ND

[a]2μ plasmids containing the indicated *RAD54* alleles (yEplac195, pNRB143, pNRB143-T58A, pNRB143-T231A, pNRB143-T132A and pNRB143-T132D respectively) were introduced into either DKB201 (*dmc1*Δ) or NH520 (*dmc1*Δ *mek1*Δ). Integrating plasmids containing indicated *RAD54* alleles (pRS306, pRS306-RAD54, pRS306-rad54-T132A, pRS306-rad54-T132K, pRS306-rad54-T132D).

[b]Spo means sporulation. Sporulation was measured by counting the number of asci present in 200 cells/transformant using phase contrast light microscopy. Three independent transformants were measured for all the alleles.

[c]S.V. means spore viability.

Table 4-6: TAP-Mek1 co-purifying proteins identified by mass spectrometry analysis.

# peptides	Xcorr	ORF	Gene
21	3.465	YOR351C	MEK1
15	3.383	YPL119C	DBP1
14	3.788	YOR204W	DED1
14	3.609	YLR259C	HSP60
13	3.745	YDL229W	SSB1
12	3.528	YER165W	PAB1
10	4.14	YNL096C	RPS7B
8	2.91	YLR441C	RPS1A
7	2.989	YAL005C	SSA1
6	4.54	YBL087C	RPL23A
6	2.808	YGR034W	RPL26B
5	4.076	YGR178C	PBP1
5	3.215	YHL024W	RIM4
5	3.186	YOR096W	RPS7A
5	3.044	YNL302C	RPS19B
5	3.015	YIL022W	TIM44
4	4.133	YER151C	UBP3
4	4.057	YDR447C	RPS17B
4	3.855	YDL075W	RPL31A
4	3.484	YHR121W	LSM12
4	3.201	YIL136W	OM45
4	3.093	YGL068W	MNP1
4	2.986	YDL083C	RPS16B
3	4.35	YFR031C-A	RPL2A
3	4.185	YJL190C	RPS22A
3	4.032	YFL016C	MDJ1
3	3.887	YBR118W	TEF2
3	3.713	YMR031C	
3	3.633	YNL085W	MKT1
3	3.455	YOL016C	CMK2
3	3.356	YKL016C	ATP7
3	3.181	YNL112W	DBP2
3	3.171	YCR031C	RPS14A
2	5.452	YBR181C	RPS6B
2	4.458	YLR061W	RPL22A
2	4.315	YGR167W	CLC1
2	3.648	YJR123W	RPS5
2	3.555	YNR051C	BRE5
2	3.507	YOL040C	RPS15
2	3.482	YER074W	RPS24A
2	3.428	YHL033C	RPL8A
2	3.394	YGL076C	RPL7A
2	3.253	YDR206W	EBS1
2	3.171	YDR064W	RPS13
2	2.731	YDL053C	PBP4
1	3.777	YHL001W	RPL14B
1	2.793	YJR094W-A	RPL43B
1	2.556	YLR340W	RPP0

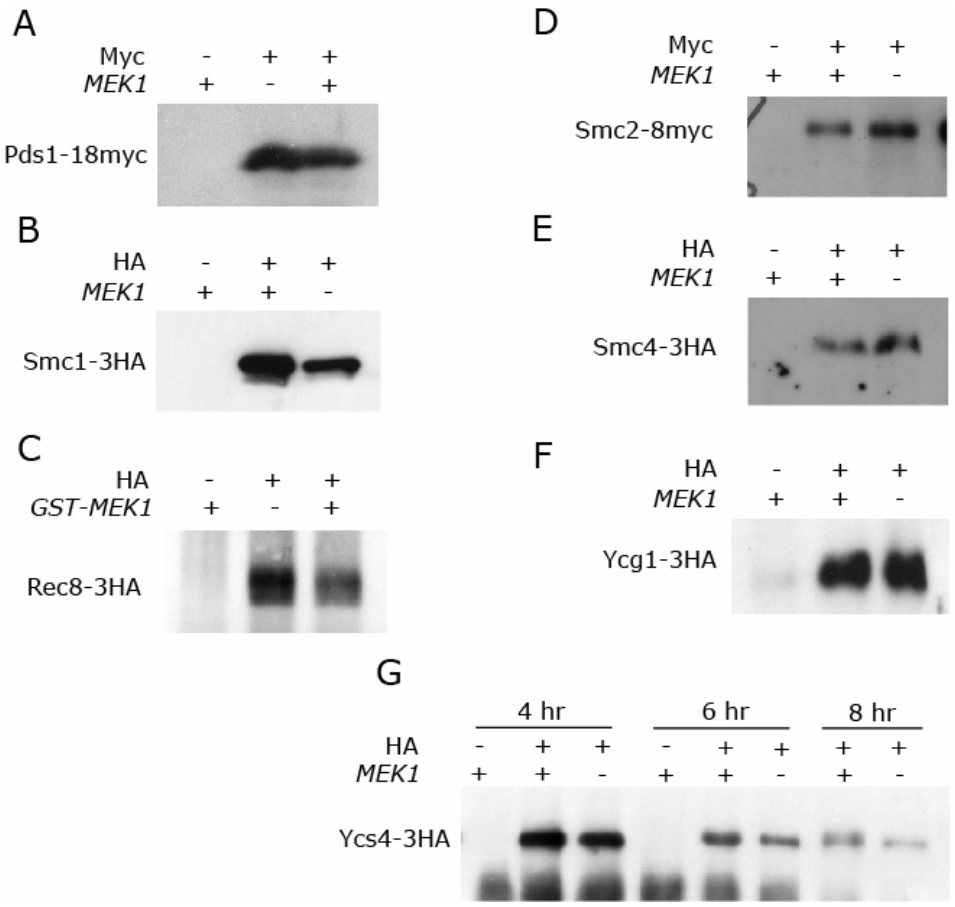

Figure 4-1. Checking for *MEK1*-dependent mobility shifts with IPed cohesin and condensin subunits. Diploid strains containing tagged candidate proteins were sporulated for 4 hours in Spo medium at 30°C. Ycs4-3HA was examined at 4, 6 and 8 hours after transfer to Spo medium. Specific strain genotypes for each panel are A. *SMC1-3HA MEK1* (NH683::pLP37), *SMC1-3HA mek1Δ* (NH683::pRS306) B. *REC8-3HA GST-MEK1* (NH621::pTS30), *REC8-3HA mek1Δ* (NH621::pRS402) C. *SMC2-8myc MEK1* (NH680::pLP37), *SMC2-8myc mek1Δ* (NH680::pRS306) D. *SMC4-3HA MEK1* (NH682::pLP37), *SMC4-3HA mek1Δ* (NH682::pRS306) E. *YCG1-3HA MEK1* (NH678::pLP37), *YCG1-3HA mek1Δ* (NH678::pRS306) F. *YCS4-3HA MEK1* (NH629::pLP37), *YCS4-3HA mek1Δ* (NH629::pRS306). The wild type strain NH144 was included in each experiment as an untagged control strain. Different HA or Myc tagged target proteins from 50 mL culture were IPed with either α-HA (12CA5) or α-myc (9E10) monoclonal antibodies and fractionated using electrophoresis on 8% Tris-Acetate gels for 14 hours, The proteins were then transferred onto nitrocellulose membrane and probed with either α-HA or α-myc antibodies.

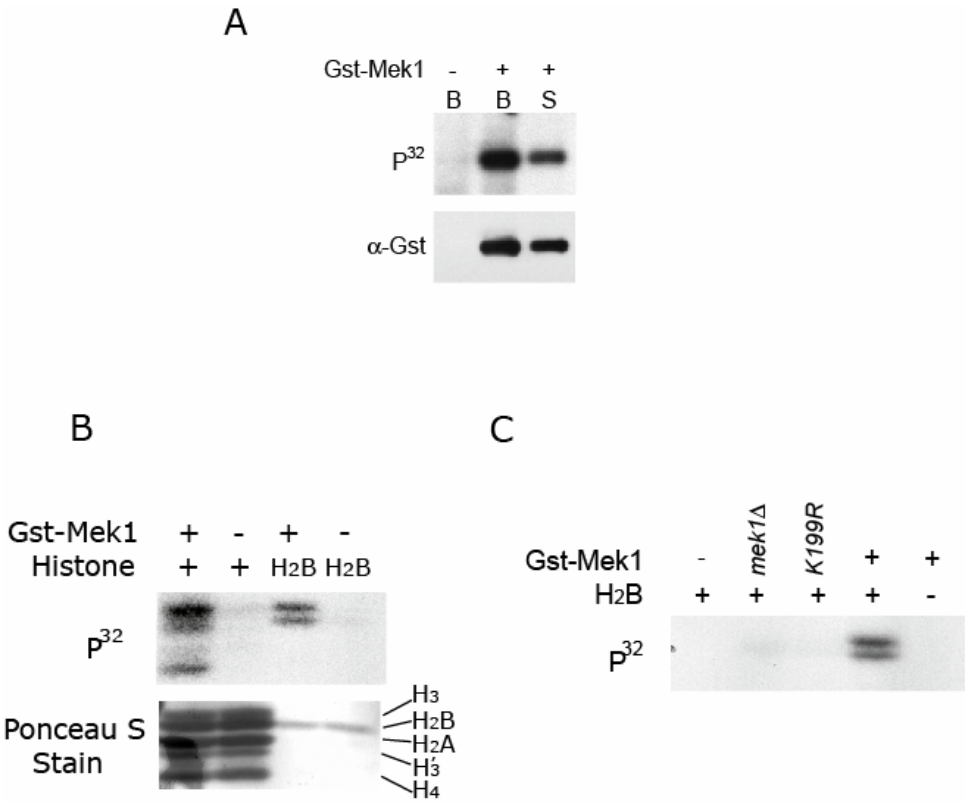

Figure 4-2. ***In vitro*** **phosphorylation of purified histone proteins by Gst-Mek1.** Soluble Mek1 was obtained by elution of the kinase off the beads using glutathione. A. Comparison of Gst-Mek1 autophosphorylation with and without elution. B: reactions without elution. S: reactions using soluble Gst-Mek1. B. *In vitro* kinase reactions using purified histones and H2B as substrates of soluble Gst-Mek1 were setup as described in materials and methods. Different histone subunits were indicated. H_3' is a histone H3 degradation product with N-terminal 21 amino acid truncated. C. Soluble Gst-Mek1 from *dmc1Δ GST-MEK1* diploid strain (NH520::pBL12) was purified as described. And as a control, catalytic inactive Gst-Mek1-K199R was purified the same way as Gst-Mek1 from diploid strain (NH520::pHN26). *In vitro* kinase assays were setup by incubating glutathione purified product from *GST-MEK1* (+), *mek1Δ* (*mek1Δ*), *GST-mek1-K199R* (*K199R*) or buffer (-) with purified H2B (+) or buffer (-).

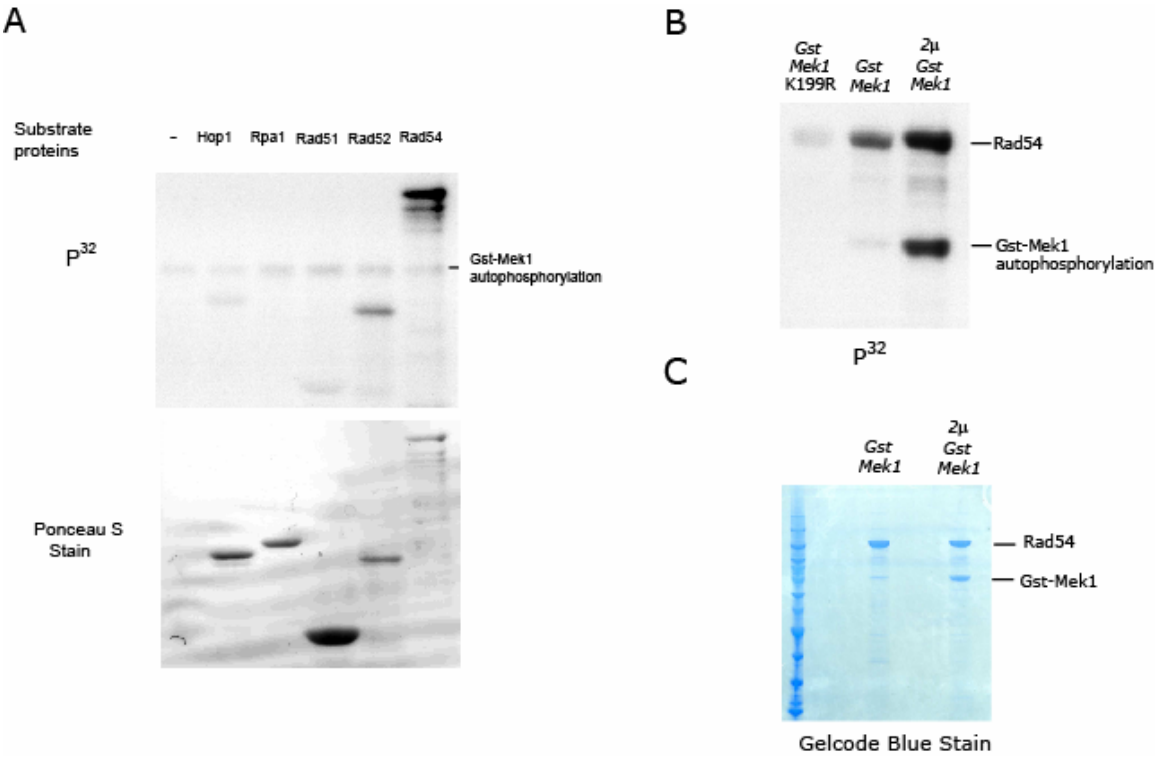

Figure 4-3. *In vitro* phosphorylation of various purified recombination factors by Gst-Mek1 A. *In vitro* kinase assays were performed using soluble Gst-Mek1 with purified candidate proteins as indicated. The amount of substrate proteins in each reaction was shown by Ponceau S staining. B. Kinase assays were setup using purified Gst-Mek1 from strains containing catalytic inactive *GST-mek1-K199R* (NH520::pHN26), *GST-MEK1* (NH520::pBL12) and *2μ GST-MEK1* (NH520/pLW1) with recombinant Rad54. C. Kinase reactions were setup the same as in B except using non-radioactive ATP. Shown is a 4-12% Bis-Tris NuPAGE gel after staining with Gelcode Blue to detect Rad54 and Gst-Mek1 as indicated.

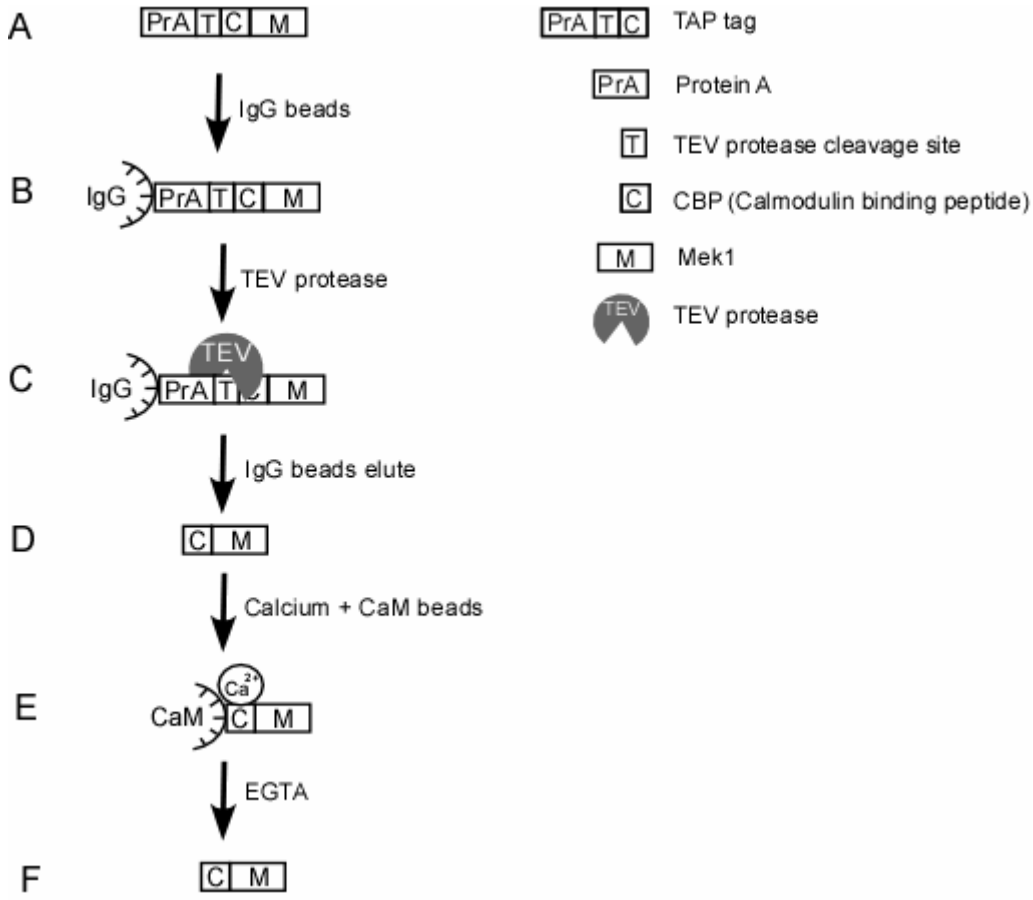

Figure 4-4. A diagram showing TAP-Mek1 purification. A. TAP-Mek1 is constructed by fusion of *MEK1* in frame with Protein A-CBP (Calmodulin binding peptide) at the N-terminus with an unique TEV protease cleavage site introduced in between Protein A and CBP. B. TAP-Mek1 binds IgG sepharose through the Protein A tag. C. Addition of TEV protease cleaves the unique target site located between Protein A and CBP. D. CBP-Mek1 is released from Protein A. E. By adding calcium, CBP-Mek1 binds calmodulin sepharose beads. F. CBP-Mek1 is eluted from calmodulin sepharose beads by adding EGTA.

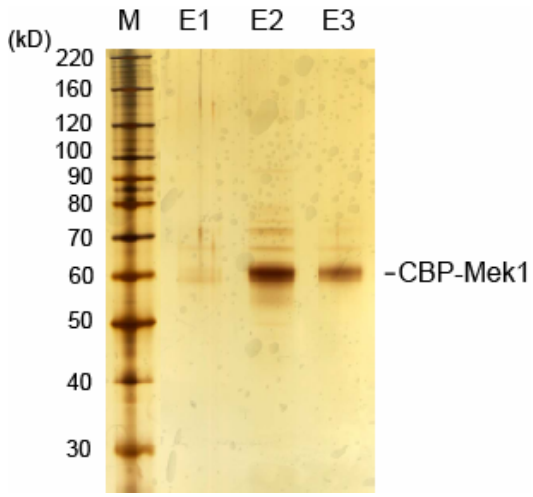

Figure 4-5. Silver staining of CBP-Mek1 and co-purified proteins. Samples from final CBP-Mek1 elute of TAP-Mek1 purification were fractionated using 4-12% Bis-Tris NuPAGE gel and silver stained. The molecule weights of markers were indicated. Three serial elution fractions were indicated as E1, E2 and E3. the band of CBP-Mek1 was marked.

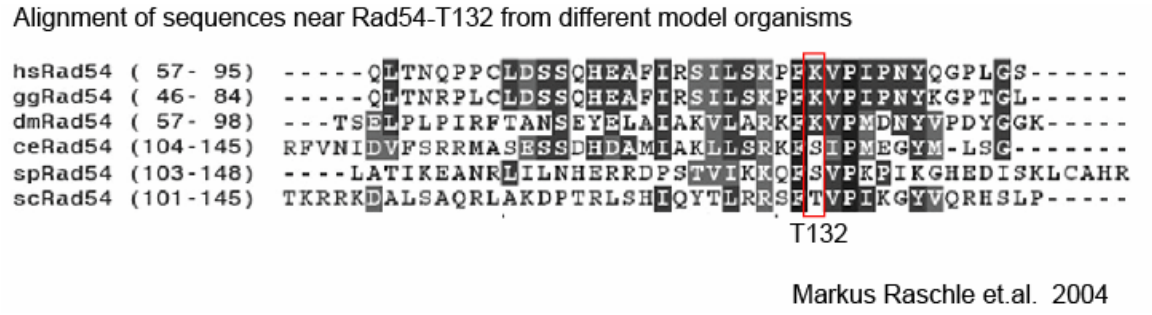

Figure 4-6. An alignment of region around T132 of Rad54 from *S. cerevisae* with Rad54 orthologs from other model organisms. The abbreviation of species names are: hs – *H. sapiens*; gg – *G. gallus*; dm – *D. melanogaster*; ce – *C. elegans*; sp – *S. pombe*; sc – *S.cerevsiae*;

CHAPTER FIVE

DISCUSSION

My thesis work focused on the Mek1 kinase, a critical factor in regulating partner choice during meiotic recombination in yeast. My goal was to answer two basic questions: (1) how is Mek1 kinase activity regulated? and (2) how do Mek1-phosphorylated substrates regulate partner choice?

With regard to the regulation of Mek1 kinase activation, my research showed that the Hop1 C-domain promotes Mek1 dimerization and that this dimerization allows autophosphorylation of Mek1 activation loop threonines at positions T327 and T331. I showed that DSBs and Hop1/Red1/Mek1 complex formation are required for Mek1 activation. Furthermore, I discovered that phosphorylation of Mek1-S320 is specifically required for *MEK1* function in *dmc1* arrested cells. Although I was not able to identify the targets of Mek1 whose phosphorylation allows formation of the BSCR, I did show that Rad54 is an *in vitro* substrate of Mek1 and that phosphorylation of Rad54 by Mek1 during meiosis down-regulates Rad54 activity.

My research, in conjunction with other data from the Hollingsworth lab, has led to a model of how Mek1 functions in meiosis to create interhomolog bias (Figure 5-1). In this model, Mek1 activation is regulated by DSBs in two steps. First, DSBs trigger recruitment of Mek1 to pre-assembled Hop1/Red1 complexes (Figure 5-1A) by binding to DSB-dependent hyper-phosphorylated Red1 through

the Mek1 FHA domain (Figure 5-1B). Second, DSBs also trigger Hop1 C-domain phosphorylation. The phosphorylated Hop1 C-domain, together with Mek1 C-terminus, then promotes Mek1 dimerization and activation by auto-phosphorylation of conserved threonines on the Mek1 activation loop (Figure 5-1C). Upon activation, Mek1 contributes to meiotic recombination partner choice in two ways (Figure 5-1D): (1) promoting *DMC1*-dependent DSB repair by down-regulating Rad51/Rad54 activity through phosphorylation of Rad54; (2) phosphorylation of yet unknown target(s) to create a BSCR.

This model describes how Hop1, Red1 and Mek1 work together to regulate meiotic recombination partner choice, an important process for almost all sexual reproducing organisms. The Red1 protein contains a coiled-coil structure and Mek1 is a protein kinase, which makes identification of their related proteins in non-fungal species based on primary sequence homology difficult. Hop1 contains a HORMA domain, a conserved structural motif, which mediates dimerization in another HORMA domain containing protein, Mad2 (ARAVIND and KOONIN 1998; LUO *et al.* 2004). Besides other fungal species, Hop1 related HORMA domain containing proteins have also been identified in worms and plants, while in humans and mice, several testis-specific putative orthologs have been found (CARYL *et al.* 2000; CHEN *et al.* 2005; MARTINEZ-PEREZ and VILLENEUVE 2005; PANGAS *et al.* 2004; ZETKA *et al.* 1999).

The worm ortholog of Hop1, Him-3, localizes to chromosome axes and is required for homolog pairing, SC formation and recombination (ZETKA *et al.* 1999). In *C.elegans*, SC formation does not require DSB formation while inter-homolog recombination depends on proper formation of SC. In *C.elegans syp* mutants, the SC central region fails to assemble and homologs fail to synapse. Him-3 still localizes to axes. Rad51 foci, used as cytological indicators of DSBs, accumulate until late pachytene in the absence of meiotic crossovers indicating a failure to repair DSBs (COLAIACOVO *et al.* 2003; MACQUEEN *et al.* 2002). In the *syp* meiocytes which reach diakinesis, chromosome integrity is dependent upon *RAD51* and *REC8*, suggesting that repair of DSBs can occur via sister chromatids, although later than interhomolog repair (COLAIACOVO *et al.* 2003). These observations suggest the presence of a BSCR in worms that prevents sister chromatids being used as templates when homologs are available. Interestingly, in *him3* mutants, Rad51 foci appear and disappear with wild-type kinetics without crossovers or synapsis, indicating a requirement for *HIM-3* in BSCR creation (COUTEAU *et al*. 2004).

There is also evidence which suggests the presence of a BSCR during meiosis in mammals. In human spermatocytes, Rad51 foci occur at early zygotene and the level of Rad51 labelling is greatly reduced in pachytene presumably due to repair of DSBs by interhomolog recombination. In contrast,

Rad51 labelling, at non-homologous asynapsed XY segments, becomes intense (BARLOW *et al.* 1997). Similar results were observed in mouse cells at early pachytene, where large Rad51 foci were also found along asynapsed axes of X chromosome. These foci disappeared when the XY chromosomes desynapsed (ASHLEY *et al.* 1995). Both results can be explained by the presence of a BSCR, which, when removed upon desynapsis, allows DSB repair off sisters.

The presence of a BSCR in yeast and muticelluar eukaryotes makes identification of Mek1 substrates involved in BSCR formation very important. Recently, a new model for BSCR creation was proposed by our lab. In this model, Mek1 creates a BSCR by preventing the post-replicative loading of Mcd1 containing cohesion complexes to meiotic DSBs. Such post-replicative cohesion loading facilitates DSB repair using sister chromatids in vegetative cells (STROM *et al.* 2004; UNAL *et al.* 2004). If this model is correct, it may help to explain BSCR formation in higher eukaryotes.

Besides Mek1's function in BSCR creation, my work has revealed an unexpected role for Mek1 in the regulation of meiotic recombination: that of down-regulating Rad51 activity during meiosis by phosphorylation of Rad54. A yeast meiosis-specific protein, Hed1, also prevents Rad51/Rad54 interaction by binding Rad51 directly (TSUBOUCHI and ROEDER 2006). An interesting question, therefore, is whether Rad54-T132 phosphorylation works independently or is on

the same pathway as Hed1. Rad54 proteins from human and mice contain non-phosphorylatable lysine residues at positions analogous to T132 in yeast Rad54 and therefore are not phosphorylated. In addition, no apparent Hed1 orthologs have yet been found in any non-fungal species, therefore whether these mechanisms for down-regulating Rad51/Rad54 activity are conserved is unclear (TSUBOUCHI and ROEDER 2006).

Why is Rad51 down-regulated in meiosis? One possibility is that in those organisms in which Dmc1 is used for strand invasion, competition by Rad51 must be suppressed. If true, organisms containing *DMC1* may down-regulate Rad51 during meiosis and those that lack *DMC1* may not. Like yeast, *DMC1* is required for meiotic progression in mice, which argues for down-regulation of Rad51 activity in mammals (PITTMAN *et al.* 1998; YOSHIDA *et al.* 1998). Unlike budding yeast, where meiosis fails to progress when both *RAD54* and *TID1* are mutated, mice with both *RAD54* and *RAD54B* (*TID1* ortholog in mice) deleted show normal meiotic progression (BANNISTER and SCHIMENTI 2004; WESOLY *et al.* 2006). Thereby, Rad51 activity may be regulated through *RAD51* co-factors other than Rad54. Recently, a meiosis-specific Rad51 interacting protein, Rad51AP2, was identified in humans and could be a potential regulator of Rad51 (KOVALENKO *et al.* 2006; Patrick Sung, personal communication).

Releasing *dmc1* arrest in budding yeast by either deleting *HED1*,

overexpressing *RAD51* or *rad54-T132A* produces viable spores, indicating that Rad51 alone can catalyze inter-homolog recombination efficiently during meiosis (TSUBOUCHI and ROEDER 2006). Consistent with this idea, in worms and fruit flies, no *DMC1* orthologs have been reported leaving Rad51 as the only recombinase. The ability of Rad51 to substitute for Dmc1 raises the question of why organisms have evolved a meiotic recombinase at all. The fact that Rad51 activity is down-regulated in budding yeast where *DMC1* is essential for interhomolog recombination under otherwise wild type condition argues that Dmc1 possesses a unique function and does not simply compensate for Rad51 recombinase activity during meiosis. One phenotype of *dmc1 hed1* is that the crossover levels are significantly lower than wild type suggesting Dmc1 enhances crossover formation (TSUBOUCHI and ROEDER 2006). Consistent with this idea, in *S. pombe*, *dmc1Δ* mutants exhibit no defects in spore formation or spore viabililty, but crossover levels are decreased to ~20% of wild type (FUKUSHIMA *et al.* 2000).

How might Dmc1 facilitate inter-homolog crossovers? In budding yeast, the crossover/non-crossover decision is made prior to or during strand exchange (ALLERS and LICHTEN 2001; HUNTER and KLECKNER 2001). The non-crossover pathway does not utilize dHJs and has been proposed instead use synthesis-dependent strand annealing (SDSA). In this pathway, one or both of the 3′ ends invade the template DNA transiently to allow limited extension. The

extended strand then is released and anneals with complementary sequences on the other side of the breaks to allow DSB repair (ALLERS and LICHTEN 2001). Although SDSA has not been demonstrated in meiosis, it has been shown to mediate Rad51-dependent DSB repair in vegetative cells to produce gene conversion (PAQUES and HABER 1999). One possibility is that Dmc1 promotes crossover formation between homologs by stabilizing the pairing between the invading ends and non-sister chromatids.

Support for this idea comes from comparing meiosis from budding yeast and humans which contain *DMC1* orthologs with meiosis from worms and fruit flies which do not. One difference is the requirement of recombination for SC formation. In budding yeast and mouse, *DMC1*-dependent strand invasion is required for SC formation (BISHOP *et al.* 1992; PITTMAN *et al.* 1998; YOSHIDA *et al.* 1998), but SC formation in worms and fruit flies is independent of recombination (DERNBURG *et al.* 1998; MCKIM *et al.* 1998). It is possible that in organisms where SC formation requires strand invasion to establish interhomolog interactions, *DMC1* is evolved to stabilize the interhomolog interactions by stabilizing the interactions between invading strand and non-sister chromatids.

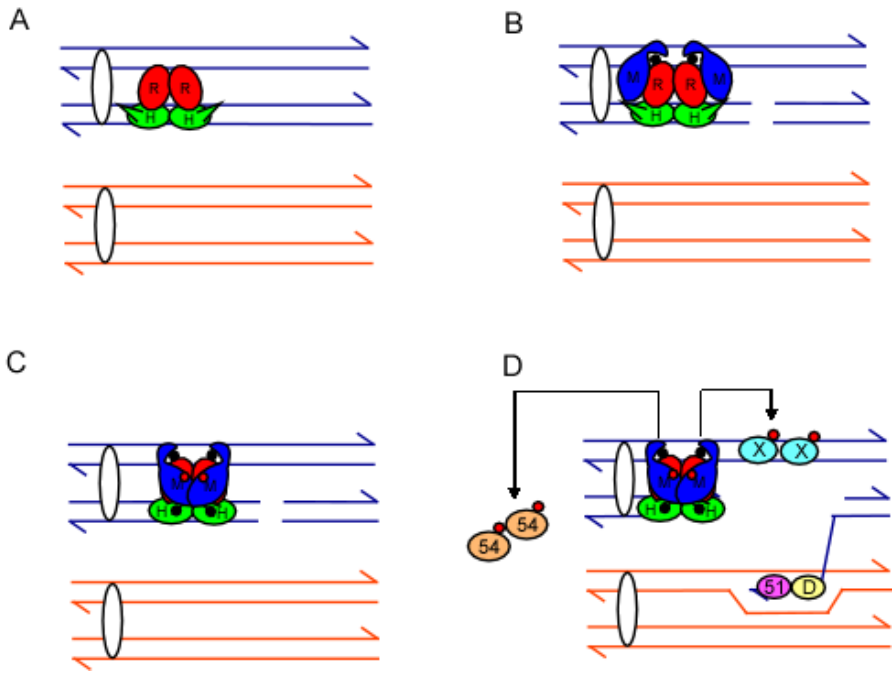

Figure 5-1: **The model of Mek1 regulation of meiotic partner choice.** A. Hop1/Red1 complexes assemble on DNA prior to DSB formation. B. DSBs trigger Red1 hyper-phosphorylation, which then recruits Mek1 through the Mek1 FHA domain. C. DSBs also trigger Hop1 C-domain phosphorylation, which promotes Mek1 dimerization and auto-activation. D. Activated Mek1 phosphorylates Rad54 to promote down-regulation of Rad51 at the same time as a yet unknown target (X) to create a BSCR. Sister chromatids from pair of homologous chromosomes are in red and blue repectively. Centromeres are labeled as black circles. Red1 is in red, Hop1 is in green and Mek1 is in blue. Rad51 is in purple, Dmc1 is in yellow and Rad54 is in orange. Mek1-independent phosphorylation events were shown as black node and Mek1-dependent phosphorylation events were shown as red1 node.

REFERENCES

ADAMS, J. A., 2003 Activation loop phosphorylation and catalysis in protein kinases: is there functional evidence for the autoinhibitor model? Biochemistry **42:** 601-607.

AHN, S. H., K. A. HENDERSON, S. KEENEY and C. D. ALLIS, 2005 H2B (Ser10) phosphorylation is induced during apoptosis and meiosis in *S. cerevisiae*. Cell Cycle **4:** 780-783.

AIHARA, H., T. NAKAGAWA, K. YASUI, T. OHTA, S. HIROSE, N. DHOMAE, K. TAKIO, M. KANEKO, Y. TAKESHIMA, M. MURAMATSU and T. ITO, 2004 Nucleosomal histone kinase-1 phosphorylates H2A Thr 119 during mitosis in the early Drosophila embryo. Genes Dev **18:** 877-888.

AKAMATSU, Y., D. DZIADKOWIEC, M. IKEGUCHI, H. SHINAGAWA and H. IWASAKI, 2003 Two different Swi5-containing protein complexes are involved in mating-type switching and recombination repair in fission yeast. Proc Natl Acad Sci U S A **100:** 15770-15775.

ALANI, E., R. PADMORE and N. KLECKNER, 1990 Analysis of wild-type and *rad50* mutants of yeast suggests an intimate relationship between meiotic chromosome synapsis and recombination. Cell **61:** 419-436.

ALLERS, T., and M. LICHTEN, 2001 Differential timing and control of noncrossover and crossover recombination during meiosis. Cell **106:** 47-57.

ARAVIND, L., and E. V. KOONIN, 1998 The HORMA domain: a common structural denominator in mitotic checkpoints, chromosome synapsis and DNA repair. Trends Biochem Sci **23:** 284-286.

ARBEL, A., D. ZENVIRTH and G. SIMCHEN, 1999 Sister chromatid-based DNA repair is mediated by *RAD54*, not by *DMC1* or *TID1*. Embo J **18:** 2648-2658.

ASHLEY, T., A. W. PLUG, J. XU, A. J. SOLARI, G. REDDY, E. I. GOLUB and D. C. WARD, 1995 Dynamic changes in Rad51 distribution on chromatin during meiosis in male and female vertebrates. Chromosoma **104:** 19-28.

BAILIS, J. M., and G. S. ROEDER, 1998 Synaptonemal complex morphogenesis and sister-chromatid cohesion require Mek1-dependent phosphorylation of a meiotic chromosomal protein. Genes Dev. **12:** 3551-3563.

BANNISTER, L. A., and J. C. SCHIMENTI, 2004 Homologous recombinational repair proteins in mouse meiosis. Cytogenet Genome Res **107:** 191-200.

BARLOW, A. L., F. E. BENSON, S. C. WEST and M. A. HULTEN, 1997 Distribution of the Rad51 recombinase in human and mouse spermatocytes. Embo J **16:** 5207-5215.

BISHOP, D. K., 1994 RecA homologs Dmc1 and Rad51 interact to form multiple nuclear complexes prior to meiotic chromosome synapsis. Cell **79:** 1081-1092.

BISHOP, D. K., Y. NIKOLSKI, J. OSHIRO, J. CHON, M. SHINOHARA and X. CHEN 1999 High copy number suppression of the meiotic arrest caused by a *dmc1* mutation: *REC114* imposes an early recombination block and *RAD54* promotes a *DMC1*-independent DSB repair pathway. Genes Cells **4:** 425-443.

BISHOP, D. K., D. PARK, L. XU and N. KLECKNER, 1992 *DMC1*: a meiosis-specific yeast homolog of *E. coli recA* required for recombination, synaptonemal complex formation and cell cycle progression. Cell **69:** 439-456.

BISHOP, D. K., and D. ZICKLER, 2004 Early decision; meiotic crossover interference prior to stable strand exchange and synapsis. Cell **117:** 9-15

.

BULLARD, S. A., S. KIM, A. M. GALBRAITH and R. E. MALONE, 1996 Double strand breaks at the *HIS2* recombination hotspot in *Saccharomyces cerevisiae*.

BUONOMO, S. B., R. K. CLYNE, J. FUCHS, J. LOIDL, F. UHLMANN and K. NASMYTH, 2000 Disjunction of homologous chromosomes in meiosis I depends on proteolytic cleavage of the meiotic cohesin Rec8 by separin. Cell **103:** 387-398.

CAO, L., E. ALANI and N. KLECKNER, 1990 A pathway for generation and processing of double-strand breaks during meiotic recombination in *S. cerevisiae*. Cell **61:** 1089-1101.

CARYL, A. P., S. J. ARMSTRONG, G. H. JONES and F. C. FRANKLIN, 2000 A homologue of the yeast *HOP1* gene is inactivated in the *Arabidopsis* meiotic mutant *asy1*. Chromosoma **109:** 62-71.

CHAMPION, M. D., and R. S. HAWLEY, 2002 Playing for half the deck: the molecular biology of meiosis. Nat Cell Biol **4 Suppl:** s50-56.

CHEN, Y. T., C. A. VENDITTI, G. THEILER, B. J. STEVENSON, C. ISELI, A. O. GURE, C.V. JONGENEEL, L. J. OLD and A. J. SIMPSON, 2005 Identification of CT46/HORMAD1, an immunogenic cancer/testis antigen encoding a putative meiosis-related protein. Cancer Immun **5:** 9.

CHENG, H., T. ADDONA, H. KESHISHIAN, E. DAHLSTRAND, C. LU, M. DORSCH, Z. LI, A. WANG, T. D. OCAIN, P. LI, T. F. PARSONS, B. JAFFEE and Y. XU, 2006 Regulation of IRAK-4 kinase activity via autophosphorylation within its activation loop. Biochem Biophys Res Commun.

COLAIACOVO, M. P., A. J. MACQUEEN, E. MARTINEZ-PEREZ, K. MCDONALD, A. ADAMO *et al.*, 2003 Synaptonemal complex assembly in *C. elegans* is dispensable for loading strand-exchange proteins but critical for proper completion of recombination. Dev Cell **5:** 463-474.

COUTEAU, F., K. NABESHIMA, A. VILLENEUVE and M. ZETKA, 2004 A component of *C. elegans* meiotic chromosome axes at the interface of homolog alignment, synapsis, nuclear reorganization, and recombination. Curr Biol **14:** 585-592.

D'AMOURS, D., F. STEGMEIER and A. AMON, 2004 Cdc14 and condensin control the dissolution of cohesin-independent chromosome linkages at repeated DNA. Cell **117:** 455-469.

DAI, J., and J. M. HIGGINS, 2005 Haspin: a mitotic histone kinase required for metaphase chromosome alignment. Cell Cycle **4:** 665-668.

DE, A., B. D. PAUL, V. RAMESH and V. NAGARAJA, 1997 Use of protein A gene fusions for the analysis of structure-function relationship of the transactivator protein C of bacteriophage Mu. Protein Eng **10:** 935-941.

DE LOS SANTOS, T., and N. M. HOLLINGSWORTH, 1999 Red1p, a *MEK1*-dependent phosphoprotein that physically interacts with Hop1p during meiosis in yeast. J Biol Chem **274:** 1783-1790.

DE LOS SANTOS, T., N. HUNTER, C. LEE, B. LARKIN, J. LOIDL and N. M. HOLLINGSWORTH, 2003 The Mus81/Mms4 endonuclease acts independently of double-Holliday junction resolution to promote a distinct subset of crossovers during meiosis in budding yeast. Genetics **164:** 81-94.

DEMINOFF, S. J., S. C. HOWARD, A. HESTER, S. WARNER and P. K. HERMAN, 2006 Using substrate-binding variants of the cAMP-dependent protein kinase to identify novel targets and a kinase domain important for substrate interactions in *Saccharomyces cerevisiae*. Genetics **173:** 1909-1917.

DERNBURG, A. F., K. MCDONALD, G. MOULDER, R. BARSTEAD, M. DRESSER and A. M. VILLENEUVE, 1998 Meiotic recombination in *C. elegans* initiates by a conserved mechanism and is dispensable for homologous chromosome synapsis. Cell **94:** 387-398.

DRESSER, M. E., D. J. EWING, M. N. CONRAD, A. M. DOMINGUEZ, R. BARSTEAD, H. JIANG, and T. KODADEK, 1997 *DMC1* functions in a *Saccharomyces cerevisiae* meiotic pathway that is largely independent of the *RAD51* pathway. Genetics **147:** 533-544.

DUROCHER, D., J. HENCKEL, A. R. FERSHT and S. P. JACKSON, 1999 The FHA domain is a modular phosphopeptide recognition motif. Mol Cell **4:** 387-394.

ELLERMEIER, C., H. SCHMIDT and G. R. SMITH, 2004 Swi5 acts in meiotic DNA joint molecule formation in *Schizosaccharomyces pombe*. Genetics **168:** 1891-1898.

FRIEDMAN, D. B., N. M. HOLLINGSWORTH and B. BYERS, 1994 Insertional mutations in the yeast *HOP1* gene: evidence for multimeric assembly in meiosis. Genetics **136:** 449-464.

FUKUSHIMA, K., Y. TANAKA, K. NABESHIMA, T. YONEKI, T. TOUGAN, S. TANAKA and H. NOJIMA, 2000 Dmc1 of Schizosaccharomyces pombe plays a role in meiotic recombination. Nucleic Acids Res **28:** 2709-2716.

GASIOR, S. L., A. K. WONG, Y. KORA, A. SHINOHARA and D. K. BISHOP, 1998 Rad52 associates with RPA and functions with Rad55 and Rad57 to assemble meiotic recombination complexes. Genes Dev **12:** 2208-2221.

.

GAVIN, A. C., M. BOSCHE, R. KRAUSE, P. GRANDI, M. MARZIOCH, A. BAUER, J. SCHULTZ, J. M. RICK, A. M. MICHON, C. M. CRUCIAT, M. REMOR, C. HOFERT, M. SCHELDER, M. BRAJENOVIC, H. RUFFNER, A. MERINO, K. KLEIN, M. HUDAK, D. DICKSON, T. RUDI, V. GNAU, A. BAUCH, S. BASTUCK, B. HUHSE, C. LEUTWEIN, M. A. HEURTIER, R. R. COPLEY, A. EDELMANN, E. QUERFURTH, V. RYBIN, G. DREWES, M. RAIDA, T. BOUWMEESTER, P. BORK, B. SERAPHIN, B. KUSTER, G. NEUBAUER and G. SUPERTI-FURGA, 2002 Functional organization of the yeast proteome by systematic analysis of protein complexes. Nature **415:** 141-147.

GILBERT, C. S., C. M. GREEN and N. F. LOWNDES, 2001 Budding yeast Rad9 is an ATP-dependent Rad53 activating machine. Mol Cell **8:** 129-136.

GOTO, H., Y. TOMONO, K. AJIRO, H. KOSAKO, M. FUJITA, M. SAKURAI, K. OKAWA, A. IWAMATSU, T. OKIGAKI, T. TAKAHASHI and M. INAGAKI, 1999 Identification of a novel phosphorylation site on histone H3 coupled with mitotic chromosome condensation. J Biol Chem **274:** 25543-25549.

GRUBER, S., C. H. HAERING and K. NASMYTH, 2003 Chromosomal cohesin forms a ring. Cell **112:** 765-777.

GUO, X. W., J. P. TH'NG, R. A. SWANK, H. J. ANDERSON, C. TUDAN, E. M. BRADBURY and M. ROBERGE, 1995 Chromosome condensation induced by fostriecin does not require p34cdc2 kinase activity and histone H1 hyperphosphorylation, but is associated with enhanced histone H2A and H3 phosphorylation. Embo J **14:** 976-985.

HAAS, W., B. K. FAHERTY, S. A. GERBER, J. E. ELIAS, S. A. BEAUSOLEIL, C. E. BAKALARSKI, X. LI, J. VILLEN and S. P. GYGI, 2006 Optimization and use of peptide mass measurement accuracy in shotgun proteomics. Mol Cell Proteomics **5:** 1326-1337.

HAERING, C. H., J. LOWE, A. HOCHWAGEN and K. NASMYTH, 2002 Molecular architecture of SMC proteins and the yeast cohesin complex. Mol Cell **9:** 773-788.

HAERING, C. H., and K. NASMYTH, 2003 Building and breaking bridges between sister chromatids. Bioessays **25:** 1178-1191.

HARUTA, N., Y. KUROKAWA, Y. MURAYAMA, Y. AKAMATSU, S. UNZAI, Y. TSUTSUI and H. IWASAKI, 2006 The Swi5-Sfr1 complex stimulates Rhp51/Rad51- and Dmc1-mediated DNA strand exchange *in vitro*. Nat Struct Mol Biol **13:** 823-830.

HASSOLD, T., and P. HUNT, 2001 To err (meiotically) is human: the genesis of human aneuploidy. Nature reviews **2:** 280-291.

HAYASE, A., M. TAKAGI, T. MIYAZAKI, H. OSHIUMI, M. SHINOHARA and A. SHINOHARA, 2004 A protein complex containing Mei5 and Sae3 promotes the assembly of the meiosis-specific RecA homolog Dmc1. Cell **119:** 927-940.

HENDZEL, M. J., Y. WEI, M. A. MANCINI, A. VAN HOOSER, T. RANALLI, B. R. BRINKLEY, D. P. BAZETT-JONES and C. D. ALLIS, 1997 Mitosis-specific phosphorylation of histone H3 initiates primarily within pericentromeric heterochromatin during G2 and spreads in an ordered fashion coincident with mitotic chromosome condensation. Chromosoma **106:** 348-360.

HOLLINGSWORTH, N. M., and S. J. BRILL, 2004 The Mus81 solution to resolution: generating meiotic crossovers without Holliday junctions. Genes Dev **18:** 117-125.

HOLLINGSWORTH, N. M., and B. BYERS, 1989 *HOP1*: a yeast meiotic pairing gene. Genetics **121:** 445-462.

HOLLINGSWORTH, N. M., L. GOETSCH and B. BYERS, 1990 The *HOP1* gene encodes a meiosis-specific component of yeast chromosomes. Cell **61:** 73-84.

HOLLINGSWORTH, N. M., and A. D. JOHNSON, 1993 A conditional allele of the *Saccharomyces cerevisiae HOP1* gene is suppressed by overexpression of two other meiosis-specific genes: *RED1* and *REC104*. Genetics **133:** 785-797.

HOLLINGSWORTH, N. M., L. PONTE and C. HALSEY, 1995 *MSH5*, a novel MutS homolog, facilitates meiotic reciprocal recombination between homologs in *Saccharomyces cerevisiae* but not mismatch repair. Genes Dev. **9:** 1728-1739.

HOLZEN, T. M., P. P. SHAH, H. A. OLIVARES and D. K. BISHOP, 2006 Tid1/Rdh54 promotes dissociation of Dmc1 from nonrecombinogenic sites on meiotic chromatin. Genes Dev **20:** 2593-2604.

HSU, J. Y., Z. W. SUN, X. LI, M. REUBEN, K. TATCHELL, D. K. BISHOP, J. M. GRUSHCOW, C. J. BRAME, J. A. CALDWELL, D. F. HUNT, R. LIN, M. M. SMITH and C. D. ALLIS, 2000 Mitotic phosphorylation of histone H3 is governed by Ipl1/aurora kinase and Glc7/PP1 phosphatase in budding yeast and nematodes. Cell **102:** 279-291.

HUGERAT, Y., and G. SIMCHEN, 1993 Mixed segregation and recombination of chromosomes and YACs during single-division meiosis in *spo13* strains of *Saccharomyces cerevisiae*. Genetics **135:** 297-308.

HUNTER, N., and N. KLECKNER, 2001 The single-end invasion: an asymmetric intermediate at the double- strand break to double-holliday junction transition of meiotic recombination. Cell **106:** 59-70.

HUSE, M., and J. KURIYAN, 2002 The conformational plasticity of protein kinases. Cell **109:** 275-282.

IVANOV, E. L., N. SUGAWARA, C. I. WHITE, F. FABRE and J. E. HABER, 1994 Mutations in *XRS2* and *RAD50* delay but do not prevent mating-type switching in Saccharomyces cerevisiae. Mol Cell Biol **14:** 3414-3425

IVANOVSKA, I., and T. L. ORR-WEAVER, 2006 Histone modifications and the chromatin scaffold for meiotic chromosome architecture. Cell Cycle **5:** 2064-2071

JASKELIOFF, M., S. VAN KOMEN, J. E. KREBS, P. SUNG and C. L. PETERSON, 2003 Rad54p is a chromatin remodeling enzyme required for heteroduplex DNA joint formation with chromatin. J Biol Chem **278:** 9212-9218.

JIANG, H., Y. XIE, P. HOUSTON, K. STEMKE-HALE, U. H. MORTENSEN, R. ROTHSTEIN and T. KODADEK, 1996 Direct association between the yeast Rad51 and Rad54 recombination proteins. J Biol Chem **271:** 33181-33186.

JOHNSON, L. N., M. E. M. NOBLE and D. J. OWEN, 1996 Active and inactive protein kinases: structural basis for regulation. Cell **19:** 149-158.

KADYK, L. C., and L. H. HARTWELL, 1992 Sister chromatids are preferred over homologs as substrates for recombinational repair in *Saccharomyces cerevisiae*. Genetics **132:** 387-402.

KALDIS, P., A. SUTTON and M. J. SOLOMON, 1996 The Cdk-activating kinase (CAK) from budding yeast. Cell **86:** 553-564.

KEENEY, S., 2001 Mechanism and control of meiotic recombination initiation. Curr Top Dev Biol **52:** 1-53.

KEENEY, S., C. N. GIROUX and N. KLECKNER, 1997 Meiosis-specific DNA double-strand breaks are catalyzed by Spo11, a member of a widely conserved protein family.

Cell **88:** 375-384.

KEENEY, S., and M. J. NEALE, 2006 Initiation of meiotic recombination by formation of DNA double-strand breaks: mechanism and regulation. Biochem Soc Trans **34:** 523-525.

KIRONMAI, K. M., K. MUNIYAPPA, D. B. FRIEDMAN, N. M. HOLLINGSWORTH and B. BYERS, 1998 DNA-binding properties of Hop1 protein, a synaptonemal complex component from *Saccharomyces cerevisiae*. Mol. Cell. Biol. **18:** 1424-1435.

KLAPHOLZ, S., and R. E. ESPOSITO, 1980 Recombination and chromosome segregation during the single division meiosis in *spo12-1* and *spo13-1* diploids. Genetics **96:** 589-611.

KLEIN, H. L., 1997 *RDH54*, a *RAD54* homologue in *Saccharomyces cerevisiae*, is required for mitotic diploid-specific recombination and repair and for meiosis. Genetics **147:** 1533-1543.

KOVALENKO, O. V., C. WIESE and D. SCHILD, 2006 RAD51AP2, a novel vertebrate- and meiotic-specific protein, shares a conserved RAD51-interacting C-terminal domain with RAD51AP1/PIR51. Nucleic Acids Res **34:** 5081-5092.

KROGH, B. O., and L. S. SYMINGTON, 2004 Recombination proteins in yeast. Annu Rev Genet **38:** 233-271.

LEU, J. Y., P. R. CHUA and G. S. ROEDER, 1998 The meiosis-specific Hop2 protein of *S. cerevisiae* ensures synapsis between homologous chromosomes. Cell **94:** 375-386.

LI, J., D. MOAZED and S. P. GYGI, 2002 Association of the histone methyltransferase Set2 with RNA polymerase II plays a role in transcription elongation. J Biol Chem **277:** 49383-49388.

LI, W., and W. T. MILLER, 2006 Role of the activation loop tyrosines in regulation of the insulin-like growth factor I receptor-tyrosine kinase. J Biol Chem **281:** 23785-23791.

LI, X., S. A. GERBER, A. D. RUDNER, S. A. BEAUSOLEIL, W. HAAS, J. VILLEN, J. E. ELIAS and S. P. GYGI, 2007 Large scale phosphorylation analysis of alpha-factor-arrested *Saccharomyces cerevisiae*. Journal of Proteome Research .6: 1190-1197 (2007)

LIM, K., J. X. HO, K. KEELING, G. L. GILLILAND, X. JI, F. RUKER and D. C. CARTER, 1994 Three-dimensional structure of *Schistosoma japonicum* glutathione S-transferase fused with a six-amino acid conserved neutralizing epitope of gp41 from HIV. Protein Sci **3:** 2233-2244.

LOIDL, J., F. KLEIN and J. ENGEBRECHT, 1998 Genetic and morphological approaches for the analysis of meiotic chromosomes in yeast. Methods Cell Biol **53:** 257-285.

LOIDL, J., F. KLEIN and H. SCHERTHAN, 1994 Homologous pairing is reduced but not abolished in asynaptic mutants of yeast. J. Cell Biol. **125:** 1191-1200.

LORENZ, A., J. L. WELLS, D. W. PRYCE, M. NOVATCHKOVA, F. EISENHABER *et al.*, 2004 *S. pombe* meiotic linear elements contain proteins related to synaptonemal complex components. J Cell Sci **117:** 3343-3351.

LUI, D. Y., T. L. PEOPLES-HOLST, J. C. MELL, H. Y. WU, E. W. DEAN and S. M. BURGESS, 2006 Analysis of close stable homolog juxtaposition during meiosis in mutants of *Saccharomyces cerevisiae*. Genetics **173:** 1207-1222.

LUO, X., Z. TANG, G. XIA, K. WASSMANN, T. MATSUMOTO, J. RIZO and H. YU, 2004 The Mad2 spindle checkpoint protein has two distinct natively folded states. Nat Struct Mol Biol **11:** 338-345.

LYDALL, D., Y. NIKOLSKY, D. K. BISHOP and T. WEINERT, 1996 A meiotic recombination checkpoint controlled by mitotic checkpoint genes. Nature **383:** 840-843.

MACHIN, F., K. PASCHOS, A. JARMUZ, J. TORRES-ROSELL, C. PADE *et al.*, 2004 Condensin regulates rDNA silencing by modulating nucleolar Sir2p. Curr Biol **14:** 125-130.

MACQUEEN, A. J., M. P. COLAIACOVO, K. MCDONALD and A. M. VILLENEUVE, 2002 Synapsis-dependent and -independent mechanisms stabilize homolog pairing during meiotic prophase in *C. elegans*. Genes Dev **16:** 2428-2442.

MAHADEVAIAH, S. K., J. M. TURNER, F. BAUDAT, E. P. ROGAKOU, P. DE BOER, J. BLANCO-RODRIGUEZ, M. JASIN, S. KEENEY, W. M. BONNER and P. S. BURGOYNE, 2001 Recombinational DNA double-strand breaks in mice precede synapsis. Nat Genet **27:** 271-276.

MALONE, R. E., and R. E. ESPOSITO, 1981 Recombinationless meiosis in *Saccharomyces cerevisiae*. Mol. Cell. Biol. **1:** 891-901.

MANIATIS, T., E. F. FRITSCH and J. SAMBROOK, 1982 *Molecular Cloning: A Laboratory Manual*, Cold Spring Harbor, N.Y.

MAO-DRAAYER, Y., A. M. GALBRAITH, D. L. PITTMAN, M. COOL and R. E. MALONE, 1996 Analysis of meiotic recombination pathways in the yeast *Saccharomyces cerevisiae*. Genetics **144:** 71-86.

MARTE, B. M., and J. DOWNWARD, 1997 PKB/Akt: connecting phosphoinositide 3-kinase to cell survival and beyond. Trends Biochem Sci **22:** 355-358.

MARTINEZ-PEREZ, E., and A. M. VILLENEUVE, 2005 HTP-1-dependent constraints coordinate homolog pairing and synapsis and promote chiasma formation during *C. elegans* meiosis. Genes Dev **19:** 2727-2743.

MCKEE, A. H., and N. KLECKNER, 1997 A general method for identifying recessive diploid-specific mutations in *Saccharomyces cerevisiae*, its application to the isolation of mutants blocked at intermediate stages of meiotic prophase and characterization of a new gene *SAE2*. Genetics **146:** 797-816.

MCKIM, K. S., B. L. GREEN-MARROQUIN, J. J. SEKELSKY, G. CHIN, C. STEINBERG, R. KHODOSH and R. S. HAWLEY, 1998 Meiotic synapsis in the absence of recombination. Science **279:** 876-878.

MILLER, T., N. J. KROGAN, J. DOVER, H. ERDJUMENT-BROMAGE, P. TEMPST, M. JOHNSTON, J. F. GREENBLATT and A. SHILATIFARD, 2001 COMPASS: a complex of proteins associated with a trithorax-related SET domain protein. Proc Natl Acad Sci U S A **98:** 12902-12907.

MOHANA-BORGES, R., A. B. F. PACHECO, F. J. R. SOUSA, D. FOGUEL, D. F. ALMEIDA and J. L. SILVA, 2000 LexA repressor forms stable dimers in solution. J. Biol. Chem. **275:** 4708-4712.

NEALE, M. J., J. PAN and S. KEENEY, 2005 Endonucleolytic processing of covalent protein-linked DNA double-strand breaks. Nature **436:** 1053-1057.

NEIMAN, A. M., and I. HERSKOWITZ, 1994 Reconstitution of a yeast protein kinase cascade *in vitro*: Activation of the yeast MEK homolog STE7 by STE11. Proceedings of the National Academy of Science USA **91:** 3398-3402.

NEW, J. H., T. SUGIYAMA, E. ZAITSEVA and S. C. KOWALCZYKOWSKI, 1998 Rad52 protein stimulates DNA strand exchange by Rad51 and replication protein A. Nature **391:** 407-410.

NIU, H., X. LI, E. JOB, C. PARK, D. MOAZED, S. P. GYGI and N. M. HOLLINGSWORTH, 2007 Mek1 Kinase Is Regulated To Suppress Double-Strand Break Repair between Sister Chromatids during Budding Yeast Meiosis. Mol Cell Biol **27:** 5456-5467.

NIU, H., L. WAN, B. BAUMGARTNER, D. SCHAEFER, J. LOIDL and N. M. HOLLINGSWORTH, 2005 Partner choice during meiosis is regulated by Hop1-promoted dimerization of Mek1. Mol Biol Cell **16:** 5804-5818.

NOLEN, B., S. TAYLOR and G. GHOSH, 2004 Regulation of protein kinases; controlling activity through activation segment conformation. Mol Cell **15:** 661-675.

OHTA, K., A. NICOLAS, M. FURUSE, A. NABETANI, H. OGAWA and T. SHIBATA, 1998 Mutations in the *MRE11*, *RAD50*, *XRS2*, and *MRE2* genes alter chromatin

configuration at meiotic DNA double-stranded break sites in premeiotic and meiotic cells. Proc Natl Acad Sci U S A **95:** 646-651.

PANGAS, S. A., W. YAN, M. M. MATZUK and A. RAJKOVIC, 2004 Restricted germ cell expression of a gene encoding a novel mammalian HORMA domain-containing protein. Gene Expr Patterns **5:** 257-263.

PAQUES, F., and J. E. HABER, 1999 Multiple pathways of recombination induced by double-strand breaks in *Saccharomyces cerevisiae*. Microbiol Mol Biol Rev **63:** 349-404.

PECINA, A., K. N. SMITH, C. MEZARD, H. MURAKAMI, K. OTHA and A. NICOLAS, 2002 Target stimulation of meiotic recombination. Cell **111:** 173-184.

.

PELLICIOLI, A., and M. FOIANI, 2005 Signal transduction: how Rad53 kinase is activated. Curr Biol **15:** R769-771.

PENG, J., and S. P. GYGI, 2001 Proteomics: the move to mixtures. J Mass Spectrom **36:** 1083-1091.

PETRONCZKI, M., M. F. SIOMOS and K. NASMYTH, 2003 Un menage a quatre: the molecular biology of chromosome segregation in meiosis. Cell **112:** 423-440.

PETUKHOVA, G., S. STRATTON and P. SUNG, 1998 Catalysis of homologous DNA pairing by yeast Rad51 and Rad54 proteins. Nature **393:** 91-94.

PETUKHOVA, G., P. SUNG and H. KLEIN, 2000 Promotion of Rad51-dependent D-loop formation by yeast recombination factor Rdh54/Tid1. Genes Dev **14:** 2206-2215.

PETUKHOVA, G., S. VAN KOMEN, S. VERGANO, H. KLEIN and P. SUNG, 1999 Yeast Rad54 promotes Rad51-dependent homologous DNA pairing via ATP hydrolysis-driven change in DNA double helix conformation. J. Biol. Chem. **274:** 29453-29462.

PETUKHOVA, G. V., R. J. PEZZA, F. VANEVSKI, M. PLOQUIN, J. Y. MASSON and R. D. CAMERINI-OTERO, 2005 The Hop2 and Mnd1 proteins act in concert with Rad51 and Dmc1 in meiotic recombination. Nat Struct Mol Biol **12:** 449-453.

PITTMAN, D. L., J. COBB, K. J. SCHIMENTI, L. A. WILSON, D. M. COOPER, E. BRIGNULL, M. A. HANDEL and J. C. SCHIMENTI, 1998 Meiotic prophase arrest with failure of chromosome synapsis in mice deficient for Dmc1, a germline-specific RecA homolog. Mol Cell **1:** 697-705.

PLOQUIN, M., G. V. PETUKHOVA, D. MORNEAU, U. DERY, A. BRANSI, A. STASIAK, R. D. CAMERINI-OTERO and J. Y. MASSON, 2007 Stimulation of fission yeast and mouse Hop2-Mnd1 of the Dmc1 and Rad51 recombinases. Nucleic Acids Res **35:** 2719-2733.

PREUSS, U., G. LANDSBERG and K. H. SCHEIDTMANN, 2003 Novel mitosis-specific phosphorylation of histone H3 at Thr11 mediated by Dlk/ZIP kinase. Nucleic Acids Res **31:** 878-885.

PRINZ, S., A. AMON and F. KLEIN, 1997 Isolation of *COM1*, a new gene required to complete meiotic double-strand break-induced recombination in *Saccharomyces cerevisiae*. Genetics **146:** 781-795.

PROWSE, C. N., and J. LEW, 2001 Mechanism of activation of ERK2 by dual phosphorylation. J Biol Chem **276:** 99-103.

PUIG, O., F. CASPARY, G. RIGAUT, B. RUTZ, E. BOUVERET, E. BRAGADO-NILSSON, M. WILM and B. SERAPHIN, 2001 The tandem affinity purification (TAP) method: a general procedure of protein complex purification. Methods **24:** 218-229.

RASCHLE, M., S. VAN KOMEN, P. CHI, T. ELLENBERGER and P. SUNG, 2004 Multiple interactions with the Rad51 recombinase govern the homologous recombination function of Rad54. J Biol Chem **279:** 51973-51980.

RIEDER, C. L., R. W. COLE, A. KHODJAKOV and G. SLUDER, 1995 The checkpoint delaying anaphase in response to chromosome monoorientation is mediated by an inhibitory signal produced by unattached kinetochores. J Cell Biol **130:** 941-948
.

RIGAUT, G., A. SHEVCHENKO, B. RUTZ, M. WILM, M. MANN and B. SERAPHIN, 1999 A generic protein purification method for protein complex characterization and proteome exploration. Nat Biotechnol **17:** 1030-1032.

ROCKMILL, B., and G. S. ROEDER, 1988 *RED1*: a yeast gene required for the segregation of chromosomes during the reductional division of meiosis. Proc Natl Acad Sci U S A **85:** 6057-6061.

ROCKMILL, B., and G. S. ROEDER, 1990 Meiosis in asynaptic yeast. Genetics **126:** 563-574.

ROCKMILL, B., and G. S. ROEDER, 1991 A meiosis-specific protein kinase homolog required for chromosome synapsis and recombination. Genes Dev **5:** 2392-2404.

ROEDER, G. S., and J. M. BAILIS, 2000 The pachytene checkpoint. Trends Genet. **16:** 395-403.

SCHMUCKLI-MAURER, J., and W. D. HEYER, 2000 Meiotic recombination in *RAD54* mutants of *Saccharomyces cerevisiae*. Chromosoma **109:** 86-93.

SCHWACHA, A., and N. KLECKNER, 1995 Identification of double Holliday junctions as intermediates in meiotic recombination. Cell **83:** 783-791.

SCHWACHA, A., and N. KLECKNER, 1997 Interhomolog bias during meiotic recombination: meiotic functions promote a highly differentiated interhomolog-only pathway. Cell **90:** 1123-1135.

SCHWARTZ, M. F., J. K. DUONG, Z. SUN, J. S. MORROW, D. PRADHAN and D. F. STERN, 2002 Rad9 phosphorylation sites couple Rad53 to the *Saccharomyces cerevisiae* DNA damage checkpoint. Mol. Cell **9:** 1055-1065.

SHINOHARA, A., and T. OGAWA, 1998 Stimulation by Rad52 of yeast Rad51-mediated recombination. Nature **391:** 404-407.

SHINOHARA, A., and M. SHINOHARA, 2004 Roles of RecA homologues Rad51 and Dmc1 during meiotic recombination. Cytogenet Genome Res **107:** 201-207.

SHINOHARA, M., S. L. GASIOR, D. K. BISHOP and A. SHINOHARA, 2000 Tid1/Rdh54 promotes colocalization of Rad51 and Dmc1 during meiotic recombination. Proc Natl Acad Sci U S A **97:** 10814-10819.

SHINOHARA, M., E. SHITA-YAMAGUCHI, J. M. BUERSTEDDE, H. SHINAGAWA, H. OGAWA and A. SHINOHARA, 1997 Characterization of the roles of the *Saccharomyces cerevisiae RAD54* gene and a homologue of *RAD54*, *RDH54/TID1*, in mitosis and meiosis. Genetics **147:** 1545-1556.

SMITH, A. V., and G. S. ROEDER, 1997 The yeast Red1 protein localizes to the cores of meiotic chromosomes. J. Cell Biol. **136:** 957-967.

SMITH, A. V., and G. S. ROEDER, 2000 Cloning and characterization of the *Kluyveromyces lactis* homologs of the *Saccharomyces cerevisiae RED1* and *HOP1* genes. Chromosoma **109:** 50-61.

SOLINGER, J. A., K. KIIANITSA and W. D. HEYER, 2002 Rad54, a Swi2/Snf2-like recombinational repair protein, disassembles Rad51:dsDNA filaments. Mol Cell **10:** 1175-1188.

SONG, B., and P. SUNG, 2000 Functional interactions among yeast Rad51 recombinase, Rad52 mediator, and replication protein A in DNA strand exchange. J Biol Chem **275:** 15895-15904.

SOUSHKO, M., and A. P. MITCHELL, 2000 An RNA-binding protein homologue that promotes sporulation-specific gene expression in *Saccharomyces cerevisiae*. Yeast **16:** 631-639.

STRAHL, B. D., and C. D. ALLIS, 2000 The language of covalent histone modifications. Nature **403:** 41-45.

STROM, L., H. B. LINDROOS, K. SHIRAHIGE and C. SJOGREN, 2004 Postreplicative recruitment of cohesin to double-strand breaks is required for DNA repair. Mol Cell **16:** 1003-1015.

SUGAWARA, N., X. WANG and J. E. HABER, 2003 In vivo roles of Rad52, Rad54, and Rad55 proteins in Rad51-mediated recombination. Mol Cell **12:** 209-219.

SULLIVAN, M., T. HIGUCHI, V. L. KATIS and F. UHLMANN, 2004 Cdc14 phosphatase induces rDNA condensation and resolves cohesin-independent cohesion during budding yeast anaphase. Cell **117:** 471-482.

SUNG, P., 1997a Function of yeast Rad52 protein as a mediator between replication protein A and the Rad51 recombinase. J Biol Chem **272:** 28194-28197.

SUNG, P., 1997b Yeast Rad55 and Rad57 proteins form a heterodimer that functions with replication protein A to promote DNA strand exchange by Rad51 recombinase. Genes Dev **11:** 1111-1121.

SWEENEY, F. D., F. YANG, A. CHI, J. SHABANOWITZ, D. F. HUNT and D. DUROCHER, 2005 *Saccharomyces cerevisiae* Rad9 acts as a Mec1 adaptor to allow Rad53 activation. Curr Biol **15:** 1364-1375.

SYM, M., J. ENGEBRECHT and G. S. ROEDER, 1993 Zip1 is a synaptonemal complex protein required for meiotic chromosome synapsis. Cell **72:** 365-378.

SYM, M., and G. S. ROEDER, 1995 Zip1-induced changes in synaptonemal complex structure and polycomplex assembly. J. Cell Biol. **128:** 455-466.

SYMINGTON, L. S., 2002 Role of *RAD52* Epistasis Group Genes in Homologous Recombination and Double-Strand Break Repair. Microbiol Mol Biol Rev **66:** 630-670.

THOMPSON, D. A., and F. W. STAHL, 1999 Genetic control of recombination partner preference in yeast meiosis. Isolation and characterization of mutants elevated for meiotic unequal sister-chromatid recombination. Genetics **153:** 621-641.

THOMPSON, E., and G. S. ROEDER, 1989 Expression and DNA sequence of *RED1*, a gene required for meiosis I chromosome segregation in yeast. Molecular and General Genetics **218:** 293-301.

TSUBOUCHI, H., and G. S. ROEDER, 2003 The importance of genetic recombination for fidelity of chromosome pairing in meiosis. Dev Cell **5:** 915-925.

TSUBOUCHI, H., and G. S. ROEDER, 2004 The budding yeast Mei5 and Sae3 proteins act together with Dmc1 during meiotic recombination. Genetics **168:** 1219-1230.

TSUBOUCHI, H., and G. S. ROEDER, 2006 Budding yeast Hed1 down-regulates the mitotic recombination machinery when meiotic recombination is impaired. Genes Dev **20:** 1766-1775.

TSUBOUCHI, H., and H. OGAWA, 1998 A novel *mre11* mutation impairs processing of double-strand breaks of DNA during both mitosis and meiosis. Mol Cell Biol **18:** 260-268.

UHLMANN, F., F. LOTTSPEICH and K. NASMYTH, 1999 Sister-chromatid separation at anaphase onset is promoted by cleavage of the cohesin subunit Scc1. Nature **400:** 37-42.

UHLMANN, F., and K. NASMYTH, 1998 Cohesion between sister chromatids must be established during DNA replication. Curr Biol **8:** 1095-1101.

UNAL, E., A. ARBEL-EDEN, U. SATTLER, R. SHROFF, M. LICHTEN, J. E. HABER and D. KOSHLAND, 2004 DNA damage response pathway uses histone modification to assemble a double-strand break-specific cohesin domain. Mol Cell **16:** 991-1002.

USUI, T., H. OGAWA and J. H. PETRINI, 2001 A DNA damage response pathway controlled by Tel1 and the Mre11 complex. Mol Cell **7:** 1255-1266.

VAN KOMEN, S., G. PETUKHOVA, S. SIGURDSSON and P. SUNG, 2002 Functional cross-talk among Rad51, Rad54, and replication protein A in heteroduplex DNA joint formation. J Biol Chem **277:** 43578-43587.

VARGO, M. A., L. NGUYEN and R. F. COLMAN, 2004 Subunit interface residues of glutathione S-transferase A1-1 that are important in the monomer-dimer equilibrium. Biochemistry **43:** 3327-3335.

VERSHON, A. K., N. M. HOLLINGSWORTH and A. D. JOHNSON, 1992 Meiotic induction of the yeast *HOP1* gene is controlled by positive and negative regulatory elements. Mol. Cell. Biol. **12:** 3706-3714.

VILLENEUVE, A. M., and K. J. HILLERS, 2001 Whence meiosis? Cell **106:** 647-650.

WAGSTAFF, J. E., S. KLAPHOLZ and R. E. ESPOSITO, 1982 Meiosis in haploid yeast. Proceedings of the National Academy of Science USA **79:** 2986-2990.

WALLIS, J. W., M. RYKOWSKI and M. GRUNSTEIN, 1983 Yeast histone H2B containing large amino terminus deletions can function in vivo. Cell **35:** 711-719.

WAN, L., T. DE LOS SANTOS, C. ZHANG, K. SHOKAT and N. M. HOLLINGSWORTH, 2004 Mek1 kinase activity functions downstream of *RED1* in the regulation of meiotic double strand break repair in budding yeast. Mol Biol Cell **15:** 11-23.

WANG, X., and J. E. HABER, 2004 Role of Saccharomyces single-stranded DNA-binding protein RPA in the strand invasion step of double-strand break repair. PLoS Biol **2:** E21.

WESOLY, J., S. AGARWAL, S. SIGURDSSON, W. BUSSEN, S. VAN KOMEN, J. QIN, H. VAN STEEG, J. VAN BENTHEM, E. WASSENAAR, W. M. BAARENDS, M. GHAZVINI, A. A. TAFEL, H. HEATH, N. GALJART, J. ESSERS, J. A. GROOTEGOED, N. ARNHEIM, O. BEZZUBOVA, J. M. BUERSTEDDE, P. SUNG and R. KANAAR, 2006 Differential contributions of mammalian Rad54 paralogs to recombination, DNA damage repair, and meiosis. Mol Cell Biol **26:** 976-989.

WILTZIUS, J. J., M. HOHL, J. C. FLEMING and J. H. PETRINI, 2005 The Rad50 hook domain is a critical determinant of Mre11 complex functions. Nat Struct Mol Biol **12:** 403-407.

WOLTERING, D., B. BAUMGARTNER, S. BAGCHI, B. LARKIN, J. LOIDL, T. DE LOS SANTOS and N. M. HOLLINGSWORTH, 2000 Meiotic segregation, synapsis, and recombination checkpoint functions require physical interaction between the chromosomal proteins Red1p and Hop1p. Mol. Cell. Biol. **20:** 6646-6658.

WU, T.-C., and M. LICHTEN, 1994 Meiosis-induced double-strand break sites determined by yeast chromatin structure. Science **263:** 515-518.

XU, L., B. M. WEINER and N. KLECKNER, 1997 Meiotic cells monitor the status of the interhomolog recombination complex. Genes Dev. **11:** 106-118.

XU, Y. J., M. DAVENPORT and T. J. KELLY, 2006 Two-stage mechanism for activation of the DNA replication checkpoint kinase Cds1 in fission yeast. Genes Dev **20:** 990-1003.

YOSHIDA, K., G. KONDOH, Y. MATSUDA, T. HABU, Y. NISHIMUNE and T. MORITA, 1998 The mouse RecA-like gene Dmc1 is required for homologous chromosome synapsis during meiosis. Mol Cell **1:** 707-718.

YVES-MASSON, J., and S. C. WEST, 2001 The Rad51 and Dmc1 recombinases: a non-identical twin relationship. Trends Biochem Sci. **26:** 131-136.

ZETKA, M. C., I. KAWASAKI, S. STROME and F. MULLER, 1999 Synapsis and chiasma formation in *Caenorhabditis elegans* require HIM-3, a meiotic chromosome core component that functions in chromosome segregation. Genes Dev **13:** 2258-2270

ZIERHUT, C., M. BERLINGER, C. RUPP, A. SHINOHARA and F. KLEIN, 2004 Mnd1 is required for meiotic interhomolog repair. Curr Biol **14:** 752-762.